
Doctoral

Science

2007-01-01

Physiochemical Indicators of Single Walled Carbon Nanotube Toxicity

Alan Casey

Technological University Dublin, alan.casey@tudublin.ie

Follow this and additional works at: <https://arrow.tudublin.ie/sciendoc>



Part of the [Nanoscience and Nanotechnology Commons](#)

Recommended Citation

Casey, A. (2007). *Physiochemical indicators of single walled carbon nanotube toxicity*. Doctoral thesis. Technological University Dublin. doi:10.21427/D73P4J

This Theses, Ph.D is brought to you for free and open access by the Science at ARROW@TU Dublin. It has been accepted for inclusion in Doctoral by an authorized administrator of ARROW@TU Dublin. For more information, please contact arrow.admin@tudublin.ie, aisling.coyne@tudublin.ie, vera.kilshaw@tudublin.ie.



Physiochemical Indicators of Single Walled Carbon Nanotube Toxicity

By

Alan Casey, Dip App Sc, BSc

A thesis submitted to the Dublin Institute of Technology,
For the degree of Doctor of Philosophy (PhD)

School of Physics

Dublin Institute of Technology

Kevin Street, Dublin 8

2007

Abstract

Numerous toxicity studies have been conducted to date both *in vivo* and *in vitro* on refined and raw Single Walled Carbon Nanotubes (SWCNT). Differences in SWCNT toxicity and biocompatibility have been observed between these studies, and whilst these discrepancies have been attributed to factors such as varying percentages of remnant catalytic particles, differences in dispersion methods etc. the mechanisms underlying these inconsistencies have not been investigated. This study used standard spectroscopic and cellular techniques to elucidate the origins of these inconsistencies and also to estimate the validity of toxicological data evaluated from standard cytotoxic endpoints.

Spectroscopic studies were conducted in order to demonstrate and elucidate the interactions of HiPco[®] SWCNT with cell culture medium and its components, prepared both with and without foetal bovine serum. Upon addition of raw SWCNT to the medium a noticeable colour change was observed. UV/Vis absorption spectroscopy revealed a dramatic reduction in the absorption attributable to the phenol red, a pH indicator within the medium, without an associated change in pH. Reductions were also observed in absorbance features attributed to various components of the medium indicating an interaction with the SWCNT. Fluorescence spectroscopy also revealed reductions in emission features associated with the components of the medium giving further support to an interaction. Concentration dependent studies of the fluorescent emission of the various components of the media were modelled to show a differing degree of interaction between the SWCNT and the various components. Finally, notable differences were observed between the behaviour with and without serum. Raman spectroscopy gave no indication of differences between raw SWCNT and those

deposited from the medium suspension indicating that no debundling of the SWCNT occurred. The results and their implications for toxicity and *in vitro* studies are discussed.

To investigate if these interactions could induce a secondary toxicity by medium depletion, further spectroscopic and cytotoxicity studies were performed. SWCNT media suspensions were created, centrifuged and filtered (0.2µm cellulose acetate filters) to remove the SWCNT. Spectroscopic analysis was carried out on the filtered samples to verify the removal of the SWCNT from the suspension but also to assess the degree of alteration of the medium due to the aforementioned interactions. Cytotoxicity studies were performed on human alveolar A549 cells with the depleted media. Two cytotoxic endpoints were employed to evaluate cytotoxicity, namely Alamar blue and neutral red. Concentration dependant exposures over different time periods revealed low acute cytotoxicity after 72 and 96 hour exposure to the filtered samples, verifying the proposed notion of a secondary toxicity due to medium depletion.

Finally the direct cytotoxicity of single walled carbon nanotubes was evaluated in the A549 human alveolar carcinoma cell line. Cell viability was assessed using the following indicator dyes, Commassie Blue, Alamar Blue[™], Neutral Red, MTT and WST-1. Exposure of the A549 cells revealed the nanotubes to have low acute toxicity. However considerable variation was found depending on the dye employed. Spectroscopic analysis of the nanotubes' interactions with the dyes revealed interactions in all cases, resulting in the reduction of the associated absorption/fluorescent emission which is used to evaluate particle toxicity. In addition to being sensitive, simple, safe and cost-effective the ideal test for *in vitro* cell cytotoxicity must also not interfere with the compound to be tested. The results therefore have comprehensively confirmed that

the indicator dyes used in this study were not appropriate for the quantitative toxicity assessment of carbon nanotubes highlighting the pressing need for the development of alternative screening techniques.

Declaration

I certify that this thesis which I now submit for examination for the award of doctor of philosophy, is entirely my own work and has not been taken from the work of others save and to the extent that such work has been cited and acknowledged within the text of my work.

This thesis was prepared according to the regulations for postgraduate study by research of the Dublin Institute of Technology and has not been submitted in whole or in part for an award in any other Institute or University.

The work reported on in this thesis conforms to the principles and requirements of the Institute's guidelines for ethics in research.

The Institute has permission to keep, or lend or to copy this thesis in whole or in part, on condition that any such use of the material or the thesis be duly acknowledged.

Signature _____ Date ____/____/____

Candidate

Acknowledgements

Over the course of my study numerous people have provided invaluable help without which I don't know what I would have done. So cheers everyone! Firstly thanks to all the staff in the Focas institute past and present Garrett Farrell, Louisa Hartnett, Anne Shanahan, Teresa Hedderman and Andrew Hartnett without all of you I would probably be still sitting in front of a spectrometer or thrown my computer out the window long ago!

Thanks to Dr. Mary McNamara and my advisory supervisor Dr. Hugh Byrne for taking a chance on an undergraduate student with somewhat questionable history many moons ago (one summer working in a lab and look what happened) without your help and guidance none of this would have ever been possible. Hugh thanks for all the advising even if it didn't seem fully appreciated at the time (because it generally meant more work!) your constant ideas, heated debates and rational explanations (well some of them were rational) were a constant source of inspiration (and many a headache!).

A special thanks to my supervisor Dr. Gordon Chambers for giving me the opportunity to carry out a PhD, your "lash the tubes in and see what happens" attitude while stressful at times did yield some very interesting results! Seriously though thanks for all the help, advice and pep talks (which were generally needed after the heated debates with Hugh) without your support and calming influence on one stressed out physicist I would have given up. I can only hope that one day I will be as good a teacher and supervisor as you are so thanks Gordon.

To everyone in the radiation and environmental science lab (Eva, Fiona, Orla, Ailbhe, James Rocky) without your patience and guidance many a cell would have died of natural causes (to be honest I am sure I was more toxic to them in the beginning). Dr. Maria Davoren what would I have done without you, I know nanotubes in general (and maybe me) were a constant source of stress, headaches and possibly a few grey hairs but without your constant explanation of everything biological, reading of many a paper and chapters, sound advice and just always being there to help this study could not have been done, your one “Bonza Shelia” Maria.

To everyone one of my friends in the ground floor office the laughs, nights out and general madness made it a very happy place to be every day cheers guys.

Finally to my family, Mam and Dad nothing I can ever say or do could truly show how much your support through out my collage years meant to me (they went on for a while I admit). Without you I would have never even went to collage let alone carried out a PhD. So to say thanks I dedicate this thesis to the most loving and supportive people I know my family.

PS. I promise I will leave collage and get a job someday!

List of Abbreviations

| | |
|--|---------------------|
| Alamar Blue TM | AB |
| Atomic force microscopy | AFM |
| Buckminster Fullerene | C ₆₀ |
| Carbon black | CB |
| Coomassie Brilliant Blue | COMMASSIE |
| Carbon nanotubes | CNT |
| Cobalt | Co |
| Carbon dioxide | CO ₂ |
| Chemical vapour deposition | CVD |
| N dimethylformamide | DMF |
| Environmental Protection Agency | EPA |
| Foetal Bovine serum | FBS |
| Iron | Fe |
| Iron pentacarbonyl | Fe(CO) ₅ |
| Human Dermal Fibroblasts | HDF |
| Hydrochloric acid | HCl |
| High pressure carbon monoxide | HiPco |
| 3-(4,5-dimethylthiazol-2-yl)-2,5-diphenyltetrazolium bromide | MTT |
| Multi-walled carbon nanotubes | MWCNT |
| Human Liver Carcinoma Cells | HepG2 |
| Neuronal Human Astrocytes | NHA |
| Nickel | Ni |

| | |
|---|-------|
| Nanoparticles | NP |
| 3-amino- <i>m</i> -dimehtylamino-2-methyl-phenazine hydrochloride | NR |
| Reactive oxygen species | ROS |
| Sodium dodecyl sulphate | SDS |
| Scanning electron microscopy | SEM |
| Scanning tunnelling spectroscopy | STS |
| Single-walled carbon nanotubes | SWCNT |
| Thiobarbituric Acid assay | TBA |
| Transmission electron microscopy | TEM |
| 2-(4-iodophenyl)-3-(4-nitrophenyl)-5-(2,4- disulfophenyl)-2H-tetrazolium | WST-1 |
| Zinc oxide | ZnO |

List of Figures

| Figure | Caption | Page |
|---------------|---|-------------|
| Figure 2.1 | Left; schematic of a single-walled carbon nanotube (SWCNT), Right; schematic of a multi-walled carbon nanotube (MWCNT). | 12 |
| Figure 2.2 | Schematic of water cooled CO flow tube reactor. | 15 |
| Figure 2.3 | Diameter distributions of SWCNT produced at 1200°C at various CO pressures . | 16 |
| Figure 2.4 | Schematic diagrams showing the different ways of rolling a sheet of graphite to make various types of single walled carbon nanotubes. | 19 |
| Figure 2.5 | Unrolled honeycomb lattice of a nanotube. When the sites O and A coincide as well as B and B', a nanotube can be constructed | 20 |
| Figure 2.6 | Schematic Diagram showing Carbon nanotubes (n, m) that are metallic and semiconducting, and are denoted by open and solid circles respectively on the map of chiral vectors (n, m). | 22 |
| Figure 2.7 | I-V curves of isolated carbon nanotubes. | 23 |
| Figure 2.8 | Schematic of a Nanotube Rope (left) High resolution TEM of SWCNT bundled nanotubes produced by the arc discharge technique (right) . | 24 |
| Figure 3.1 | Proposed mechanisms by which nanomaterials interact with biological tissue. | 38 |

| Figure | Caption | Page |
|---------------|---|-------------|
| Figure 3.2 | Proposed properties of SWCNT which may induce toxicity. | 43 |
| Figure 4.1 | Jablonski diagram showing the sequence of steps leading to radiative decay. | 62 |
| Figure 4.2 | Absorption Spectrum of HiPco Carbon Nanotubes. | 64 |
| Figure 4.3 | Schematic diagram of electronic density of states for (a) metallic and (b) semiconducting SWCNT. Arrows indicate the optically allowed Inter band transitions | 65 |
| Figure 4.4 | Absorption (Blue) and Fluorescent Emission (Red) spectra of HiPco SWCNT in SDS. | 68 |
| Figure 4.5 | Infrared Spectrum of HiPco Carbon Nanotubes carried out in transmittance with a KBr disc. | 73 |
| Figure 4.6 | Raman Spectrum obtained for pristine HiPco SWCNT at 514nm excitation divided into characteristic Low, Medium and High Frequency Regions. | 74 |
| Figure 4.7 | Schematic representations of RBM vibrations of SWCNT | 75 |
| Figure 4.8 | Raman Spectra of the RBM region of pristine HiPco SWCNT (a) 514 nm excitation and (b) 633nm excitation. | 76 |
| Figure 4.9 | Raman Signal for Raw HiPco Carbon Nanotubes (a) 514.5nm Excitation and (b) 633nm Excitation. | 78 |
| Figure 4.10 | Raman Signals of SWCNT at various excitation wavelengths. | 80 |
| Figure 4.11 | Fitted Radial Breathing Modes for Raw HiPco Carbon Nanotubes 514nm excitation. | 81 |

| Figure | Caption | Page |
|---------------|--|-------------|
| Figure 4.12 | Diameter Distribution of pristine HiPco Carbon Nanotubes from RBM analysis at 514 and 632nm excitation. | 82 |
| Figure 4.13 | TEM of Raw as Purchased HiPco® SWCNT. | 84 |
| Figure 5.1. | Absorption Spectra of (a) 5%-FBS-F12K containing 0.7 mg/ml SWCNT (b) 5%-FBS-F12K medium only. | 100 |
| Figure 5.2. | Plot of the emission ratios at 450nm by 360nm excitation of (●) 0%-FBS-F12K $C_0 = 0.135 \pm 0.020$ mg/ml and (Δ) 5%-FBS-F12K $C_0 = 0.125 \pm 0.020$ mg/ml. | 105 |
| Figure 5.3. | Plot of emission ratios against SWCNT concentration by (●) 268nm excitation $C_0 = 0.145 \pm 0.02$ mg/ml and (Δ) 410nm excitation $C_0 = 0.2 \pm 0.02$ mg/ml for 5%- FBS-F12K cell culture medium. | 106 |
| Figure 5.4. | Plot of emission ratios against SWCNT concentration for a 1:1 ratio dilution of FBS at (●) 268nm excitation $C_0 = 0.2 \pm 0.02$ mg/ml and (Δ) 410nm excitation $C_0 = 0.275 \pm 0.02$ mg/ml. | 107 |
| Figure 5.5 | G-line region for 514.5nm excitation (a) Raw SWCNT Soot. (b) 5%-FBS-F12K containing 0.1 mg/ml SWCNT. | 110 |
| Figure 5.6 | Radial breathing mode region for 514nm excitation (a) Raw SWCNT Soot (b) 5%-FBS-F12K containing 0.1mg/ml SWCNT. | 111 |

| Figure | Caption | Page |
|---------------|--|-------------|
| Figure 5.7 | Plot of emission ratios at 500nm by 360nm excitation against concentration for a 1:1 mass ratio dilution of Riboflavin and SWCNT in deionised water. $C_0 = 0.0045 \pm 0.002$ mg/ml. | 114 |
| Figure 5.8 | Radial breathing mode region for 514.5nm excitation (a) Raw SWCNT Soot (b) 0.125mg/ml SWCNT in 0.125mg/ml riboflavin taken from a drop cast sample. | 116 |
| Figure 5.9 | Plot of emission ratios at 425nm against SWCNT concentration for a 1:1 mass ratio dilution of Phenylalanine in deionised water. $C_0 = 0.15 \pm 0.02$ mg/ml. | 117 |
| Figure 5.10 | Plot of emission ratios against SWCNT concentration for a 1:1 mass ratio dilution of Glutamic Acid in deionised water. $C_0 = 0.008 \pm 0.002$ mg/ml. | 118 |
| Figure 5.11 | Radial breathing mode region for 514.5nm excitation (a) Raw SWCNT Soot (b) 0.125mg/ml SWCNT in equal concentration glutamic acid (c) 0.0315mg/mg SWCNT in equal concentration phenylalanine, taken from a drop cast sample. | 119 |
| Figure 6.1 | Raman Spectra by 514.5 nm excitation of (a) Unfiltered 5% FBS Medium containing HiPco SWCNT 0.8mg/ml (b) Unfiltered 5% FBS Medium containing HiPco SWCNT 0.00156 mg/ml (c) Arc Discharge SWCNT Filtrate 0.8mg/ml (d) Carbon Black Filtrate 0.8mg/ml (e) HiPco SWCNT Filtrate 0.8mg/ml. | 134 |
| Figure 6.3 | UV-Vis Absorption Spectra of (a) HiPco SWCNT Filtered medium 0.8mg/ml and (b) 5 % FBS medium. | 136 |
| Figure 6.4 | UV-Vis Absorption Spectra of (a) Arc Discharge SWCNT Filtered medium 0.8mg/ml and (b) 5 % FBS medium. | 137 |

| Figure | Caption | Page |
|---------------|--|-------------|
| Figure 6.5 | UV-Vis Absorption Spectra of (a) Carbon Black Filtered medium 0.8mg/ml and (b) 5 % FBS medium. | 137 |
| Figure 6.6 | Plot of emission ratios of 5%-FBS-F12K filtered cell culture medium against (a) HiPco SWCNT (b) Arc Discharge SWCNT (c) Carbon black concentration (initial) by excitation at (□) 268nm excitation, (●) 360nm excitation and (Δ) 410nm excitation. | 141 |
| Figure 6.7 | Cytotoxicity of HiPco SWCNT filtered medium to A549 cells after 24, 48, 72 and 96 hour exposures determined by the NR assay. | 144 |
| Figure 6.8 | Cytotoxicity of Arc Discharge SWCNT filtered medium to A549 cells after 24, 48, 72 and 96 hour exposures determined by the NR assay. | 144 |
| Figure 6.9 | Cytotoxicity of Carbon Black filtered medium to A549 cells after 24, 48, 72 and 96 hour exposures determined by the NR assay. | 146 |
| Figure 6.10 | Cytotoxicity of HiPco SWCNT filtered medium to A549 cells after 24, 48, 72 and 96 hour exposures determined by the AB assay. | 148 |
| Figure 6.11 | Cytotoxicity of Arc Discharge SWCNT filtered medium to A549 cells after 24, 48, 72 and 96 hour exposures determined by the AB assay. | 149 |
| Figure 6.12 | Cytotoxicity of Carbon Black filtered medium to A549 cells | 151 |

| Figure | Caption | Page |
|---------------|---|-------------|
| | after 24, 48, 72 and 96 hour exposures determined by the AB assay | |
| Figure 7.1 | (a) Cytotoxicity of SWCNT to A549 cells after 24 hour exposure determined by the COMMASSIE assay (b) Plots of COMMASSIE absorbance at 615nm versus concentration mg/ml (●) COMMASSIE and (○) COMMASSIE and SWCNT. | 166 |
| Figure 7.2 | (a) Cytotoxicity of SWCNT to A549 cells after 24 hour exposure determined by the AB assay (b) Plot of emission ratios at 595nm by 540nm excitation for the AB assay against SWCNT concentration mg/ml. | 168 |
| Figure 7.3 | (a) Cytotoxicity of SWCNT to A549 cells after 24 hour exposure determined by the NR assay (b) Plot of emission ratios for the NR assay against SWCNT concentration mg/ml. | 173 |
| Figure 7.4 | (a) Cytotoxicity of SWCNT to A549 cells after 24 hour exposure determined by the MTT assay (b) Plot of the absorbance ratio of the converted MTT formazan against SWCNT concentration mg/ml. | 175 |
| Figure 7.5 | (a) Cytotoxicity of SWCNT to A549 cells after 24 hour exposure determined by the WST-1 assay (b) Plot of the absorbance ratios for the WST-1 assay against SWCNT concentration mg/ml. | 178 |

List of Tables

| Table | Caption | Page |
|--------------|---|-------------|
| Table 2.1 | Production rates and yield for varying temperatures at a CO pressure of 10atm. | 17 |
| Table 2.2 | Production rates and yields for varying CO pressures at a temperature of 1200°C. | 17 |
| Table 7.1 | displays a list of all cytotoxic dyes tested, the spectroscopic property from which cytotoxic data is evaluated, the SWCNT concentration at which toxicity was observed and the lowest SWCNT concentration at which absorptive interferences were detected. | 179 |

Table of Contents

| <u>Section Title</u> | <u>Page</u> |
|--|-------------|
| <u>Chapter 1 “Introduction”</u> | |
| 1.1 Nanotechnology. | 1 |
| 1.2 The Importance of Carbon Nanotubes. | 2 |
| 1.3 Societal Impacts of Nanotechnology. | 2 |
| 1.4 Current Knowledge. | 4 |
| 1.5 Thesis Outline. | 5 |
| References. | 7 |
| | |
| <u>Chapter 2 “Single walled carbon nanotubes”</u> | |
| 2.1 Introduction to single walled carbon nanotubes. | 12 |
| 2.2 High Pressure Carbon Monoxide Method (HiPco). | 14 |
| 2.3 Physical Properties of carbon nanotubes. | 18 |
| 2.3.1 <i>Structure and types of SWCNT.</i> | 18 |
| 2.3.2 <i>Electronic properties of SWCNT.</i> | 21 |
| 2.4 SWCNT interactions. | 24 |
| 2.4.1 <i>Surfactants and solvents.</i> | 25 |
| 2.4.2 <i>Synthetic molecules.</i> | 26 |
| 2.4.3 <i>Biological molecules.</i> | 27 |
| 2.4.4 <i>Saccharide systems.</i> | 28 |
| 2.5 Chapter summary. | 29 |
| References. | 31 |
| | |
| <u>Chapter 3 “Nanotoxicology”</u> | |
| 3.1 Introduction | 36 |
| 3.2 Toxicity of carbon based materials. | 39 |
| 3.2.1 <i>Carbon Black.</i> | 39 |
| 3.2.2 <i>The Buckminster Fullerene.</i> | 41 |
| 3.3 Factors contributing to SWCNT toxicity. | 42 |
| 3.3.1 <i>Surface area.</i> | 44 |
| 3.3.2 <i>Length.</i> | 45 |

| Section Title | Page |
|------------------------------------|-------------|
| 3.3.3 <i>Chemical composition.</i> | 46 |
| 3.4 Toxicity of SWCNT. | 47 |
| 3.5 Chapter Summary. | 50 |
| References. | 52 |

Chapter 4 “Experimental”

| | |
|--|----|
| 4.1 Introduction. | 61 |
| 4.2 Electronic spectroscopy. | 61 |
| 4.2.1 <i>Absorption spectroscopy.</i> | 64 |
| 4.2.2 <i>Fluorescent emission spectroscopy.</i> | 67 |
| 4.3 Vibrational spectroscopy. | 69 |
| 4.3.1 <i>Infra red spectroscopy.</i> | 69 |
| 4.3.2 <i>Raman spectroscopy.</i> | 70 |
| 4.4 Infra red spectroscopy of SWCNT. | 71 |
| 4.5 Raman analysis of SWCNT. | 73 |
| 4.5.1 <i>Low frequency Raman spectra.</i> | 74 |
| 4.5.2 <i>Medium frequency Raman spectra.</i> | 77 |
| 4.5.3 <i>High frequency Raman spectra.</i> | 77 |
| 4.5.4 <i>Radial Breathing Mode analysis of pristine HiPco SWCNT.</i> | 81 |
| 4.6 Transmission electron microscopy of pristine HiPco SWCNT. | 83 |
| 4.7 SWCNT characterisation summary. | 85 |
| 4.8 General experimental | 86 |
| 4.8.1 <i>Test materials and reagents.</i> | 86 |
| 4.8.2 <i>Dispersion of SWCNT.</i> | 87 |
| 4.8.3 <i>Spectroscopic characterisation.</i> | 87 |
| 4.8.4 <i>Cell culture.</i> | 87 |
| 4.8.5 <i>Cytotoxicity assays.</i> | 88 |
| 4.8.6 <i>Statistical analysis.</i> | 90 |
| References. | 91 |

Chapter 5 “Nanotube medium interactions”

| | |
|------------------|----|
| 5.1 Introduction | 97 |
|------------------|----|

| Section Title | Page |
|---|-------------|
| 5.2 Experimental. | 99 |
| 5.2.1 <i>Dispersion of SWCNT.</i> | 99 |
| 5.3 Results and discussion. | 99 |
| 5.3.1 <i>Initial observations.</i> | 99 |
| 5.3.2 <i>UV/Visible absorption spectroscopy.</i> | 100 |
| 5.3.3 <i>Fluorescent emission spectroscopy.</i> | 102 |
| 5.3.4 <i>Raman spectroscopy.</i> | 109 |
| 5.4 Individual components. | 112 |
| 5.4.1 <i>Riboflavin.</i> | 113 |
| 5.4.2 <i>Amino Acids (Phenylalanine and Glutamic Acid).</i> | 116 |
| 5.5 Chapter Summary. | 120 |
| References. | 123 |

Chapter 6 “Can interactions induce medium depletion?”

| | |
|---|-----|
| 6.1 Introduction | 130 |
| 6.2 Experimental | 131 |
| 6.2.1 <i>Preparation of test samples.</i> | 131 |
| 6.2.2 <i>Cytotoxicity assays.</i> | 132 |
| 6.3 Spectroscopic analysis. | 132 |
| 6.3.1 <i>Initial observations</i> | 133 |
| 6.3.2 <i>Raman spectroscopy.</i> | 133 |
| 6.3.3 <i>UV/Visible absorption spectroscopy.</i> | 135 |
| 6.3.4 <i>Fluorescent emission spectroscopy.</i> | 139 |
| 6.3.5 <i>Spectroscopic analysis summary.</i> | 142 |
| 6.4 Indirect cytotoxicity of SWCNT by medium depletion. | 143 |
| 6.4.1 <i>Neutral Red</i> | 143 |
| 6.4.2 <i>Alamar Blue.</i> | 146 |
| 6.5 Chapter summary. | 152 |
| References. | 155 |

Chapter 7 “SWCNT interfere with cytotoxicity endpoints”

| | |
|-------------------|-----|
| 7.1 Introduction. | 161 |
|-------------------|-----|

| <u>Section Title</u> | <u>Page</u> |
|---|--------------------|
| 7.2 Experimental. | 163 |
| 7.2.1 <i>Dispersion of SWCNT.</i> | 163 |
| 7.2.2 <i>Cytotoxicity assays.</i> | 163 |
| 7.3 Results and discussion. | 163 |
| 7.3.1 <i>Commassie Blue.</i> | 164 |
| 7.3.2 <i>Alamar Blue.</i> | 167 |
| 7.3.3 <i>Neutral Red.</i> | 170 |
| 7.3.4 <i>MTT.</i> | 173 |
| 7.4.5 <i>WST-1.</i> | 177 |
| 7.4 Chapter summary. | 179 |
| References. | 181 |
| | |
| <u>Chapter 8 “Conclusions”</u> | |
| 8.1 Summary of findings. | 187 |
| 8.2 Further work. | 191 |
| 8.3 Concluding remarks. | 193 |
| References. | 195 |
| | |
| <u>Appendices.</u> | 196 |
| | |
| <u>Peer reviewed publications.</u> | 212 |
| | |
| <u>Conference list.</u> | 213 |

Chapter 1

“Introduction”

1.1 Nanotechnology.

Nanoscience is defined as “the study of phenomena and the manipulation of materials at atomic, molecular, and macromolecular scales, where properties differ significantly from those at larger scale”, and nanotechnologies as “the design, characterization, production, and application of structures, devices, and systems by controlling shape and size at the nanometre scale” (The Royal Society, 2004). Richard P. Feynman was the first to mention the concept of nanoscience during his key lecture at the annual American Physical Society meeting in 1959 (Feynman, 1959). A Japanese researcher, Norio Taniguchi, spoke about nanotechnology in 1974 and gave this definition “Nanotechnology consists of the processing, separation, consolidation and deformation of materials by one atom or another” (Taniguchi, 1974). Although this description is over 30 years old it still encompasses the aims of many researchers working in the Nanotechnology field.

Nanotechnology is widely perceived as one of the key technologies of the 21st century and accordingly there have been huge advances and increased funding in global technological research on nanomaterials. Its incorporation into main stream scientific research understandably has had considerable effects. The development of a vast battery of engineered nanoparticles has resulted in an ever increasing range of potential

applications based primarily on their one common property-their size.

1.2 The importance of carbon nanotubes.

Within the family of nanomaterials, carbon nanotubes (CNT) have shown great potential, with a multitude of proposed applications in such disciplines as, for example, materials science (Guzmán de Villoria *et al.*, 2006), electronics (Singh *et al.*, 2006), and biomedicine (Bianco *et al.*, 2005; Pantarotto *et al.*, 2004). Of the CNT, single wall carbon nanotubes (SWCNT) are considered to have extensive commercial applications potential due to their excellent mechanical, electrical and magnetic properties (Paradise and Goswami, 2006). The broad and increasing range of nanotechnological applications for SWCNT, many of which are biological, will almost certainly result in the increased potential for both human and environmental exposures to this nanomaterial. It is, therefore, imperative that toxicological research to evaluate the biocompatibility and possible adverse effects on both the health of humans and the environment is conducted parallel with technological research and the development of nanomaterials (Dreher, 2004; Oberdörster *et al.*, 2005; Thomas and Sayre, 2005).

1.3 Societal impacts of nanotechnology.

Nanotechnology has a huge number and variety of applications across many different sectors. Potentially it could lead to more efficient and sustainable use of resources and have a beneficial impact for the vast majority of people throughout the world. However, as with all technologies, there are also potential negative impacts on society. With an increasing range of engineered nanoparticles finding their way in to mainstream consumer products there will undoubtedly be societal impacts. The main issues include

social divide, communication, and risk. As with previous technologies such as information technology, nanotechnology could have the effect of widening the divide between the rich and the poor, or more specifically the developed and developing world. Primarily this can be through advances in healthcare, transport, energy supplies, *etc.* which may be more available to the wealthy. However, paradoxically, it may also come about through a decreased use of natural resources. Many of the precious metals and minerals that new nanomaterials are expected to replace, and thereby reduce our dependency on non-renewable sources, are mined in the developing world. The loss of this revenue without a strategy for its replacement will have a negative impact on the economy and development of these countries. Acceptance of new developments and in particular the wide-ranging effects of nanotechnology, can only be achieved through communication and dialogue between scientists, industrialists, governments and wider society. All too often in the past this has been ignored and resulted in misinformation and misunderstanding of the risks and benefits associated with the new development. This has been recognised by governments, research funding agencies and industry, and there are currently emerging many initiatives that actively explore dialogue with social scientists and interested citizens, allowing the implications of new developments to be explained, concerns explored, and opinions of different members of society incorporated into future planning.

Nanomaterials are being developed because they offer advantages over conventional materials such as improved electronic properties, strength and optical properties. However, information regarding the health and safety of engineered nanoparticles has been slow to filter to the public. There are of course concerns regarding the safety of this every increasing range of nanomaterials which are slowly filtering into main stream consumer products such as cosmetics, sun creams and food packaging to name a few.

With the shrinkage in size to the nano scale, the intrinsic properties can be significantly altered in comparison to that of the bulk material which may induce adverse effects to health. Also the nano scale dimensions are such that cellular and indeed intra cellular interactions of the nanoparticles are feasible. Despite the increase in public exposures due to their use in a number of consumer products, toxicological information and risk assessments of many nanoparticles have been slow to emerge. This is primarily due to scientific difficulties in evaluating the potential health risks of a variety of different nanoparticles.

1.4 Current Toxicological Knowledge.

Very little is known about the long term effects of exposure to different nanoparticles. However toxicological studies do exist for a variety of different types of nanoparticles (Carero *et al*, 2001; Cedervall *et al*, 2007; Donaldson *et al*, 2002; Donaldson *et al*, 2004; Duncan *et al*, 2005; Ghio *et al*, 1999; Kamat *et al* 2000; Lin *et al*, 2006; Monteiro-Riviere *et al*, 2006; Murphy *et al*, 1999; Oberdorster *et al* 2000; Pulskamp *et al*, 2007; Sayes *et al* 2005; Shvedova *et al*, 2005; Smart *et al*, 2006; Wang *et al*, 2007). Although some of these materials are considered to be biologically compatible in their bulk form, studies are showing that in the nano form they can induce adverse effects. This phenomenon is primarily due to the fact that reduction in size to the nano scale increases the surface area ratio of these particles increasing the potential for adverse interactions which are not possible in the larger form. Many mechanisms have been suggested as to how a nanoparticle induces a toxic effect. The different electronic properties of nanoparticles in comparison to their bulk form have been suggested as a potential contributing factor (Donaldson *et al*, 2002; Oberdorster *et al*, 2005). The

different surface chemistry of the nanoparticles (chemically active or inactive, hydrophobic or hydrophilic) (Cedervall *et al*, 2007; Nel *et al*, 2006) can also contribute. Recently the generation of Reactive Oxygen Species (ROS) has been identified as a potential marker for a toxic response of carbonaceous nanoparticles (Shvedova *et al*, 2005; Pulskamp *et al*, 2007). It is clear that both a full physio-chemical characterisation of these nanomaterials and an identification of the critical factors which affect a toxic response are required.

This thesis will focus on the cytotoxicity of SWCNT. Although the number of research groups looking specifically at SWCNT toxicity both *in vitro* and *in vivo* (Huczko *et al*, 2001; Kagan *et al*, 2006; Muller *et al*, 2006; Shvedova *et al*, 2005; Smart *et al*, 2006; Warheit *et al*, 2004) has increased dramatically over the last 5 years, there are conflicting reports in the literature regarding the toxicity profile and general biocompatibility of these materials. Due to the inconsistent toxicological profile of SWCNT which exists currently, this study will seek to address a number of factors which have been alluded to in literature as possible contributors. The study will employ both standard spectroscopic and microscopic techniques in conjunction with standard *in vitro* cytotoxicity protocols to verify the existence of these contributing factors and to assess their effects on the overall toxicological profile of SWCNT.

1.5 Thesis Outline.

In chapter 2 a brief account into the evolution of carbon nanotube fabrication methods focusing on the HiPco method will be described. Carbon nanotubes will be classified

according to their physical structure. The electronic properties of SWCNT will then be discussed. The aggregative nature of 'as produced' SWCNT and the role it has played in SWCNT research will be discussed. Finally a review of SWCNT composite systems will be discussed highlighting the range of different molecules capable of interacting with SWCNT.

Chapter 3 gives an introduction to nanotoxicology, in which the key properties of many engineered nanoparticles that may induce a toxic response will be discussed. The chapter then focuses on the mechanisms by which carbon based materials elicit toxicity. A review of the properties of SWCNT and the role they may play in the generation of toxicity is given. The chapter concludes with a review of SWCNT toxicity highlighting discrepancies in the current toxicological profile of SWCNT.

Chapter 4 will detail the experimental techniques employed throughout this study. A characterisation of pristine SWCNT both spectroscopically and microscopically will be described using the outlined experimental techniques. The origins of the observed spectral features will be discussed. Chapter 5 will use spectroscopic analysis to study the interactions of SWCNT upon their dispersion within a cell culture medium. Chapter 6 will employ both cytotoxicity and spectroscopic techniques to investigate the role the interactions discussed in chapter 5 play in SWCNT toxicity. Chapter 7 will again use cytotoxicity and spectroscopic techniques to evaluate SWCNT cytotoxicity. The validity of the cytotoxicity evaluation will then be assessed, for each cytotoxicity endpoint employed, by spectroscopic analysis. Chapter 8 will present a summary of the findings over the course of the research and detail some potential areas which warrant future study.

References

- Bianco, A., Kostarelos, K., Prato, M. "Applications of carbon nanotubes in drug delivery. *Current Opinion in Chemical Biology*", 2005, 9, 674-679.
- Carero ADP, Hoet PHM, Verschaeve L, Schoeters G, Nemery B. "Genotoxic effects of carbon black particles, diesel exhaust particles, and urban air particulates and their extracts on a human alveolar epithelial cell line (A549) and a human monocytic cell line (THP-1)" *Environmental and molecular Mutagenesis*, 2001, 37, 155-163.
- Cedervall T, Lynch I, Lindman S, Berggard T, Thulin E, Nilsson H, Dawson KA, Linse S. "Understanding the nanoparticle-protein corona using methods to quantify exchange rates and affinities of proteins for nanoparticles" *Proceedings of the national academy of sciences of the united states of America*, 104 (7): 2050-2055 FEB 13 2007.
- Donaldson K, Stone V, Tran CL, Kreyling W, Borm PJA. "Nanotoxicology", *Occupational Environmental Medicine*, 2004, 61, 727-728.
- Donaldson K, Tran CL. "Inflammation caused by particles and fibers", *Inhalation Toxicology*, 2002, 14, 5-27.
- Duncan R, Izzo L "Dendrimer biocompatibility and toxicity" *Advanced Drug Delivery Reviews*, 2005, 57, 2215-2237
- Dreher, K.L "Health and environmental impact of nanotechnology: toxicological assessment of manufactured nanoparticles". *Toxicological Sciences*, 2004, 77, 3-5.

Feynman R., “*There’s plenty of room at the bottom*”, Talk on December 26, 1959, annual meeting of the American Physical Society at the Californian Institute of Technology. Also published in “Miniaturisation” Horace D Gilbert, Reinhold Publishing Corporation, NY 10003.

Huczko, A., Lange, H., Calko, E., Grubek-Jaworska, H., Droszez, P. “Physiological testing of carbon nanotubes: are they asbestos-like?” *Fullerene Science and Technology*, 2001, 9, 251-254.

Ghio AJ, Carter JD, Dailey LA, Devlin RB, Samet JM. “Respiratory epithelial cells demonstrate lactoferrin receptors that increase after metal exposure”. *American journal of physiology-lung cellular and molecular physiology*, 1999, 276 (6): L933-L940.

Guzmán de Villoria, R., Miravete, A., Cuartero, J., Chiminelli, A., Tolosana, N. “Mechanical properties of SWNT/epoxy composites using two different curing cycles”. *Composites: Part B*, 2006, 37, 273-277.

Kagan VE, Tyurina YY, Tyurin VA, Konduru NV, Potapovich AI, Osipov AN, Kisin ER, Schwegler-Berry D, Mercer R, Castranova V, Shvedova AA “Direct and indirect effects of single walled carbon nanotubes on RAW 264.7 macrophages: Role of iron.” *Toxicology Letters*. 2006; 165 (1): 88-100.

Kamat JP, Devasagayam TPA, Priyadarsini KI, Mohan H. “Reactive oxygen species mediated membrane damage induced by fullerene derivatives and its possible biological implications”. *Toxicology*, 2000, 155; 55-61.

Lin W, Huang Y, Zhou XD, Ma Y. “In vitro toxicity of silica nanoparticles in human lung cancer cells” *Toxicology and Applied Pharmacology*, 2006, 217, 252–259.

Monteiro-Riviere NA, Inman AO. “Challenges for assessing carbon nanomaterial toxicity to the skin.” *Carbon*, 2006; 44: 1070-78.

Muller J, Huaux F, Lison D. “Respiratory toxicity of carbon nanotubes: How worried should we be?” *Carbon*, 2006; 44; 1048-1056.

Murphy SAM, BeruBe KA, Richards RJ. “Bioreactivity of carbon black and diesel exhaust particles to primary Clara and type II epithelial cell cultures” *Occupational and Environmental Medicine*, 1999, 56 (12): 813-819.

Nel A. “Air pollution-related illness: Effects of particles”, *Science*, 2005, 308, 804-806.

Oberdorster G, Oberdorster E, Oberdorster J. “Nanotoxicology: An emerging discipline evolving from studies of ultrafine particles”, *Environmental Health Perspectives*, 2005, 113, 823-839.

Oberdorster G. "Toxicology of ultrafine particles: in vivo studies". *Philosophical Transactions of the Royal Society of London Series – A – Mathematical Physical and Engineering Sciences*, 2000; 358 (1775): 2719-2739.

Pantarotto, D., Singh, R., McCarthy, D., Erhardt, M., Briand, J-P, Prato, M., Kostarelos, K., Bianco, A., "Functionalized carbon nanotubes for plasmid DNA gene delivery." *Angewandte Chemie International Edition*, 2004. 43, 5242-5246.

Paradise, M., Goswami, T. "Carbon nanotubes-Production and industrial applications." *Materials and Design*, 2006, (In press)

Pulskamp K, Diabate S, Krug HK. "Carbon nanotubes show no sign of acute toxicity but induce intracellular reactive oxygen species in dependence on contaminants." *Toxicology Letters*, 2007, 168, 58-74.

Sayes CM, Gobin AM, Ausman KD, Mendez J, West JL, Colvin VL. "Nano-C₆₀ cytotoxicity is due to lipid peroxidation" *Biomaterials*, 2005, 26, 7587-7595.

Shvedova AA, Kisin ER, Mercer R, Murray AR, Johnson VJ, Potapovich AI, Tyurina YY, Gorelik O, Arepalli S, Schwegler-Berry D, Hubbs AF, Antonini J, Evans DE, Ku BK, Ramsey D, Maynard A, Kagan VE, Castranova V, Baron P. "Unusual inflammatory and fibrogenic pulmonary responses to single-walled carbon nanotubes in mice", *American Journal of Physiology*, 2005, 289, L698-L708.

Smart SK, Cassady AI, Lu GQ, Martin DJ. “The biocompatibility of carbon nanotubes.” *Carbon*, 2006, 44, 1034-1047.

Singh, K.V., Pandey, R.R., Wang, X., Lake, R., Ozkan, C.S., Wang, K., Ozkan, M.. “Covalent functionalization of single walled carbon nanotubes with peptide nucleic acid: Nanocomponents for molecular level electronics.” *Carbon*, 2006, 44, 1730-1739.

Taniguchi N. Proceedings. ICPE Tokyo (1974)

The Royal Society & The Royal Academy of Engineering (2004). Nanoscience and nanotechnologies: opportunities and uncertainties.

Thomas, K., Sayre, P. “Research strategies for safety evaluation of nanomaterials, part I: evaluating the human health implications of exposure to nanoscale materials”. *Toxicological Sciences*, 2005, 87, 316-321.

Wang JJ, Sanderson BJS, Wang H. “Cyto- and genotoxicity of ultrafine TiO₂ particles in cultured human lymphoblastoid cells” *Mutation Research*, 2007, 628, 99–106.

Warheit, D.B., Laurence, B.R., Reed, K.L., Roach, D.H., Reynolds, G.A., Webb, T.R. “Comparative pulmonary toxicity assessment of single-wall carbon nanotubes in rats.” *Toxicological Sciences* 2004, 77, 117-125.

Chapter 2

“Single Walled Carbon Nanotubes”

2.1 Introduction to single walled carbon nanotubes.

Carbon nanotubes (CNT) were first observed by Sumio Iijima (1991) and have sparked an abundance of research since their discovery. They are unique, one-dimensional macromolecules, comprising entirely of carbon. They consist of extended tubes of rolled graphene sheets with an axial symmetry and a diameter in the nanometre range and can grow up to microns in length (Saito, 1999). Two types of CNT can be differentiated by their structures (Figure 2.1); they can be single walled (Iijima *et al*, 1993) which are hollow tubes of carbon capped at either end with a hemi-fullerene, or multiwalled, consisting of concentric layers of graphene sheets rolled up, where smaller diameter tubes are encased in larger diameter tubes (Ebbesen *et al*, 1993).

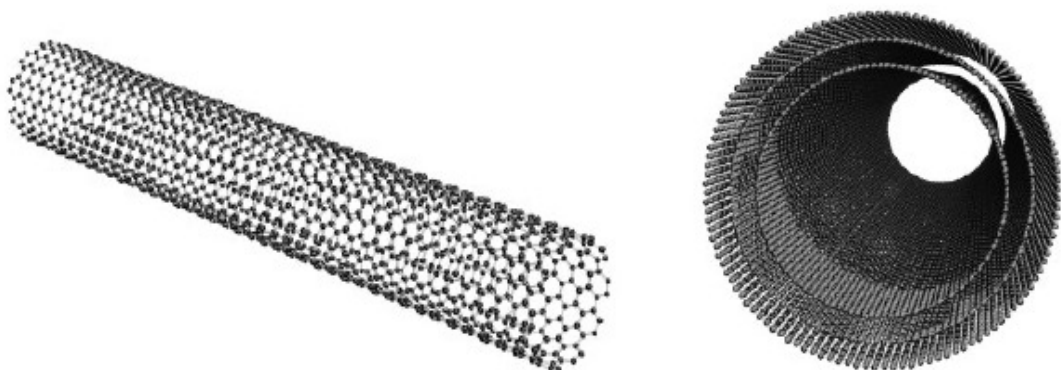


Figure 2.1 Left; schematic of a single-walled carbon nanotube (SWCNT), Right; schematic of a multi-walled carbon nanotube (MWCNT) (Royal Society, 2004).

Since their discovery, several production techniques have evolved. SWCNT were first synthesised primarily in an arc-discharge chamber using metal catalysts, such as Fe or Co during the synthesis process (Harris, 1999). The arc discharge chamber (Ebbesen *et al.*, 1992) in essence consists of two graphite rods, which are separated by a distance typically of the order of millimetres. A current is then passed through the rods causing the formation of an arc which vaporises the carbon into a hot plasma and upon cooling the carbon nanotubes form. This method can produce both multi and single walled tubes and has a typical yield of approximately 30% nanotubes. The nanotubes produced by this method tend to be short and of varying size. Initial experiments showed varying diameter ranges and lengths with low yield and purity (Bethune *et al.*, 1993; Iijama and Ichihashi, 1993, Saito *et al.*, 1998). The impurities comprised of amorphous carbon and catalytic particles. Through experimentation, Journet *et al.*, (1997) showed that high yields of SWCNT could be achieved using the arc technique. Yields of 70 % SWCNT, average diameter of 1.4 nm and lengths of many micrometers were obtained in gram quantities.

A breakthrough in the synthesis of SWCNT, making significant amounts of material available for experimental study, was the laser vaporisation method developed by Rice University in 1996 (Thess *et al.*, 1996). High yields with >70 % SWCNT and an average diameter of 1.4 nm were reported. The remaining 30 % consists of amorphous carbon and catalytic particles. The laser vaporisation technique was surpassed in 1999 by high pressure decomposition of carbon monoxide, commonly referred to as the HiPco method, which can produce >90 % pure SWCNT with an average diameter of 1.1 nm, the only impurity being iron particles (Nikolaev *et al.*, 1999). This fabrication process will be discussed in detail in the next section as HiPco SWCNT were used

throughout this study. However mass production with a yield of 100 % SWCNT is yet to be achieved. Also, irrespective of the production technique, SWCNT are found to form hexagonal-packed bundles during the growth process with the properties of the bundle in general being inferior to those of individual SWCNT (Zhang, 2004). As a result of their tendency to aggregate into these bundles, substantial effort has been put into the dispersion and separation of bulk samples.

2.2 High Pressure Carbon Monoxide Method (HiPco).

As HiPco Carbon Nanotubes were predominantly used in this study, the production method will be discussed in depth (Nikolaev *et al*, 1999). It is a continuous gas flow synthetic method in which SWCNT are grown and separated in a furnace with a continuous flowing gaseous feedstock mixture (Figure 2.2). This technique uses a mixture of carbon monoxide (CO) and iron pentacarbonyl (Fe(CO)₅). Carbon monoxide is used as a carbon feed stock gas and the Fe(CO)₅ as an iron containing catalyst precursor. The yield and diameter distribution can vary substantially and are highly dependant on fabrication conditions, particularly heat and pressure. Inside the furnace, thermal decomposition of the Fe(CO)₅ produces iron clusters, which then serve as sites upon which the SWCNT nucleate and grow. The solid carbon is produced by CO disproportionation through a reaction known as the “Boudouard reaction” (Nikolaev *et al*, 1999),



This reaction occurs catalytically on the surface of the iron particles. A model has been

proposed for the gas phase nanotube growth in which the metal clusters form first. The metal clusters form by aggregation of iron atoms from the decomposition of $\text{Fe}(\text{CO})_5$, then grow by collision with other metal particles and eventually reach the size of a SWCNT diameter (0.7-1.4nm), which corresponds to approximately 50-200 iron atoms.

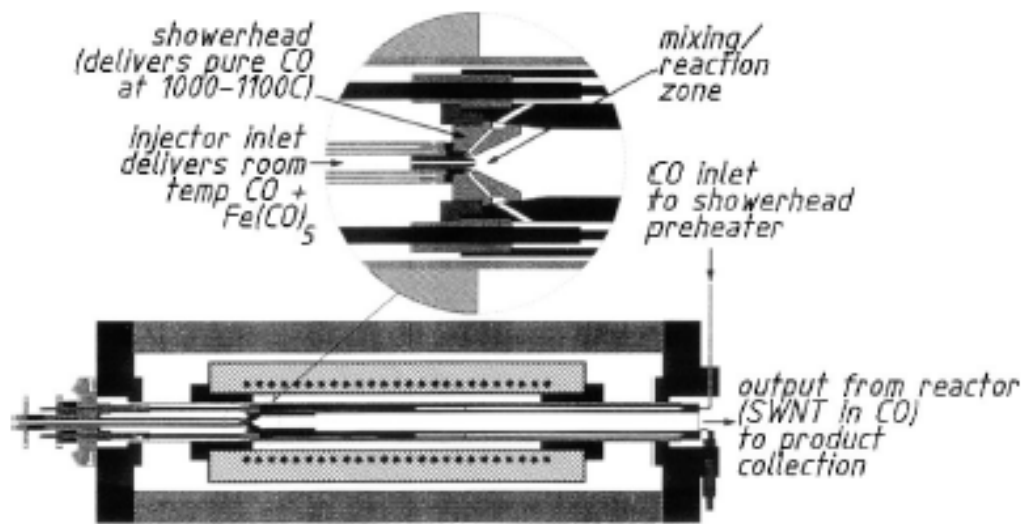


Figure 2.2 Schematic of water cooled CO flow tube reactor (Nikolaev *et al*, 1999).

When the iron atoms cluster to the required size the CO can disproportionate on the surface of the clusters via the “Boudouard Reaction” to yield solid carbon. The SWCNT will nucleate and grow from them by the ‘Yarmulke’ mechanism (Dai *et al*, 1996). That is, a hemi fullerene cap forms on the partially carbon-coated particle, lifts off, and additional carbon atoms are continuously added to the edge of the cap, forming a hollow tube of constant diameter which grows away from the particle.

The size and diameter distribution of the SWCNT can be roughly selected by controlling the pressure of the CO in which the reaction occurs (figure 2.3). A study carried out by P. Nikolaev *et al* (1999) showed that the highest yield and narrowest tubes are produced at the highest accessible temperature and pressure, 1200°C and

10atm, (Nikolaev *et al*, 1999). Furthermore they showed that operating temperature in conjunction with operating pressure had a considerable effect on the production rate of tubes and ultimately on the percentage yield of SWCNT (see tables 2.1 and 2.2).

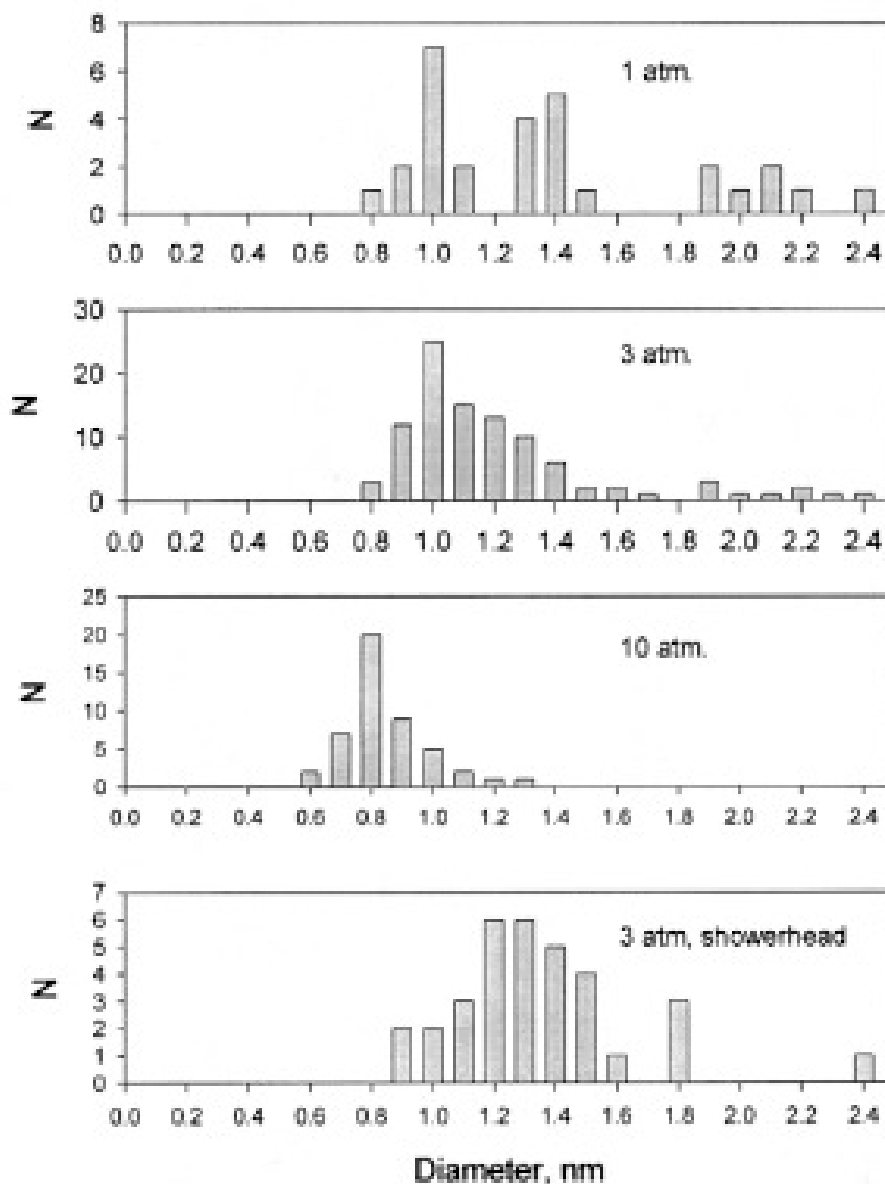


Figure 2.3 Diameter distributions of SWCNT produced at 1200°C at various CO pressures (Nikolaev *et al*, 1999).

Table 2.1 Production rates and yield for varying temperatures at a CO pressure of 10atm
(Nikolaev *et al*, 1999).

| Temperature (°C) | Production Rate (mg/h) | SWCNT Yield (mole%) | SWCNT (wt.%) |
|------------------|---------------------------|------------------------|--------------|
| 850 | 0.68 | 73 | 37 |
| 1000 | 1.00 | 71 | 34 |
| 1200 | 1.24 | 79 | 44 |

Table 2.2 Production rates and yields for varying CO pressures at a temperature of 1200°C
(Nikolaev *et al*, 1999).

| Pressure (atm) | Production Rate (mg/h) | SWCNT Yield (mole%) | SWCNT (wt.%) |
|----------------|---------------------------|------------------------|--------------|
| 1 | 1.16 | 61 | 25 |
| 3 | 1.38 | 67 | 30 |
| 10 | 1.24 | 79 | 44 |

Another important issue is the mechanism by which nanotube growth ceases. The metal catalyst particles in the product material are 3–5 nm in diameter, substantially larger than SWCNT diameters of ~ 1 nm, suggesting that the particles continue to grow even after nucleating a tube. The additional aggregating Fe atoms could come from several sources: direct gas-phase collisions with other Fe atoms, Fe clusters, or Fe(CO)₅ molecules (by adsorption/decomposition), or by adsorption of Fe atoms, clusters or adsorption/decomposition of Fe(CO)₅ molecules onto the growing nanotube followed by iron atom diffusion to the particle at the end. As a catalytic particle grows larger, more and more catalytically active surface area is created, and eventually a graphitic

shell or other structures not associated with the growing nanotube will begin to form on the particle. Eventually the particle will become covered with carbon, preventing the diffusion of additional CO to the particle's surface and terminating further nanotube growth. Another potential contributing factor to cessation of growth of a nanotube is evaporation of its attached cluster. As discussed above, small iron clusters (fewer than 10 atoms) will tend to evaporate quickly at temperatures where SWCNT growth is rapid. The cessation of growth of the nucleated nanotubes would thus derive from a combination of these two effects: some nanotubes would stop growing when their attached catalyst particle evaporates or grows too small, some would stop when their catalyst cluster grows too large.

2.3 Physical properties of carbon nanotubes.

Carbon nanotubes, as mentioned earlier, are cylindrical graphene sheets of sp^2 -bonded carbon atoms. These nanotubes are single molecules measuring a few nanometres in diameter and several microns in length. Carbon nanotubes come in a variety of diameters and length, depending on fabrication technique and growth process the length of the tube can be from approximately 100 nanometres to 1mm while the diameters can vary from less than 1 to 100 nanometres. Furthermore they can be metallic or semiconducting. The following sections will give a brief overview of their structural and electronic properties.

2.3.1 Structure and types of SWCNT.

As stated there are two types of carbon nanotubes Single walled carbon nanotubes (SWCNT) which consist of a single graphene sheet seamlessly wrapped into a

cylindrical tube and Multiwalled carbon nanotubes (MWCNT) comprising of an array of such nanotubes that are concentrically nested like rings of a tree trunk (Iijima, 1991). Despite the structural similarity to a single sheet of graphite which is a zero-bandgap semiconductor, SWCNT may be either metallic or semi conducting, depending on how the graphene sheet is rolled to form the nanotube cylinder (Dreselhaus *et al*, 1996).

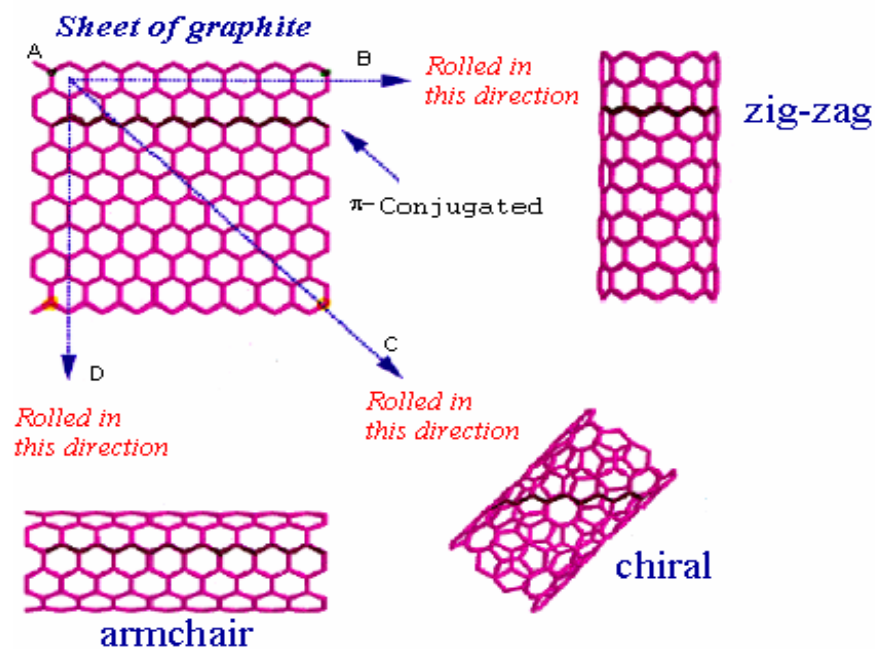


Figure 2.4 Schematic diagrams showing the different ways of rolling a sheet of graphite to make various types of single walled carbon nanotubes.

Figure 2.4 shows three ways in which the graphene sheet can be rolled, in order to form a SWCNT. It can be seen in the graphene sheet (Figure 2.4) that the π - electron conjugation lies horizontally in a zigzag across the nanotube as highlighted by the darkened line. If the tube is formed by rolling the graphene sheet along the line AB, then a tube is formed with this “zigzag” around its circumference and a confined radial π - conjugation. If however the sheet is rolled along the direction AD then we obtain an “armchair” nanotube, which is metallic in nature due to its longitudinal π - conjugation

and is often referred to as a 1-D conductor. Finally the last type of tube which can be formed is a “chiral” tube when the sheet is rolled along the line AC (where C is an arbitrary direction between B and D); this type of tube is often semi-conducting due to its π - electron configuration.

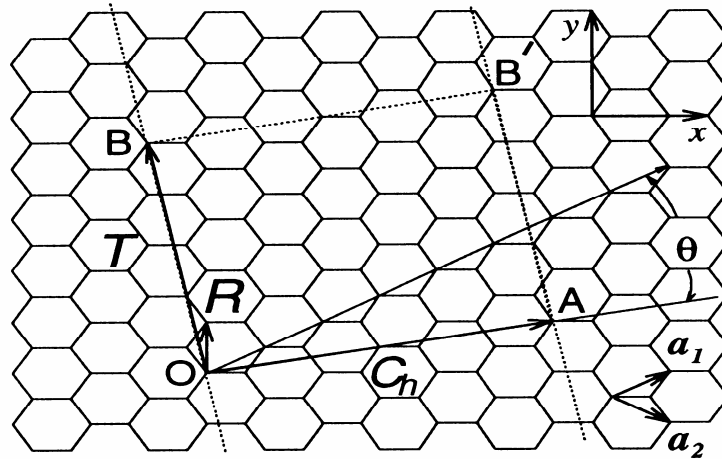


Figure 2.5 Unrolled honeycomb lattice of a nanotube. When the sites O and A coincide as well as B and B', a nanotube can be constructed. The rectangle OABB defines the unit cell for the nanotube. The vector R denotes a symmetry vector (Saito *et al.*, 1998).

The basic structure of a SWCNT is specified by a single vector called the chiral vector (C_h). In figure 2.5, this vector is defined as OA and this is the section of the nanotube perpendicular to the nanotube axis, which when rolled up is the circumference of the tube. Figure 2.5 shows the unrolled lattice of the nanotube, and in this case, the direction of the nanotube axis is given by the vector OB. The lattice can then be rolled to form a cylinder by lining up the points so that O is on top of A and B is on top of B. The chiral vector C_h is then determined by the real space lattice vectors a_1 and a_2 , which are also defined in figure 2.5 and this leads to the following equation:

$$C_h = na_1 + ma_2 \equiv (n, m) \quad \text{Equation 2.2}$$

The main symmetry classification of a tube is defined as being either achiral or chiral.

An achiral tube is defined as one where the mirror image of the tube is identical to the original one. A chiral tube is then defined as a tube where the mirror image cannot be superposed onto the original tube and they show spiral symmetry. There are two types of achiral tubes, which are named armchair and zigzag nanotubes. These two types can be seen in figure 2.3 where (a) is an armchair tube and (b) is a zigzag tube. These two tubes get their names from the shape of the cross-sectional ring at the edge of the nanotubes.

An armchair nanotube is then defined as the case where $n = m$ in equation 1, a zigzag corresponds to the case where $m = 0$. All other chiral vectors correspond to the production of a chiral nanotube but this is subject to the constraint that m is less than or equal to n . While the structure and type of SWCNT, be they armchair, zigzag or chiral, are likely to be of lesser importance in terms of toxicity testing, it is these differing structural and electronic properties that have made them attractive for an array of applications, many of them being “Bio-based”, highlighting the need for the development of reliable screening techniques for the bio compatibility of these truly remarkable materials.

2.3.2 Electronic properties of SWCNT.

Rolled graphene (*i.e.* a nanotube) can be described as a “semi-metal” as it is metallic in some directions and semi-conducting in others. The condition for metallic nanotubes is that $(2n + m)$ or equivalently $(n - m)$ is a multiple of three. In particular the armchair tube denoted by $(n = m)$ is always metallic and the zigzag tubes $(n, 0)$ are only metallic when n is a multiple of three. Figure 2.6 shows carbon nanotubes which are metallic and semiconducting, denoted by open and solid circles respectively. It also shows that

approximately one third of carbon nanotubes are metallic and the remaining two thirds are semiconducting.

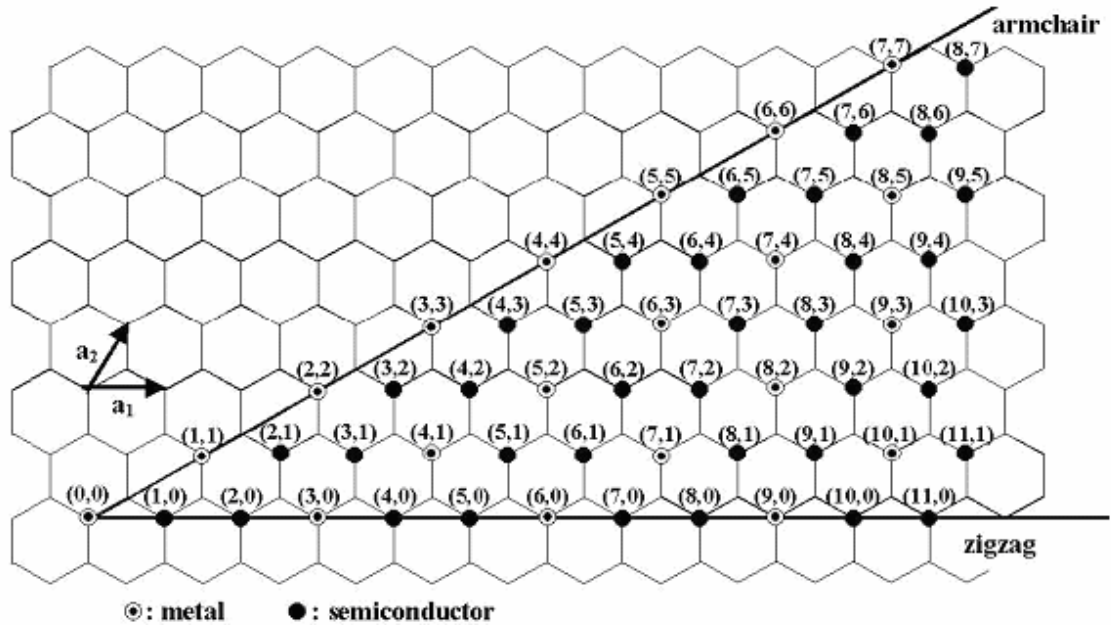


Figure 2.6 Schematic Diagram showing Carbon nanotubes (n, m) that are metallic and semiconducting, and are denoted by open and solid circles respectively on the map of chiral vectors (n, m) (Dresselhaus *et al.*, 2001).

Smalley *et al.*, have experimentally shown the electronic structure of isolated carbon nanotubes. Figure 2.7 depicts an I-V curve obtained by STS (Scanning tunnelling spectroscopy) of isolated chiral carbon nanotubes. Curves 1-4 have well-defined energy gaps between 0.55 -0.65eV. These gap values coincide with theoretical energy gap values of the order of 0.5eV for semiconducting tubes. Curves 5-7 have significantly larger energy gaps of 1.7-1.9eV, which coincide with theoretical gap values for metallic tubes.

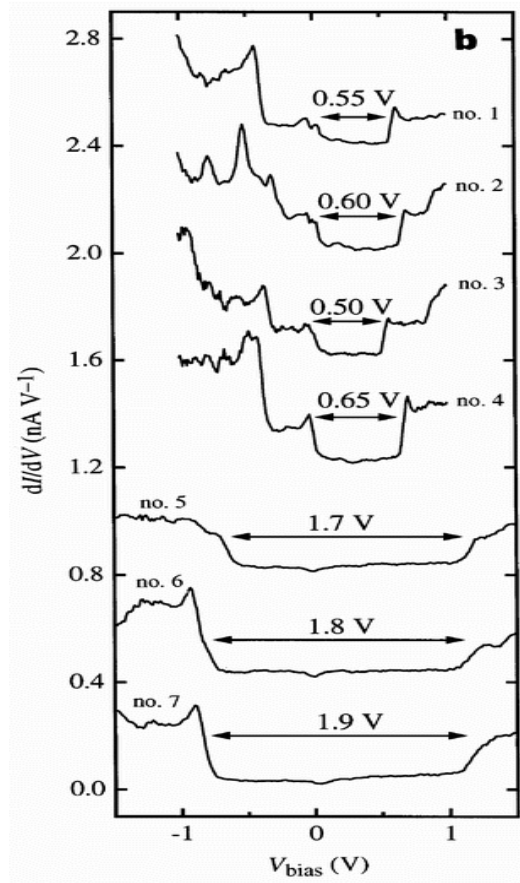


Figure 2.7, I-V curves of isolated carbon nanotubes (Smalley *et al*, 1998).

Each carbon nanotube has its own signature band structure, and hence its own density of states. The energy gap is inversely proportional to the diameter of the nanotube (Wilder *et al*, 1998). This can be understood as the curvature of the lattice induces a strain in the graphene sheet manifesting itself in the bandgap. The bandgap reduces with increasing tube diameter and as the diameter goes to infinity, the bandgap goes to zero.

The experimentally determined bandgaps presented by Smalley *et al*, (1998) are based on isolated SWCNT, that is, they are not in bundles. As well as unwanted amorphous carbon, one of the main consequences of production methods to date is that tubes form ropes or bundles, which are difficult to dissociate (Nikolaev *et al*, 1999). Synthesis

techniques and related problems have been discussed earlier. All electronic properties that are discussed in this section are in relation to structurally sound isolated nanotubes. In reality this can be difficult to achieve in the laboratory.

2.4 SWCNT interactions.

As stated, all current fabrication techniques result in an “impure” sample, the type of impurities present being dependant on the fabrication process. Regardless of the purity levels of produced samples all fabrication techniques produce an inhomogeneous sample. In any given batch there are a variety of types of SWCNT, there are different diameters and lengths, the SWCNT can be metallic or semiconducting and they have a tendency to aggregate into large bundles or ropes of tubes of similar diameter (figure 2.8).

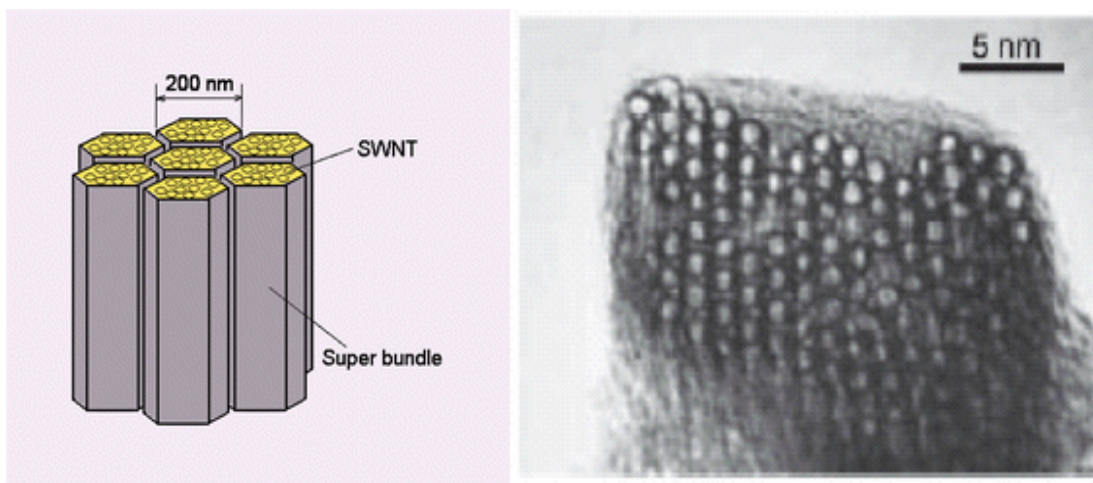


Figure 2.8 Schematic of a Nanotube Rope (left) High resolution TEM of SWCNT bundled nanotubes produced by the arc discharge technique (right) (Thess *et al.*, 1996).

The tube-tube interactions within SWCNT bundles are weak, similar to the coupling between adjacent graphene planes in 3D crystalline graphite or the inter-ball coupling

found in solid fullerene C₆₀. This weak inter-tube coupling is dominated by the van der Waals interaction, but contains a nonzero covalent component that has been shown theoretically and experimentally to have significant influence on the vibrational and electronic states for carbon nanotubes. Most of the properties discussed in the previous sections are attributed to an individual nanotube and are not applicable to bulk samples due to the range of diameters, types and bundles of nanotubes which are currently available. As a result of this, substantial effort has been put into the development of methods to disperse and separate individual tubes from bulk samples. Composite systems and various other techniques have been comprehensively studied, with the result that the mechanisms of the interaction of SWCNT with a battery of different molecules is extensively documented (Bandyopadhyaya *et al*, 2002; Chambers *et al*, 2003; Chen *et al*, 2001; Hedderman *et al*, 2006; Kawamoto *et al*, 2006; Keogh *et al*, 2005; Moulten *et al*, 2005; Roman *et al*, 2006; Salvador-Morales *et al*, 2006; Yu *et al*, 2003). The following subsections will give a brief summary of the interactions of SWCNT with various classifications of molecules and where applicable their relevance to this research will be discussed.

2.4.1 Surfactants and solvents.

A variety of different techniques is now routinely used for the dispersion of bulk SWCNT samples. These include acid washing (Lu *et al*, 1996), sonication (Lu *et al*, 1996) and centrifuging and also the use of a variety of organic solvents (Gregan *et al*, 2006). To date, the best solvents reported for generating SWCNT dispersions are amides, particularly, N-dimethylformamide (DMF), 1,2 dichloroethane (DCE) and N-methylpyrrolidone (NMP) (Boul *et al*, 1999; Gregan *et al*, 2006; Lui *et al*, 1999; Giordani *et al*, 2006). However, the dispersions aggregate on a time-scale of days. With

the aid of surfactants, carbon nanotubes have been solubilised in water. Surfactants, such as SDS, can deposit on the surface of nanotubes (Lui *et al*, 1999) and help form stable colloidal dispersions of SWCNT (Krstic *et al*, 1998; Duesberg *et al*, 1998). The surfactant acts as a coupling agent and may introduce a steric repulsive force between the carbon nanotubes. The repulsive force overcomes the van der Waals attractive force between the carbon surfaces, *i.e.* the SWCNT bundles. However, removing the surfactant afterward is problematic although the intrinsic structure of the nanotube is not destroyed.

2.4.2 Synthetic molecules.

The use of conjugated polymers (Curran *et al*, 1998; Keogh *et al*, 2005) to isolate carbon nanotubes from bulk samples systems has been shown to hold good promise. However one inherent problem in using synthetic polymers is that they rely heavily on the use of harsh organic solvents (to initially solubilise the polymer) severely limiting biological applications. Notably, the interaction of the polymer with the nanotubes was characterised by a quenching of the polymer fluorescence, a phenomenon which becomes relevant to the analysis of the dispersion of nanotubes in the cell growth medium in this study.

A similar study (Hedderman *et al*, 2006) using synthetic dye molecules to structurally select different types of SWCNT (metallic or semiconducting) was also shown to uniformly disperse and separate individual SWCNT, based on their structure, from bulk samples. However, the studied system again utilised harsh organic solvents limiting biological applications. Again the interaction was characterised according to quenching of the molecular fluorescence and indeed numerous studies exist in the literature

studying the interactions of SWCNT with various different dye molecules and other fluorescent species, showing a reduction in the associated absorption or emission upon interaction with SWCNT (Coleman *et al*, 2005; Hedderman *et al*, 2006; Keogh *et al*, 2004). These studies are of great relevance in this research, as in cytotoxicity studies multiple endpoints are generally employed to evaluate toxicity, such as cell counts, cell morphology and cell apoptosis, the most common of which is the use of colorimetric indicator dyes. These dyes are added to the cell line under test following exposure to the suspected toxicant, and their binding, conversion or uptake (process is assay dependant) by the exposed cells is detected spectroscopically either by absorption or emission (detection process is assay dependant) and is then compared to unexposed controls. This raises obvious questions, given that SWCNT are known to interact with dye molecules (Hedderman *et al*, 2006), regarding to what degree SWCNT will interact with these dyes and more significantly will these interactions result in a false toxicity profile being evaluated. This will be explored in chapter 7.

2.4.3 Biological Molecules.

Composite systems are not solely limited to synthetic matrices and extensive studies have also been carried out employing more natural matrices such as proteins (Moulten *et al*, 2005; Salvador-Morales *et al*, 2006), enzymes (Yu *et al*, 2003), amino acids (Roman *et al*, 2006) and DNA (Kawamoto *et al*, 2006). Standard *in vitro* cytotoxicity protocol relies on the dispersion of a suspected toxicant within a cell culture medium followed by its exposure to a cell line under test for a set time period and cytotoxicity is then evaluated by comparison to unexposed controls. Cell culture medium is a complex mixture of many different components (see appendix 1) vital for cell growth, many of which SWCNT are known to interact to varying degrees. The potential for the SWCNT

to interact with these various components when dispersed in the medium will be discussed in chapter 5. It has been shown in the literature that functionalisation of SWCNT actually reduces observed toxicity; therefore it is plausible that if SWCNT interact with the various components of the medium these interactions may influence the recorded cytotoxic data. This will be discussed in chapter 6.

2.4.4 Saccharide Systems.

Saccharide systems have also been extensively studied (Bandyopadhyaya *et al*, 2002; Chambers *et al*, 2003; Chen *et al*, 2001). In an earlier study (Casey *et al*, 2005; see appendix 2) it was shown that using a composite system with starch, stable aqueous suspensions of SWCNT could be created. Such systems offer considerable advantages over polymer based composites due to their biocompatibility and noncovalent coupling which can potentially preserve the unique properties of the tubes. The mechanism of interaction for such systems has been proposed to be dominated by hydrophobic and hydrophilic interactions along the surface of the tube. However efforts to characterise and rationalise such noncovalent interactions between the sugar-based materials and the carbon nanotubes were not evident in the literature. In the aforementioned study (Casey *et al*, 2005) a composite system was formed using HiPco SWCNT and starch (extracted from rice). This composite was characterised using a range of spectroscopic techniques, which showed clear evidence of an intermolecular interaction between the SWCNT and starch. Although starch, a polymer of glucose, is not present in cell growth media its monomer glucose is present, and hence the possibility of an interaction is a realistic one upon their dispersion of SWCNT in the medium resulting in interferences in the toxicological evaluation of the SWCNT.

As a direct result of the drive to use composite systems to develop SWCNT technology, the process of the interaction between SWCNT with a battery of different molecules and solvents has been extensively documented (Bandyopadhyaya *et al*, 2002; Chambers *et al*, 2003; Chen *et al*, 2001;Greegan *et al*, 2005; Hedderman *et al*, 2006; Kawamoto *et al*, 2006; Keogh *et al*, 2004; Moulten *et al*, 2005; Roman *et al*, 2006; Salvador-Morales *et al*, 2006; Yu *et al*, 2003) the mechanism of these interactions is well understood as a reversible physisorption process and known to be dominated by van der Waals type interactions. The knowledge gained from these extensive studies will be utilised to assess a variety of systems and their potential to contribute to the toxicity evaluation of SWCNT *in vitro*.

2.5 Chapter Summary.

This chapter has given a brief account of the evolution of carbon nanotube fabrication methods focusing on the HiPco method. Carbon nanotubes were classified according to their physical structure, be they multi or single walled. SWCNT were then further classified structurally, zigzag, armchair or chiral. The electronic properties of SWCNT were then discussed showing that SWCNT can be metallic or semi-conducting. The idealised picture of isolated SWCNT is deceptive, however, and the inhomogeneous, impure, aggregative nature of as produced SWCNT was highlighted. A variety of composite systems which are reported in literature were discussed highlighting the range of different molecules capable of interaction with SWCNT. The chapter has raised some questions that will be addressed throughout this thesis, namely: upon dispersion of SWCNT in cell culture medium what interactions occur (chapter 5), what effects can these interactions have on the quantitative evaluation of SWCNT

cytotoxicity (chapter 6), how do SWCNT effect common cytotoxic assay based endpoints (chapter 7) and what implications does the combination of the effects have for future toxicity evaluations of nanoparticles. The next chapter will give an overview of nanotoxicology, highlighting some of the intrinsic properties of nanomaterials which may elicit adverse health effects. Finally review of the toxicity of carbonaceous nanoparticles will be given focusing on SWCNT noting any observed inconsistencies.

References

- Bandyopadhyaya R, Nativ-Roth E, Regev O and Yerushalmi-Rozen R. "Stabilization of individual carbon nanotubes in aqueous solutions" *Nanoletters*. 2002; 2: 25-28.
- Bethune, D.S., Kiang, C.H., de Vries, M.S., Gorman, G., Savoy, R., Vazquez, J., Beyers, R. "Cobalt-catalysed growth of carbon nanotubes with single-atomic-layer walls", *Nature*, 1993; 363, 605-607.
- Boul, P.J.; Liu, J.; Mickelson, E.T.; Huffman. C.B.; Ericson, L.M.; Chiang, I.W.; Smith, K.A.; Colbert, D.T.; Hauge, R.H.; Margrave, J.L.; Smalley, R.E. "Reversible sidewall functionalization of buckytubes" *Chemical Physics Letters*. 1999. 310, 367-372.
- Bronikowski M.J., Willis P.A., Colbert D.T., Smith K.A., Smalley R.E. "Gas-phase production of carbon single-walled nanotubes from carbon monoxide via the HiPco process: A parametric study". *Journal of Vacuum Science Technology. A*, 2001, 19, 1800-1805.
- Chambers G, Carroll C, Farrell GF, Dalton AB, McNamara M, in het Panhuis M, *et al.* Characterization of the interaction of gamma cyclodextrins with single walled carbon nanotubes. *NanoLetters*. 2003; 3 (6): 843-6.
- Chen J, Dyer MJ, and Yu MF. "Cyclodextrin-mediated soft cutting of single-walled carbon nanotubes" *Journal of American Chemical Society*, 2001; 123, 6201

Curran SA, Ajayan PM, Blau WJ, Carroll DL, Coleman JN, Dalton AB, *et al.* A composite from poly(m-phenylenevinylene-co-2,5-dioctoxy-p-phenylenevinylene) and carbon nanotubes: A novel material for molecular optoelectronics. *Advanced Materials* 1998; 10(14):1091-3.

Dai, HJ, Rinzler A, Thess, A, Nikolaev, P, Colbert, DT, Smalley, RE. "Single-Walled Carbon Nanotubes Produced by Metal-Catalyzed Disproportionation of Carbon Monoxide", *Chemical Physics Letters*, 1996, 260, 471.

Dresselhaus, M.S., Dresselhaus, G., Eklund, P.C. *Science of Fullerenes and Carbon Nanotubes*, 1996, Academic Press, New York.

Dresselhaus, M.S., Dresselhaus, G., Avouris, Ph., (2001), "Carbon nanotubes: Synthesis, Structure, Properties and Applications", Springer-Verlag, Berlin Heidelberg.

Duesberg, G., Blau, W., Byrne, H.J., Muster, J., Burghard, M., Roth, S. "Chromatography of carbon nanotubes", *Synthetic Metals*, 1999, 103, 2484-2485.

Ebbesen TW, Ajayan PM. "Large scale synthesis of carbon nanotubes." *Nature*, 1992; 358, 220-222.

Ebbesen, T.W., Hiura, H., Fujita, J., Ochiai, Y., Matsui, S., Tanigaki, K. "Patterns in the bulk growth of carbon nanotubes", *Chemical Physics Letters*, 1993, 209, 83-90.

Gregan E, Keogh SM, Hedderman T, Chambers G, Byrne HJ. "Use of Raman Spectroscopy in the investigation of debundling of single walled carbon nanotubes." *SPIE Conference Proceedings*, 2005, Abstract No. 5826A-7.

Harris, P.J. "Carbon nanotubes and related structures." Cambridge University Press, Cambridge, 1993.

Iijima S. "Helical microtubules of graphitic carbon" *Nature* 1991, 354, 56-58.

Iijima, S., Ichihashi, T. "Single shell nanotubes of 1-nm diameter", *Nature*, 1993; 363, 603-605.

Journet, C., Maser, W.K., Bernier, P., Loiseau, A., Lamy de la Chapelle, M., Lefrant, S., Deniard, P., Lee, R., Fisher, J.E. "Large-scale production of single-walled carbon nanotubes by the electric-arc technique", *Nature*, 1997, 388, 756-758.

Kawamoto H, Uchida T, Kojima K, Tachibana M. Raman study of DNA- wrapped single walled carbon nanotube hybrids under various humidity conditions. *Chemical Physics Letters*, 2006; 431: 118-120.

Keogh, S.M., Hedderman, T.G., Greegan, E., Chambers, G., Byrne, H.J. "Spectroscopic Analysis of Single-Walled Carbon Nanotubes and Semiconjugated Polymer Composites", *Journal of Physical Chemistry B*, 2004, 108, 6233 -6241.

Krstic V, Duesberg GS, Muster J, Burghard M, Roth S “Langmuir-Blodgett films of matrix-diluted single-walled carbon nanotubes” *Chemistry of Materials*, 1998, 10, 2338-2340.

Kroto, H.W., Heath, J.R., O'Brien, S.C., Curl, R.F., Smalley, R.E. “C₆₀: Buckminsterfullerene”, *Nature*, 1985, 318, 162-163.

Lu, K.L.; Lago, R.M.; Chen, Y.K.; Green, M.L.H.; Harris, P.J.F.; Tsang, S.C. “Mechanical damage of carbon nanotubes by ultrasound” *Carbon*, 1996, 34, 814.

Liu, J.; Casavant, M.J.; Cox, M.; Walters, D.A.; Boul, P.; Lu, W.; Rimberg, A. J.; Smith, K.A.; Colbert, D.T.; Smalley, R.E. “Controlled deposition of individual single-walled carbon nanotubes on chemically functionalized templates” *Chemical Physics Letters*. 1999, 303, 125-129.

Moulton SE, Minett AI, Murphy R, Ryan KP, McCarthy D, Coleman JN, *et al.* Biomolecules as selective dispersants for carbon nanotubes. *Carbon*, 2005; 43: 1879-84.

Nikolaev, P., Bronikowski, M.J., Bradely, R.K., Rohmund, F., Colbert, D.T., Smith, K.A., Smalley, R.E., (1999), “Gas-phase catalytic growth of single walled carbon nanotubes from carbon monoxide”. *Chemical Physics Letters*. 1999, 313, 91-97.

Saito, R., Dresselhaus, G., Dresselhaus, M.S. “*Physical properties of carbon nanotubes.*” Imperial College Press, London. 1998.

Salvador-Morales C, Flahaut E, Sim E, Sloan J, Green MLH, Sim RB. Complement activation and protein adsorption by carbon nanotubes. *Molecular Immunology*. 2006; 43: 193-201.

Smalley, R.E., (1992), "Self assembly of fullerenes", *Accounts of Chemical Research* 25. 3: 98 - 105.

The Royal Society & The Royal Academy of Engineering. Nanoscience and nanotechnologies: opportunities and uncertainties, 2004.

Thess, A.; Lee, R.; Nikolaev, P.; Dai, H.; Petit, P.; Robert, J.; Xu, C.; Lee, Y.H.; Kim, S.G.; Rinzler, A.G.; Colbert, D.T.; Scuseria, G.E.; Tomanek, D.; Fisher, J.E.; Smalley, R.E, "Crystalline Bundles of Metallic Carbon Nanotubes", *Science*, 1996, 273, 483-487.

Wildoer, JWG, Venema, LC, Rinzler, AG, Smalley, RE, Dekker, C. "Electronic structure of atomically resolved carbon nanotubes". *Nature*, 1998, 391, 59-61.

Yu X, Chattopadhyay D, Galeska I, Papadimitrakopoulos F, Rusling JF. Peroxidase activity of enzymes bound to the ends of single-wall carbon nanotube forest electrodes. *Electrochemistry Communications* 2003; 5:408-11.

Zhang XH, Sun DY, Liu ZF, Gong XG. "Structure and phase transitions of single-wall carbon nanotube bundles under hydrostatic pressure". *Physical Review B*. 2004, 70 (3): Art. No. 035422.

Chapter 3

“Nanotoxicology”

3.1 Introduction.

This chapter will give a brief introduction to the toxicity testing of nanoparticles in general, focusing on their intrinsic properties which may result in harmful effects. This will be followed by an overview of the toxicity of carbon based materials highlighting the differences in toxicity based on the structural state of the carbon. A summary of the intrinsic properties of SWCNT, physical and chemical, will be given, highlighting the potential role each property may play in the generation of a toxic response. Finally a review of SWCNT *in vitro* cytotoxicity studies summarising the main findings and highlighting the inconsistencies that have arisen in the literature is reported.

“Nanotoxicology an emerging discipline” (Oberdorster *et al*, 2005) is one which has proven to be a challenge to nanotechnology researchers, when trying to conduct a comprehensive safety evaluation of nanomaterials. As the scale of production of nanomaterials increases, so does the potential of adverse health effects in humans and environmental damage. It is first necessary to assess what physical dimensions define a nanoparticle. Some publications have used the term to describe particles with a dimension of less than 0.1 μm (Colvin, 2003). Others used the term for particles with diameters below 45 μm . In 1996, the Environmental Protection Agency (EPA) used the term to characterize a particle distribution with mass median diameter (MMD) below 0.1 μm .

Regardless of the definition of a nanoparticle, the main physical characteristic of nanoparticles is their size, which can fall in the transitional zone between individual atoms or molecules and the corresponding bulk materials. This can modify the physio-chemical properties of the material as well as create the opportunity for increased uptake and interaction with biological tissues. For instance, shrinkage in size creates discontinuous crystal planes that increase the number of structural defects as well as disrupt the well structured electronic configuration of the material, so as to give rise to altered electronic properties (figure 3.1) (Donaldson *et al*, 2002; Oberdorster *et al*, 2005). Also in parallel with the shrinkage in size there is a corresponding increase in the relative surface area. A large surface area allows a greater contact area with cellular membranes as well as greater capacity for absorption and transport of toxic substances. This combination of effects can generate adverse biological effects in living cells that would not otherwise be manifest with the same material in larger particulate form.

Nanoparticles can be hydrophilic or hydrophobic, lipophilic or lipophobic, or catalytically active or passive (figure 3.1) (Cedervall *et al*, 2007). An example of how such surface properties can lead to toxicity is the interaction of electron donor or acceptor active sites (chemically or physically activated) with molecular dioxygen (O_2). Electron capture can lead to the formation of the super oxide radical (O_2^-), which through dismutation or Fenton chemistry can generate additional reactive oxygen species (ROS). Thus, several nanoparticles characteristics can culminate in ROS generation (Shvedova *et al*, 2005; Pulskamp *et al*, 2007).

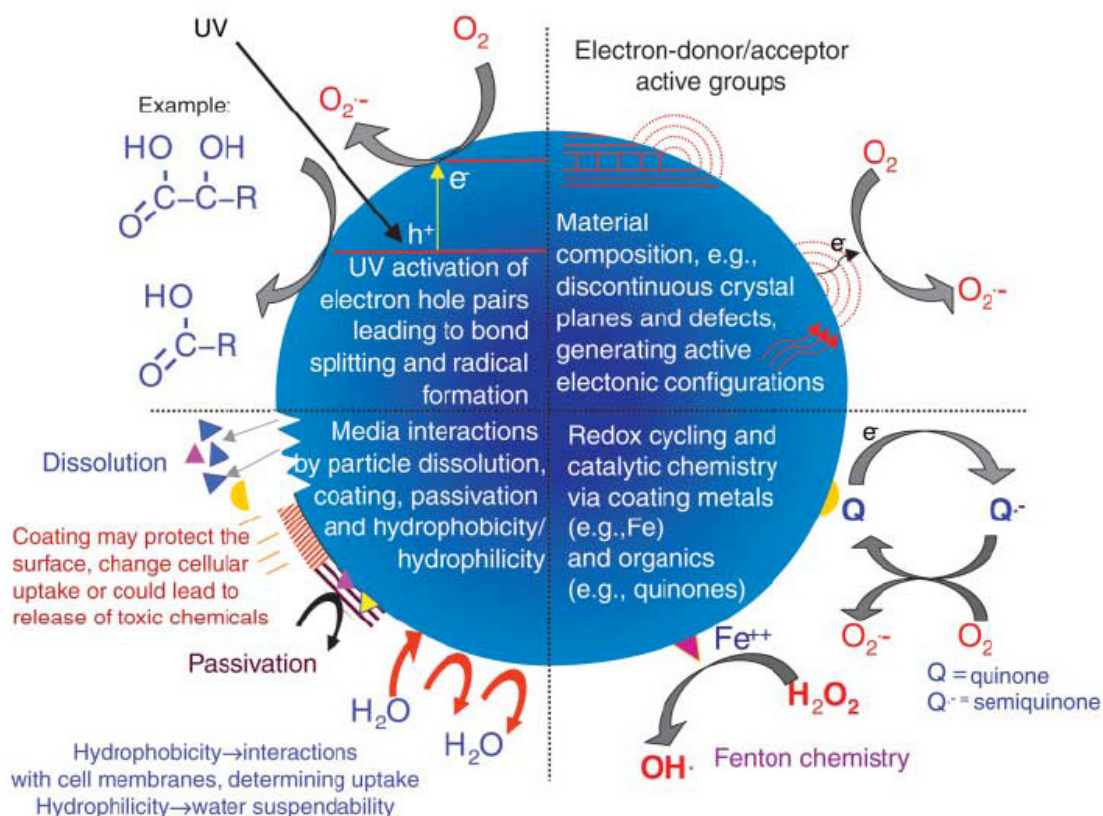


Figure 3.1 Proposed mechanisms by which nanomaterials interact with biological tissue.

Examples illustrate the importance of material composition, electronic structure, bonded surface species (e.g., metal-containing), surface coatings (active or passive), and solubility, including the contribution of surface species and coatings and interactions with other environmental factors (e.g., UV activation) (Nel *et al*, 2006).

Other nanoparticle properties such as shape, aggregation, surface coating, and solubility may also affect the specific physio-chemical and transport properties, with the possibility of negating or amplifying the size effects (figure 3.1). Studies by Sayes *et al* (2004) showed that chemical alteration of the surface of a fullerene to a water soluble form resulted in the lowering of observed cytotoxicity when compared to its bulk unaltered form.

Another point of concern is the apparent ability of nanoparticles to redistribute from their site of deposition; studies have reported that inhaled and ingested nanoparticles can readily move from the entry portal to various other sites (Hillery *et al*, 1994; Jani *et al*, 1990; Kreuter *et al*, 2002; Oberdorster *et al*, 2004). This further complicates the evaluation of their toxicity profile, as potentially the adverse effects of nanoparticles could occur in very different scenarios, dependant on nanoparticle type and portal of entry.

3.2 Toxicity of carbon based materials.

Toxicological studies involving various structural forms of carbon, primarily due to their potential applications in various biological systems, have been extensively reported in literature (Carero *et al*, 2001; Kamat *et al* 2000; Monteiro-Riviere *et al*, 2006; Murphy *et al*, 1999; Oberdorster *et al* 2000; Sayes *et al* 2005; Yang *et al* 1999). The following sections will give a brief summary of the findings about two forms of carbon which are particularly relevant to this study, namely carbon black and the Buckminster fullerene C₆₀.

3.2.1 Carbon Black.

Carbon black is a form of amorphous carbon that has an extremely high surface area to volume ratio, and as such it is one of the first nanomaterials to find common use, prior to the nanotechnology revolution, in everyday items such as inks and car tyres (It is similar to soot but with a much higher surface area to volume ratio). All carbon blacks have chemisorbed surface oxygen complexes (*i.e.*, carboxylic, quinonic, lactonic, phenolic groups and others) to varying degrees depending on the conditions of

manufacture. Extensive studies both *in vivo* and *in vitro* have been carried out on carbon black.

An *in vivo* study carried out by Yang *et al* (1999) exploring the effects of inhalation of various carbonaceous materials in rats showed that carbon black did induce pulmonary inflammation and the authors postulated that the inflammation may have resulted from the presence of organic compounds in the sample. A similar study by Oberdorster *et al* (2000), again on rats, showed that carbon black can induce a slight inflammatory response in the lungs, concluding that the increased surface area of the carbon black was key to its greater biological activity.

Numerous *in vitro* studies have resulted in the conclusion that no significant toxicity was detectable for carbon black (Carero *et al*, 2001; Murphy *et al*, 1999). However these studies did provide useful information. Murphy *et al* (1999) concluded the overall bio reactivity of carbon black was related to its size and therefore ultimately to its surface area and noted internalisation of the carbon black nanoparticles within the cells. Carero *et al* (2001) evaluated the cytotoxic and genotoxic potential of carbon black. They observed that although carbon black exhibited no significant cytotoxicity, DNA damage was noted and it was concluded that again the particle size, composition and structure may have played a key role in the damage. More recent studies exploring the dermal toxicity of carbonaceous materials (Monteiro-Riviere *et al*, 2006), including carbon black, noted that absorptive interferences with various commonly used cytotoxicity assays occurred resulting in inconsistent absorption/fluorescence data used to evaluate cytotoxicity. This raised questions about the validity of *in vitro* testing of

carbon black and advised caution even when performing standard *in vitro* testing protocols in the presence of fine quantities of carbonaceous materials.

3.2.2 Buckminster fullerene C₆₀.

The Buckminster fullerene (C₆₀) is a nanoparticle which is made up of sixty carbon atoms arranged in a cage like structure consisting of twelve pentagonal rings and twenty hexagonal rings, an icosahedral structure similar in appearance to that of a football. Its bonding structure is such that each carbon atom has a sp² hybridised bonding arrangement which gives rise to sixty delocalised electrons around the carbon cage.

Kamat *et al* (2000), using rat liver microsomes, explored the ability of C₆₀ to induce cell membrane damage. The study indicated that C₆₀ generated Reactive Oxygen Species (ROS) and induced significant lipid peroxidation/protein oxidation in the cell membranes, but it was shown that these effects could be prevented by natural antioxidants. Sayes *et al* (2004) showed a differential cytotoxicity of C₆₀ in two different mammalian cell lines and the study clearly showed a marked increase in observed toxicity in the unprocessed form of C₆₀ when compared to its water soluble, chemically altered, counterpart. The authors concluded that cell death was induced by oxidative damage upon exposure; the C₆₀ generated oxygen radicals which then induced cell membrane damage which subsequently resulted in cell death.

A later study by Sayes *et al* (2005) explored the biocompatibility of C₆₀ *in vitro*, again using different mammalian cell lines (Human Dermal Fibroblasts [HDF], Neuronal Human Astrocytes [NHA] and Human Liver Carcinoma Cells [HepG2]), in an attempt to elucidate the mechanisms by which this nanoparticle exerts a cytotoxic effect. They

concluded that C₆₀ was toxic to the cell lines tested. DNA and mitochondrial activity were not affected by the exposure as determined by the use of the DNA binding dye PicoGreen® and the MTT assay for mitochondrial activity. However it was shown that C₆₀ disrupted normal cellular functions by lipid peroxidation evaluated by the Thiobarbituric Acid (TBA) assay. Furthermore, exposure resulted in the generation of ROS which were responsible for the observed cell membrane damage and ultimately cell death.

The mechanisms proposed for C₆₀ toxicity, which from literature are dominated by the generation of ROS, are expected to be of particular relevance to SWCNT toxicity as SWCNT are considered by many to be an elongated C₆₀ molecule. The following section will discuss the potential role the intrinsic properties of SWCNT may play in the generation of a toxic response upon exposure.

3.3 Factors contributing to SWCNT toxicity.

Nanoparticles induce adverse effects as a result of two contributing factors. Firstly their reduced size increases the relative surface area of the nanoparticles therefore emphasising any intrinsic toxicity of the material (Duffin *et al*, 2002). Secondly the reactivity of the exposed surface area may play an important role in the generation of a toxic response. A relatively inert material can induce injurious effects primarily due to its increased surface area where alternatively a reactive surface can result in harm due to a combination of the increased surface area and the intrinsic toxicity of the reactive surface.

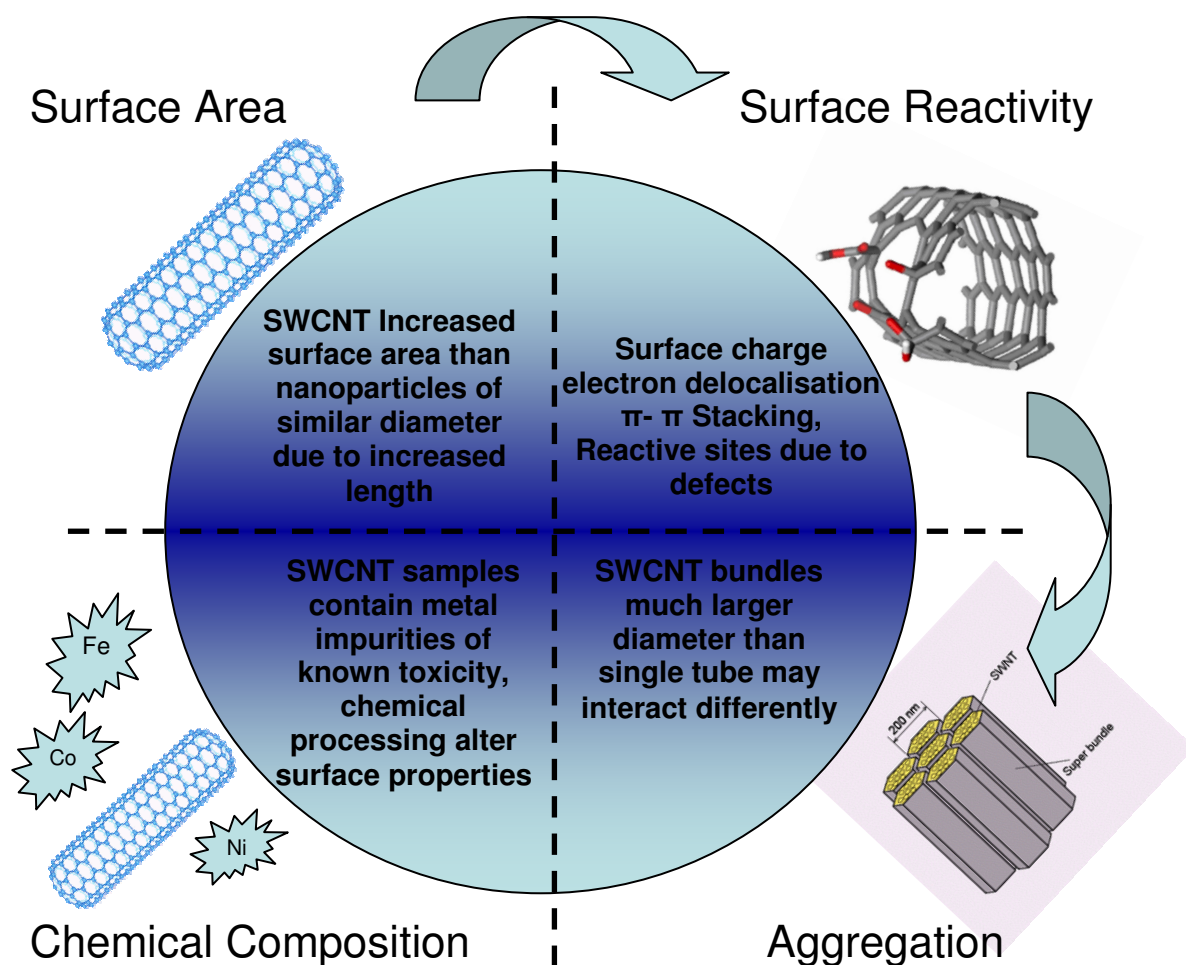


Figure 3.2 Proposed properties of SWCNT which may induce toxicity, diagram illustrates the importance of the increased surface area of SWCNT in comparison to other nanoparticles of similar diameter, surface reactivity due structural defects and chemical processing. The role aggregation of SWCNT may play as it greatly increases the size therefore reducing the surface area and finally the chemical composition highlighting the potential role of metal impurities in bulk SWCNT samples.

SWCNT exhibit these characteristics (figure 3.2) in that their physical dimensions, small diameter and relative long length; result in a substantially increased surface area in comparison to nanoparticles of similar diameters. Although considered chemically un-reactive, they readily interact with a battery of different systems (Bandyopadhyaya *et al*, 2002; Chambers *et al*, 2003; Chen *et al*, 2001; Hedderman *et al*, 2006; Kawamoto *et al*, 2006; Keogh *et al*, 2004; Moulten *et al*, 2005; Roman *et al*, 2006; Salvador-Morales

et al, 2006; Yu *et al*, 2003) many of which (amino acids, proteins and DNA) are components of biological matter. These properties are likely to contribute significantly to observed toxicity. The following subsections will discuss the intrinsic properties of SWCNT and their potential role in the in the generation of a toxic response.

3.3.1 Surface area.

The increased surface area of SWCNT, as with other nanoparticles, is expected to be a leading contributor to any observed toxicity. The overall surface area of a SWCNT is of course larger than that of a nanoparticle of similar diameter. If a per particle basis is taken it then is expected that even a “short” SWCNT of 20nm (wide) x 2000nm (long) for example, which is typical of SWCNT, would present ~100 times more surface area than that of a spherical particle of diameter 20 nm . Thus it is anticipated that SWCNT will have a pro-inflammatory potential that is driven by their surface area, as has been found for other graphitic nanoparticles such as carbon black.

As discussed in chapter 2, SWCNT have a tendency to aggregate into bundles due to van der Waals forces and although SWCNT diameters can be sub nanometre these bundles typically consist of tens of SWCNT and can have considerably larger diameters than the SWCNT from which they are formed. This is a very important factor in modifying their toxicity; for example aggregates with a much larger diameter than a SWCNT could deposit in an organ with a different anatomic pattern when compared to a SWCNT. In terms of inhalation exposure, macrophages may very well be able to clear a larger aggregate of nanotubes as a single entity, where as an individual SWCNT may be more difficult to handle due to the increased surface area and the potential to travel further into the recesses of the lungs when compared to an aggregate. Recent *in vitro*

studies (Wick *et al.*, 2007), using a lung cell model (Mesothelioma cell line MSTO-211H), revealed that larger aggregates in comparison to smaller bundles of SWCNT had an increased toxicity as determined by the MTT viability assay and DNA analysis using the Hoechst 33258 assay. The authors proposed that the aggregates induced a toxic effect similar to that of asbestos which was employed as a reference material in the study. Morphological studies of the SWCNT and asbestos exposed cells revealed similarities between the larger aggregates and the asbestos reference material allowing the comparison to be drawn. The authors concluded that the degree of dispersion and hence aggregation will be a key contributing factor to any observed SWCNT toxicity.

3.3.2 Length.

Neglecting the obvious fact that the increased length of SWCNT will obviously further increase their surface area, in terms of pulmonary toxicity, SWCNT length relative to their diameter will significantly affect their toxicity. Fibre toxicity is a mature science and many fibres are known to induce different injurious effects upon instillation within the lungs. Literature suggests that some fibre types may possess surface reactivity that imparts added pathogenicity. As of yet it is unclear if SWCNT have this potential. However they do contain reactive sites along the backbone of the SWCNT due to structural defects. Carbon particles would not normally be anticipated to have especially active surfaces. However, due to their small size, nanoparticle carbon black, composed of degenerated graphitic crystallites, is able to generate more oxidative stress *in vitro* than fine carbon black (Wilson *et al.* 2002). It is therefore plausible that as SWCNT and carbon black essentially can be considered to be different structural orientations of graphite, SWCNT may induce oxidative stress by a similar mechanism as carbon black.

3.3.3 Chemical composition.

SWCNT are generally considered chemically un-reactive; however there are points in the structure of SWCNT which are more reactive than others, such as defects due to missing carbon atoms and the more strained curved end-caps of the tubes (Lin *et al.* 2003). These sites may prove toxic “hot spots” along the backbone of the SWCNT due to the discontinuity of the electronic configuration of the SWCNT resulting from the structural defect ultimately cumulating in the generation of ROS. Furthermore recent studies have shown that nanoparticles (Cedervall *et al.*, 2007) due to their large surface area and the diversity of their surface characteristics have been shown to enhance the rate of protein fibrillation. As of yet it is unclear if SWCNT will induce similar scenarios. However it is plausible that this or a similar mechanism may occur, upon SWCNT exposure, given SWCNT’s tendency to readily interact with proteins (Moulten *et al.*, 2005).

As produced SWCNT, depending on the fabrication method, contain a number of toxic contaminant metal particles. These metals include cobalt, iron and nickel, the metal present being dependant on the fabrication process, all of which have documented toxic effects (Denkhaus and Salnikow, 2002; Ghio *et al.*, 1999). Transition metals such as iron are important toxicants as they have the ability to undergo redox reactions and to cause oxidative stress (Denkhaus and Salnikow, 2002; Ghio *et al.*, 1999). The presence of these metals is expected to play a significant role in the toxicity of bulk SWCNT samples.

Much research on SWCNT focuses on modifying these as-produced tubes by the addition of different chemical groups, leading to a significant change to many of their

properties (Banerjee *et al.* 2003). Functionalisation with different groups has been shown to result in different toxicity (Sayes *et al.*, 2005) since the particle surface is of great importance when interacting with biological systems. Chemical alteration of this surface therefore will obviously have an effect. Finally SWCNT, as discussed earlier, are known to interact with a variety of different molecular species (Bandyopadhyaya *et al.*, 2002; Chambers *et al.*, 2003; Chen *et al.*, 2001; Hedderman *et al.*, 2006; Kawamoto *et al.*, 2006; Keogh *et al.*, 2004; Moulten *et al.*, 2005; Roman *et al.*, 2006; Salvador-Morales *et al.*, 2006; Yu *et al.*, 2003) through van der Waals type interactions due to the electronic configuration of the SWCNT, used to process and purify. In some exposure scenarios these species may still be adsorbed to the tubes, in many cases they may also lead to a debundling of the tubes. Furthermore, the mechanism by which SWCNT interact with other molecular species may prove to be a significant contributor to generation of a toxic response at a cellular level.

3.4 Toxicity of SWCNT.

Due to their very light weight, SWCNT can easily become airborne and inhaled, hence the evaluation of their pulmonary effects has received a considerable amount of interest and a number of *in vivo* and *in vitro* studies have been performed to date. Several studies on the effects of both refined and raw SWCNT on the lung tissue of various animal models have been reported and there appears to be some inconsistency between the research findings (Huczko *et al.*, 2001; Shvedova *et al.*, 2005; Warheit *et al.*, 2004). These studies highlighted the inherent difficulty in testing SWCNT due to their agglomerative nature in aqueous solutions; indeed some of the observed mortality was attributed to mechanical blockage of the airways resulting in

asphyxiation (Warheit *et al*, 2004). It is now recognised that in order to elucidate the mechanisms of the pulmonary toxicity observed, specifically for SWCNT, further, more realistic *in vivo* inhalation studies with aerosolised SWCNT need to be conducted (Muller *et al*, 2006; Smart *et al*, 2006; Warheit, 2006).

Numerous *in vitro* studies have been performed on SWCNT with varying metal content and have evaluated different mechanistic endpoints. Shvedova *et al.*, (2003) tested iron-rich (30% wt iron) SWCNT on human epidermal keratinocytes (HaCaT) and following 18 hours exposure reported oxidative stress and loss of cell viability. They also observed that exposure resulted in ultra structural and morphological changes in these skin cells. The authors concluded that oxidative stress might be associated and greatly enhanced by the high levels of catalysts present in the SWCNT sample, which contained up to 30 percent iron residues per mass, and that the cytotoxicity observed might be due to the catalytic effects of iron (Shedova *et al.*, 2003). Recently, Kagan *et al*, (2006) also demonstrated that iron-rich SWCNT (26% wt iron) resulted in a significant loss of intracellular low molecular weight thiols and accumulation of lipid hydroperoxides in murine macrophages. Interestingly, a study by Sayes *et al*, (2005) evaluating the cytotoxicity of C₆₀, concluded that the observed toxicity could be attributed to lipid peroxidation and it is plausible that, although of different physical dimensions, SWCNT elicit toxicity through a similar mechanism. Tian *et al.* (2006) evaluated the *in vitro* cytotoxicity of five carbon nanomaterials, namely SWCNT, active carbon, carbon black, MWCNT and graphite on human dermal fibroblasts. The effects of refined material on cell survival and attachment were investigated and the most toxic refined material, SWCNT, was compared to its unrefined versions.

Fiorito *et al*, (2006) investigated the effects of highly purified fullerenes and SWCNT on murine and human macrophages and found these materials did not stimulate the release of the inflammatory marker nitric oxide by murine macrophage cells in culture. In addition, they also demonstrated the uptake of each material by human macrophages to be very low and that each possessed a very low toxicity against human macrophage cells. Jia *et al*, (2005) exposed SWCNT (with trace amounts of metal catalysts) to alveolar macrophages isolated from guinea pigs for 6 h and found that the SWCNT elicited a more toxic response than multi walled carbon nanotubes (MWCNT), quartz and fullerene. SWCNT have also been tested on human embryo kidney cells (HEK293) and were found to inhibit the proliferation of these cells by inducing cell apoptosis and decreasing cellular adhesive ability (Cui *et al*, 2005). As with the *in vivo* studies discussed earlier, differences in SWCNT toxicity and biocompatibility have also been observed with the various *in vitro* tests. These discrepancies have been attributed to the varying percentages of catalysts and other impurities in the tested SWCNT (Kagan *et al*, 2006), to the different dispersion methods employed to date (Smart *et al*, 2006) and additionally the functionalisation state of the nanoparticle under test has been recently shown to affect its toxicity (Sayes *et al*, 2006).

Recent literature has also revealed that the interactions of SWCNT and other carbon based nanomaterials with various commonly used cytotoxicity assays has resulted in interference with absorption/fluorescence data used to evaluate cytotoxicity (Montiero-Riviere *et al*, 2006; Worle-Knirsch *et al*, 2006). Furthermore, Hurt *et al* (2006) recently addressed this confounding issue and advised caution when

performing even established toxicity assays in the presence of significant quantities of fine carbon. While these studies highlighted the interference of SWCNT and other carbon based materials with cytotoxicity dyes, namely MTT and Neutral Red, no attempts to quantify these interferences have been realised to date although recommendations involving the use of various other cytotoxicity dyes have been made.

3.5 Chapter summary.

Although the number of research groups looking specifically at SWCNT toxicity both *in vitro* and *in vivo* has increased dramatically of the last 5 years, there are conflicting reports in the literature regarding the toxicity profile and general biocompatibility of these materials. Studies have pointed towards these discrepancies potentially originating from a number of different sources.

Firstly the different dispersion techniques employed; testing with or without an intermediate dispersion step, such as a surfactant, to initially disperse the SWCNT in the cell culture medium, has been shown to have an effect (Smart *et al*, 2006). The chemical composition of the test medium itself has recently been noted to have an effect. A study by Davoren *et al*, (2007) noted an increase in cytotoxicity of SWCNT to A549 lung cells when exposed to SWCNT in a protein free medium indicating that the presence of an added protein supplement in cell culture medium, which is general practice in mammalian cell culture techniques, may have had a protective effect reducing any observed cytotoxicity. Moreover the purity level (Fiorito *et al*, 2006) and functionalisation state (Sayes *et al*, 2006) of the SWCNT tested also seems to greatly

influence any observed cytotoxicity. Several studies (Jia *et al*, 2005; Kagan *et al*, 2006; Shedova *et al.*, 2003), have postulated the presence of remnant catalytic particles, from the relevant SWCNT fabrication techniques, may contribute significantly to SWCNT cytotoxicity. More alarming is the emergence of literature noting adsorptive interferences between SWCNT and cytotoxic assays (Montiero-Riviere *et al*, 2006; Worle-Knirsch *et al*, 2006) resulting in both false positive and negative cytotoxic effects being observed.

The upcoming chapters (5, 6 and 7) will employ both standard *in vitro* testing and spectroscopic analysis to assess contributing factors to SWCNT cytotoxicity in an attempt to elucidate the origins of these observed inconsistencies and their potential impacts for future studies evaluating SWCNT *in vitro* cytotoxicity.

References

Bandyopadhyaya R, Nativ-Roth E, Regev O and Yerushalmi-Rozen R. "Stabilization of individual carbon nanotubes in aqueous solutions" *Nanoletters*. 2002; 2: 25-28.

Banerjee S, Kahn MGC, Wong SS. "Rational chemical strategies for carbon nanotube functionalization". *Chemistry A European Journal*, 2003, 9 (9); 1899-1908.

Carero ADP, Hoet PHM, Verschaeve L, Schoeters G, Nemery B. "Genotoxic effects of carbon black particles, diesel exhaust particles, and urban air particulates and their extracts on a human alveolar epithelial cell line (A549) and a human monocytic cell line (THP-1)" *Environmental and molecular Mutagenesis*, 2001, 37, 155-163.

Cedervall T, Lynch I, Lindman S, Berggard T, Thulin E, Nilsson H, Dawson KA, Linse S. "Understanding the nanoparticle-protein corona using methods to quantify exchange rates and affinities of proteins for nanoparticles" *Proceedings of the national academy of sciences of the united states of America*, 104 (7): 2050-2055 FEB 13 2007.

Chambers G, Carroll C, Farrell GF, Dalton AB, McNamara M, in het Panhuis M, *et al.* Characterization of the interaction of gamma cyclodextrins with single walled carbon nanotubes. *NanoLetters*. 2003; 3 (6): 843-6.

Chen J, Dyer MJ, and Yu MF. "Cyclodextrin-mediated soft cutting of single-walled carbon nanotubes" *Journal of the American Chemical Society*. 2001; 123, 6201

Colvin VL. "The potential environmental impact of engineered nanomaterials", *Nature Biotechnology*. 2003, 21, 1166-1170.

Cui D, Tian F, Ozkan CS, Wang M, Gao H. "Effect of single wall carbon nanotubes on human HEK293 cells." *Toxicology Letters*, 2005, 155, 73-85.

Denkhaus E, Salnikow K. "Nickel essentiality, toxicity, and carcinogenicity". *Critical Reviews in Oncology Haematology*, 2002; 42 (1): 35-56.

Donaldson K, Stone V, Clouter A, Renwick L, Mac Nee W. "Ultrafine particles", *Occupational Environmental Medicine*. 2001, 58, 211.

Donaldson K, Tran CL. "Inflammation caused by particles and fibers", *Inhalation Toxicology*. 2002, 14, 5-27.

Donaldson K, Stone V, Tran CL, Kreyling W, Borm PJA. "Nanotoxicology", *Occupational Environmental Medicine*. 2004, 61, 727-728.

Duffin, R., Clouter, A., Brown, D., Tran, C. L., MacNee, W., Stone, V., and Donaldson, K. "The importance of surface area and specific reactivity in the acute pulmonary inflammatory response to particles". *Annals of Occupational Hygiene*, 2002, 46, 1, 242-245

Duncan R, Izzo L "Dendrimer biocompatibility and toxicity" *Advanced Drug Delivery Reviews*, 2005, 57, 2215–2237

Fiorito S, Serafino A, Andreola F, Bernier P. "Effects of fullerenes and single-wall carbon nanotubes on murine and human macrophages." *Carbon*, 2006, 44, 1100-1105.

Ghio AJ, Carter JD, Dailey LA, Devlin RB, Samet JM. "Respiratory epithelial cells demonstrate lactoferrin receptors that increase after metal exposure". *American journal of physiology-lung cellular and molecular physiology*, 1999, 276 (6): L933-L940.

Hedderman TG, Keogh SM, Chambers G, Byrne HJ. In-depth study into the interaction of single walled carbon nanotubes with anthracene and p-terphenyl. *Journal of Physical Chemistry B*. 2006; 110: 3895-901.

Hillery AM, Jani PU, Florence AT. "Comparative, Quantitative study of lymphoid and nonlymphoid uptake of 60nm polystyrene particles." *Journal of Drug Targeting*, 1994; 2; 151-156.

Hurt RH, Monthieux M, Kane A. "Toxicology of carbon nanomaterials: Status, trends, and perspectives on the special issue." *Carbon* 2006; 44: 1028-33.

Kagan VE, Tyurina YY, Tyurin VA, Konduru NV, Potapovich AI, Osipov AN, Kisin ER, Schwegler-Berry D, Mercer R, Castranova V, Shvedova AA "Direct and indirect effects of single walled carbon nanotubes on RAW 264.7 macrophages: Role of iron." *Toxicology Letters*. 2006; 165 (1): 88-100.

Kamat JP, Devasagayam TPA, Priyadarsini KI, Mohan H. "Reactive oxygen species mediated membrane damage induced by fullerene derivatives and its possible biological implications". *Toxicology*, 2000, 155; 55-61.

Kawamoto H, Uchida T, Kojima K, Tachibana M. Raman study of DNA- wrapped single walled carbon nanotube hybrids under various humidity conditions. *Chemical Physics Letters*. 2006; 431: 118-120.

Keogh, S.M., Hedderman, T.G., Greegan, E., Chambers, G., Byrne, H.J. "Spectroscopic Analysis of Single-Walled Carbon Nanotubes and Semiconjugated Polymer Composites", *Journal of Physical Chemistry B*. 2004, 108, 6233 -6241.

Kreuter J, Shamenkov D, Petrov V, Ränge P, Cychutek K, Koch-Brandt C, Alyautdin R. "Apolipoprotein-mediated transport of nanoparticle-bound drugs across the blood-brain barrier". *Journal of Drug Targeting*, 10; 317-325.

Jani P, Halbert GW, Langridge J, Florence AT. "Nanoparticle uptake by the rat gastrointestinal mucosa – Quantisation and particle size dependency." *Journal of Pharmacy and Pharmacology*, 1990; 42; 821-826.

Jia G, Wang H, Yan L, Wang X, Pei R, Yan T, Zhao Y, Guo X. "Cytotoxicity of carbon nanomaterials: Single-wall nanotube, multi-wall nanotube, and fullerene." *Environmental Science and Technology*, 2005, 39, 1378-1383.

Lin W, Huang Y, Zhou XD, Ma Y. “In vitro toxicity of silica nanoparticles in human lung cancer cells” *Toxicology and Applied Pharmacology*, 2006, 217, 252–259.

Monteiro-Riviere NA, Inman AO. “Challenges for assessing carbon nanomaterial toxicity to the skin.” *Carbon*, 2006; 44: 1070-78.

Moulton SE, Minett AI, Murphy R, Ryan KP, McCarthy D, Coleman JN, *et al.* Biomolecules as selective dispersants for carbon nanotubes. *Carbon*, 2005; 43: 1879-84.

Mosmann, T. “Rapid colorimetric assay for cellular growth and survival: Application to proliferation and cytotoxicity assays.” *Journal of Immunology Methods*. 1983, 65, 55-63

Muller J, Huaux F, Lison D. “Respiratory toxicity of carbon nanotubes: How worried should we be?” *Carbon*, 2006; 44; 1048-1056.

Murphy SAM, BeruBe KA, Richards RJ. “Bioreactivity of carbon black and diesel exhaust particles to primary Clara and type II epithelial cell cultures” *Occupational and Environmental Medicine*, 1999, 56 (12): 813-819.

Nel A. “Air pollution-related illness: Effects of particles”, *Science*, 2005, 308, 804-806.

Oberdorster G, Oberdorster E, Oberdorster J. "Nanotoxicology: An emerging discipline evolving from studies of ultrafine particles", *Environmental Health Perspectives*. 2005, 113, 823-839.

Oberdorster G. "Toxicology of ultrafine particles: in vivo studies". *Philosophical Transactions of the Royal Society of London Series A – Mathematical Physical Engineering Sciences*, 2000; 358 (1775): 2719-2739.

Pulskamp K, Diabate S, Krug HK. "Carbon nanotubes show no sign of acute toxicity but induce intracellular reactive oxygen species in dependence on contaminants." *Toxicology Letters*, 2007, 168, 58-74.

Roman T, Dino WA, Nakanishi H, Kasai H. "Glycine adsorption on single-walled carbon nanotubes". *Thin solid films*, 2006; 509; 218-222 .

Salvador-Morales C, Flahaut E, Sim E, Sloan J, Green MLH, Sim RB. Complement activation and protein adsorption by carbon nanotubes. *Molecular Immunology*. 2006; 43: 193-201.

Sayes CM, Fortner JD, Guo W, Lyon D, Boyd AM, Ausman KD, Tao YJ, Sitharaman B, Wilson LJ, Hughes JB, West JL, Colvin VL. "The differential cytotoxicity of water-soluble fullerenes". *Nanoletters*, 2004, 4, 1881-87.

Sayes CM, Gobin AM, Ausman KD, Mendez J, West JL, Colvin VL. "Nano-C₆₀ cytotoxicity is due to lipid peroxidation" *Biomaterials*, 2005, 26, 7587-7595.

Sayes CM, Liang F, Hudson JL, Mendez J, Guo W, Beach JM, Moore VC, Doyle CD, West JL, Billups WE, Ausman KL, Colvin VL. "Functionalization density dependence of single-walled carbon nanotubes cytotoxicity in vitro". *Toxicology Letters*, 2006, 161, 135-142.

Service RF, "Nanotoxicology: Nanotechnology grows up", *Science*, 2005, 304, 1732-1734.

Shvedova AA, Kisin ER, Mercer R, Murray AR, Johnson VJ, Potapovich AI, Tyurina YY, Gorelik O, Arepalli S, Schwegler-Berry D, Hubbs AF, Antonini J, Evans DE, Ku BK, Ramsey D, Maynard A, Kagan VE, Castranova V, Baron P. "Unusual inflammatory and fibrogenic pulmonary responses to single-walled carbon nanotubes in mice", *American Journal of Physiology*. 2005, 289, L698-L708.

Shvedova AA, Castranova V, Kisin ER, Schwegler-Berry D, Murray AR, Gandelsman VZ, Maynard A, Baron P. "Exposure to carbon nanotubes material: assessment of nanotubes cytotoxicity using human keratinocyte cells." *Journal of Toxicology and Environmental Health*, 2003, Part A 66, 1909-1926.

Smart SK, Cassady AI, Lu GQ, Martin DJ. "The biocompatibility of carbon nanotubes." *Carbon*, 2006, 44, 1034-1047.

Soto K, Garza KM, Murr LE. "Cytotoxic effects of aggregated nanomaterials" *Acta Biomaterialia*, 2007, 3 (3): 351-358.

Tian FR, Cui DX, Schwarz H, Estrada GG, Kobayashi H. “Cytotoxicity of single-wall carbon nanotubes on human fibroblasts”. *Toxicology in vitro*, 2006; 20 (7); 1202-1212.

Wang JJ, Sanderson BJS, Wang H. “Cyto- and genotoxicity of ultrafine TiO₂ particles in cultured human lymphoblastoid cells” *Mutation Research*, 2007, 628, 99–106.

Wick P, Manser P, Limbach LK , Dettlaff-Weglikowska U, Krumeich F , Roth S , Stark WJ, Bruinink A. “The degree and kind of agglomeration affect carbon nanotube cytotoxicity”. *Toxicology Letters*, 2007, 168; 121-131.

Wilson MR, Lightbody JH, Donaldson K, Sales J, Stone V. “Interactions between ultrafine particles and transition metals in vivo and in vitro”. *Toxicology and Applied Pharmacology*, 2002; 184 (3); 172-179.

Wörle-Knirsch JM, Pulskamp K, Krug HF. “Oops they did it again! Carbon nanotubes hoax scientists in viability assays.” *NanoLetters*. 2006; 6: 1261-68.

Yang HM, Barger MW, Castranova V, Ma JKH, Yang JJ, Ma JYC . “Effects of diesel exhaust particles (DEP), carbon black, and silica on macrophage responses to lipopolysaccharide: Evidence of DEP suppression of macrophage activity.” *Journal of toxicology and environmental health Part A*, 1999, 58 (5): 261-278.

Yu X, Chattopadhyay D, Galeska I, Papadimitrakopoulos F, Rusling JF. Peroxidase activity of enzymes bound to the ends of single-wall carbonnanotube forest electrodes. *Electrochemistry Communications* 2003; 5:408–11.

Chapter 4

“Experimental”

4.1 Introduction.

This chapter will discuss the analytical techniques used throughout this research. In this study, spectroscopic and microscopic analysis was employed to probe the interactions of SWCNT with a variety of different molecules and biological systems; their implications for the quantitative evaluation of SWCNT cytotoxicity will be discussed in later chapters as well as the possible implications for nanoparticle cytotoxicity in general.

4.2 Electronic Spectroscopy.

Two electronic spectroscopic techniques, namely absorption and fluorescent emission spectroscopy were used in this research. These complementary techniques examine the electronic transitions within a molecule and hence provide information about the electronic structure of the molecule and its local environment. The absorption and emission of light by a molecule is depicted in the Jablonski diagram in figure 4.1. The act of absorption involves the interaction of electromagnetic radiation with the components of a molecule. The initial absorption step takes the molecule to an excited electronic state. Since electronic transitions take place on a much faster time scale than nuclear motion, most electronic transitions are completed before the nuclei can alter

their spatial relationships. Such a transition is denoted as a Frank-Condon transition and is indicated in Figure 4.1 by the solid lines.

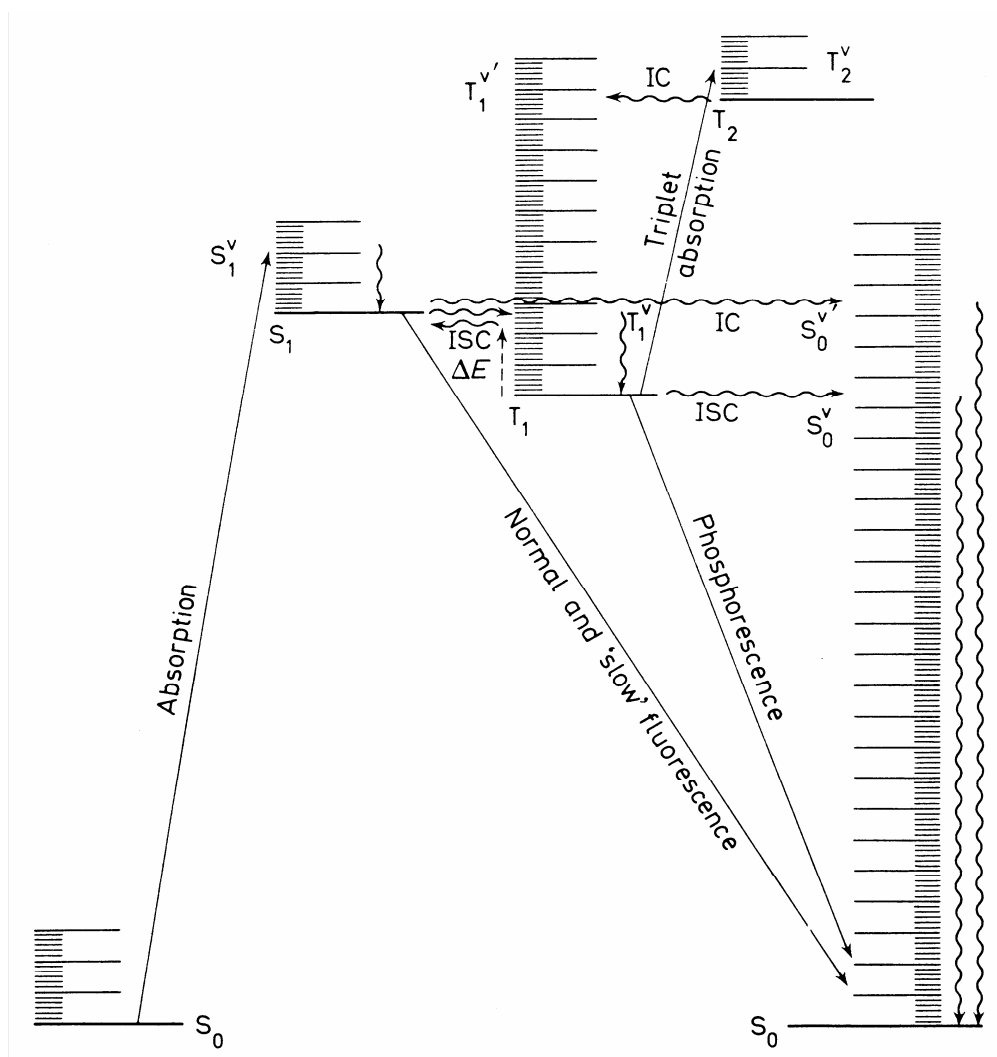


Figure 4.1 Jablonski diagram showing the sequence of steps leading to radiative decay. After initial absorption the upper excited vibrational states undergo non radiative decay by giving up energy to the surroundings. A radiative transition then occurs from the lowest vibrational level of the excited electronic state (Wayne, 1970). S_0 is the singlet ground electronic state and S_1 is the singlet excited electronic state; with T_1 representing the triplet state. ISC and IC represent intersystem crossing of an electron from the S_1 to T_1 excited states or vice versa and internal conversion where the electron orients itself so that it may return for T_1 to S_0 .

The Frank-Condon principle states that an electronic transition occurs so rapidly in comparison with vibration frequencies that no change occurs in inter-nuclear separation during the course of the transition. After excitation of the molecule to an upper vibronic state, the nuclear coordinates are not in their equilibrium configuration for the new electronic state and hence non-radiative relaxation between the vibrational states occurs. Generally after relaxing to the lowest vibrational state, the electron can return to the ground state by emitting the excess energy as a photon or by other radiationless channels of decay. The emitted photon is characteristically of longer wavelength than that of the exciting light. The crimped lines in figure 4.1 represent radiationless energy conversion: the vertical crimped lines within a particular electronic state indicate degradation of vibrational excitation, while the horizontal crimped lines indicate changes of state. The term internal conversion is applied to radiationless transitions between states of the same spin multiplicity, while intersystem crossing refers to transitions between states belonging to different spin systems.

Deactivation through emission of radiation can happen in one of two ways. These two processes were originally distinguished in terms of whether or not there was an observable afterglow. Jablonski interpreted phosphorescence as being emission from some long lived metastable electronic state lying lower in energy than the state populated by the absorption of radiation (Wayne, 1970). This was in fact a triplet state of a species. The long lifetime of the emission is a direct consequence of the forbidden nature of a transition from an excited triplet to the ground state singlet. Hence, phosphorescence can be described as a radiative transition between states of different multiplicity. Fluorescence is then understood to be a radiative transition between states of the same multiplicity (Wayne, 1970).

4.2.1 Absorption Spectroscopy.

Absorption spectroscopy probes the characteristic electronic absorption transitions of a molecule. The spectrometer used to probe the materials in this research was a Perkin Elmer Lambda 900 UV/VIS/NIR Spectrometer. The spectrometer is a double-beam, double monochromator ratio recording system with pre-aligned tungsten-halogen and deuterium lamps as sources. The wavelength range is from 175 to 3,300 nm with an accuracy of 0.08 nm in the UV-Vis region and 0.3 nm in the NIR region. It has a photometric range of ± 6 in absorbance. For all the experimental studies the absorption was measured at all times with a reference sample in a double beam arrangement.

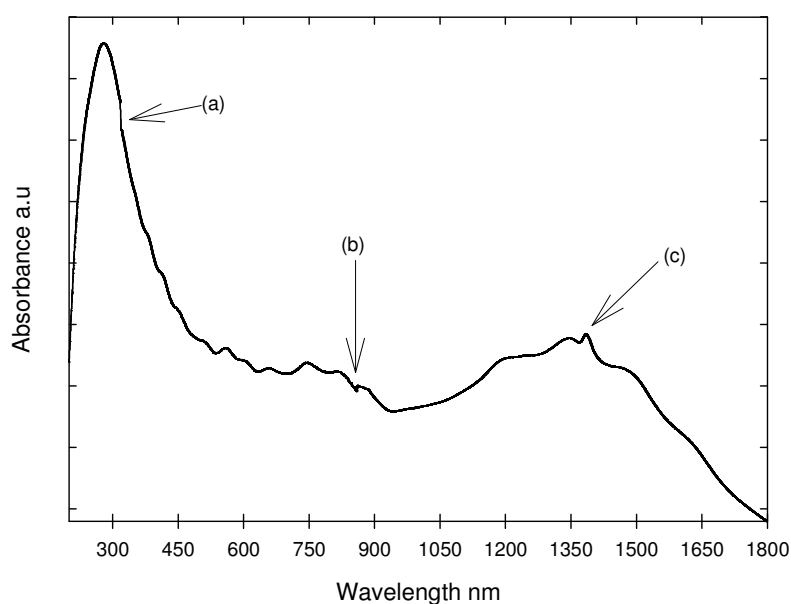


Figure 4.2 Absorption Spectrum of HiPco Carbon Nanotubes drop cast on to spectral B quartz discs. Note the following highlighted anomalies in the spectrum are due to; (a) increase in spectrum due to instrumental lamp change (b) dip in spectrum due to Instrumental detector change (c) sharp peak observed at 1400nm is due to the absorption of the quartz disk that was used as a substrate.

A solution of SWCNT in toluene (1 mg/ml) was prepared from which thin films were drop cast onto a spectrosil B disc for analysis. Toluene was chosen as it evaporates rapidly at room temperature but it also leaves no detectable absorption in the UV-VIS-NIR region (Hedderman, 2006) which is under examination here. Figure 4.2 shows the absorption spectrum of SWCNT. It can be seen that the spectrum consists of three broad absorption bands centred approximately at 1200nm, 800nm and 270nm. This spectrum agrees well with literature which also report three dominant absorbance features for HiPco SWCNT (Katura *et al*, 1999). The bands at 1200nm and 800nm are commonly agreed to be due to optical transitions between mirror image spikes in density of states.

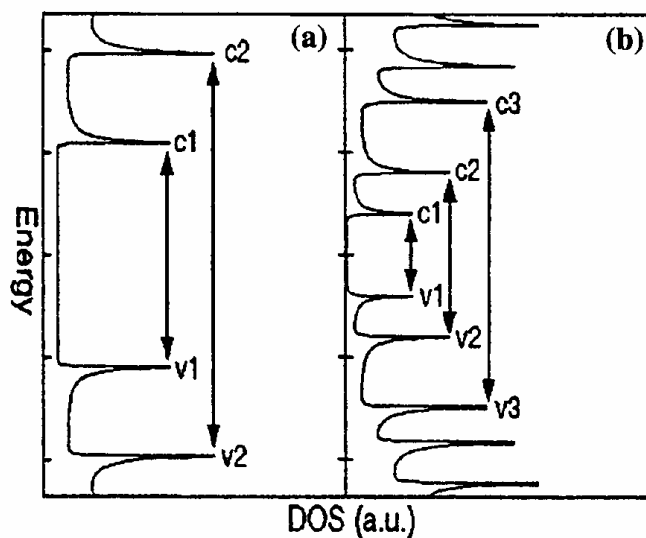


Figure 4.3 Schematic diagram of electronic density of states for (a) metallic and (b) semiconducting SWCNT. Arrows indicate the optically allowed interband transitions.

These transitions in the Density of States (DOS) of SWCNT are optically allowed and create excited electronic states as indicated in figure 4.3. The interband transition energies, $v1 \rightarrow c1$, $v2 \rightarrow c2$, and $v3 \rightarrow c3$ for semiconducting tubes $\approx 0.6\text{eV}$, 1.2eV and 2.4eV respectively, and that for $v1 \rightarrow c1$ in metallic tubes are $\approx 1.8\text{eV}$ (Satio *et al.*,

1998), are dependent on diameter and chirality of SWCNT (Bachilo *et al*, 2002; Kataura *et al*, 1999; Lian *et al*, 2005) and can be approximated by the following equations.

$$E^S_{22}(d_t) = \frac{4a_{c-c}\gamma_o}{d_t} \quad \text{Equation 4.1}$$

$$E^S_{33}(d_t) = \frac{8a_{c-c}\gamma_o}{d_t} \quad \text{Equation 4.2}$$

and

$$E^M_{11}(d_t) = \frac{6a_{c-c}\gamma_o}{d_t} \quad \text{Equation 4.3}$$

$$E^M_{22}(d_t) = \frac{12a_{c-c}\gamma_o}{d_t} \quad \text{Equation 4.4}$$

where a_{c-c} is the nearest-neighbour carbon-carbon distance, which is taken to be 1.44\AA for a SWCNT. γ_o is the nearest-neighbour carbon-carbon interaction energy, and d_t is the diameter of a SWCNT. E^S and E^M are the absorption (in eV) band positions for semiconducting and metallic tubes respectively. On the basis of this theoretical prediction, the absorption peak between 800nm and 1200nm can be assigned to the second inter-band transition $v_2 \rightarrow c_2$ in semiconducting tubes, with an energy of approximately 1.2eV, whereas peaks around 650nm are ascribed to the first inter-band transitions $v_1 \rightarrow c_1$ in metallic tubes with an energy of approximately 1.8eV. Using the previously mentioned equation and the absorbance of the SWCNT in the NIR region of the spectrum, an estimation of the tube diameter distribution for the semiconducting tubes as 0.8 – 1.36 nm can be made. The strong peak at 270nm is close to the π -plasma frequency of $\sim 4.6\text{eV}$ in carbon materials and presumed to be of similar origin.

4.2.2 Fluorescent Emission Spectroscopy.

A molecule that has absorbed a photon can discard its excess energy via radiative decay, in which an electron relaxes back into the lower energy levels of the ground electronic state and in the process generates a photon. This provides information with regards to the electronic and vibrational levels of the ground electronic state. A Perkin Elmer LS55 luminescence spectrometer was used throughout this research. In this instrument, excitation is provided by a pulsed Xenon discharge lamp with a pulse width at half peak height of $< 10 \mu\text{s}$ and pulse power 20 kW. The source is monochromated using a Monk-Gillieson type monochromator and can be scanned over the range of 200-800 nm. The luminescence is passed through a similar monochromator, which can be scanned over the range of 200-900 nm. Due to the limited range of the spectrometer used, SWCNT fluorescence could not be investigated (O'Connell *et al*, 2002). A brief description of the emission behaviour of SWCNT is given below.

The authors (O'Connell *et al*, 2002) verified that the absorption spectrum of SWCNT was dominated by the sharp inter band transitions within the DOS of SWCNT and was strongly dependant on diameter (figure 4.4). It was noted that upon 532nm excitation, the emission spectrum, although slightly red shifted, overlaid the absorption spectrum corresponding to the DOS of the SWCNT.

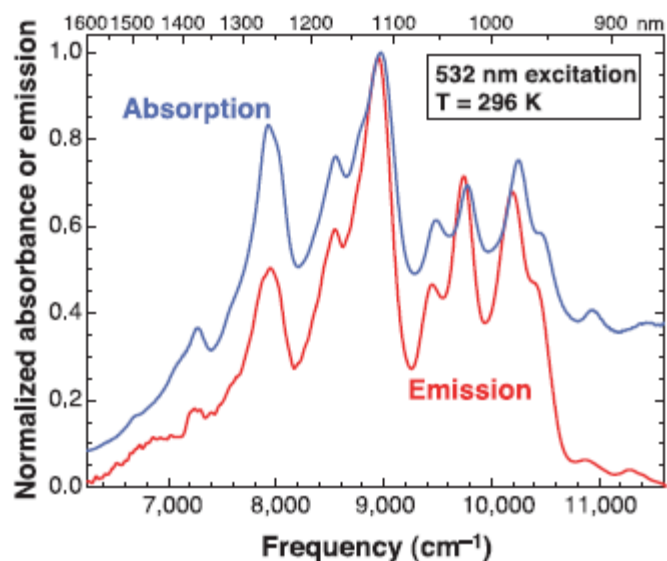


Figure 4.4 Absorption (Blue) and Fluorescent Emission (Red) spectra of HiPco SWCNT in SDS (O'Connell *et al*, 2002)

The authors concluded that the detailed correspondence of the absorption and emissions features of the HiPco SWCNT indicated that the observed emission originated from bandgap emission from the DOS of SWCNT. They furthermore noted that aggregation of the tested samples greatly reduced the observed emission.

While the direct emission of SWCNT was not carried out in this study, due to the limited spectral range of the instrument available, the effects of the incorporation of SWCNT into a fluorescent matrix have been extensively documented and SWCNT are now known to quench the emission of many fluorescent species (Curran *et al*, 1998; Coleman *et al*, 2005; Dalton *et al*, 2000; Giordani *et al*, 2006; Keogh *et al*, 2004; Hedderman *et al*, 2004; Hedderman *et al*, 2006). The mechanism is known to be dominated by π - π stacking between the electronic configurations of the SWCNT and the interacting species studies have shown these types of interaction to have a dramatic effect on both

the absorption and emission of fluorophores. In this research the effect of the incorporation of SWCNT into a fluorescent matrix will be studied to elucidate information about the interaction between SWCNT and various fluorescent species.

4.3 Vibrational spectroscopy.

Vibrations can be excited by the absorption or scattering of electromagnetic radiation at appropriate frequency and analysis of the frequencies where resonance is observed yields information about the identity of the molecule and the normal modes of vibration. Molecules interact with radiation of frequencies which exactly match the frequencies of vibrations within the molecule. The frequencies at which the molecules vibrate depend on the forces between the atoms, the mass of the atoms and the geometry of the molecule. The stronger the forces between the atoms in the molecule, the higher the vibrational frequency while heavier atoms display lower vibrational frequencies. Traditionally, there are two techniques used to obtain a vibrational spectrum; infrared absorption (IR) and Raman spectroscopy.

4.3.1 Infra Red spectroscopy.

The energies associated with the vibrations in a molecule with respect to one another are quantised and absorption of electromagnetic radiation in the infrared region gives rise to transitions between these different vibrational states. Absorption results from the coupling of a vibration with the oscillating electric field of the IR radiation and this interaction can only occur when the electric dipole moment of the molecule changes during the vibration. Since vibrating atoms are linked together by chemical bonds it is usual to refer to the vibration as a bond deformation. The simplest bond deformations

are bending and stretching. Usually, the only significant absorptions correspond to promotion of the bond deformation from their ground state to the next highest energy level, as at room temperature the molecules are normally in their ground state. IR spectroscopy is based on bond deformation and hence the vibration which is related to the atoms involved. Thus by measuring the IR absorption spectrum over a range of energies a series of absorptions corresponding to characteristic vibrations of particular bonds is obtained. Analysis of the location of the frequencies of these absorptions can aid in the identification of the material composition. In complex molecules, the constituent bond vibrations overlap and the spectrum becomes complex, but is nevertheless a characteristic fingerprint of the molecular material.

4.3.2 Raman Spectroscopy.

Transitions between vibrational states can result from the inelastic scattering of radiation from molecules. In such scattering processes, the oscillating electric field of the incident optical wave should be of an energy that is greater than the energy difference between the vibrational states, for example UV or visible radiation. The oscillating electric field of the incident optical wave can be scattered off the molecule in two different ways. The scattered light induces an oscillating polarisation in the scattering molecule and when the oscillating electric field exchanges energy with the molecule, then the scattered radiation may have a higher (anti-Stokes) or lower (Stokes) frequency than the incident electric field. The difference in frequency corresponds to vibrational modes of the molecular structure and is referred to as Raman scattering. When the incident frequency equals the scattered light, the scattering is referred to as elastic or Rayleigh scattering. In Stokes Raman scattering, the molecule starts out in a

lower vibrational energy state and as a result of the scattering process ends up in a higher energy state. Thus the interaction of the incident light with the molecule creates a vibration in the material. In anti-Stokes scattering, the molecule begins in a higher vibrational energy state and after the scattering process ends up in a lower vibrational state. Thus the vibration in the material is lost as a result of the interaction. The frequency difference between Raman lines and the exciting lines are characteristic of the scattering molecule and are independent of the excitation frequency. In IR spectroscopy a change in dipole moment is required, whereas in Raman spectroscopy a change in polarisability is required. As polar bonds are not often very susceptible to polarisation, the two techniques are often mutually complementary.

4.4 Infra Red (IR) Spectroscopy of Carbon Nanotubes.

The first vibrational technique that was applied to the current study was that of Infrared spectroscopy. The spectrometer used in this research to carry out experimental work was the Perkin Elmer Spectrum GX. It is a single-beam, Michelson interferometer based, Fourier transform infrared spectrometer. It has a dual level optical module that is sealed and desiccated. The system is configured with a mid-infrared (MIR), single source. MIR and far infrared (FIR), beam splitters allow the range 7000 to 50 cm^{-1} to be covered with a maximum resolution of 0.3 cm^{-1} . The spectrometer is configured with an AutoIMAGE microscope system which can operate in transmission and reflectance modes. All microscope operations including adjustments to aperture, focus and illumination are fully automated and the spectra are collected from the PC. The instrument includes a built-in 35W tungsten halogen illuminator, a motorised stage and a CCD video camera. The medium beam MCT detector covers the range from 5500 to

550 cm^{-1} . An ATR attachment with a micro germanium crystal with a range from 5500 to 600 cm^{-1} can be used for micro samples and ATR mapping for surface studies.

Although theoretical studies of single walled carbon nanotubes have been carried out (Branca *et al*, 2004, Kuhlmann *et al*, 1998) and have predicted that there are 6 to 9 IR active modes for a single walled carbon nanotube, very little infrared spectral data has been reported in literature (Branca *et al*, 2004). . By comparison to the IR active modes of graphite, it is the spectral region below 1800 cm^{-1} , which is of interest when examining nanotube samples. Of particular interest is its IR active E_{1u} mode at 1590 cm^{-1} attributed to the stretching mode of C=C which forms the frame work of the grapheme plane or the carbon nanotube back-bone. Figure 4.5 shows the recorded IR spectrum of nanotubes using potassium bromide (KBr) discs. The E_{1u} mode is present in the IR Spectra of single walled carbon visible but is shifted by 10 cm^{-1} to 1600 cm^{-1} . Also in this region one would expect a contribution from the aromatic rings of the hexagonal array, potentially broadened slightly by the presence of C=C bending usually visible at 1700 cm^{-1} .

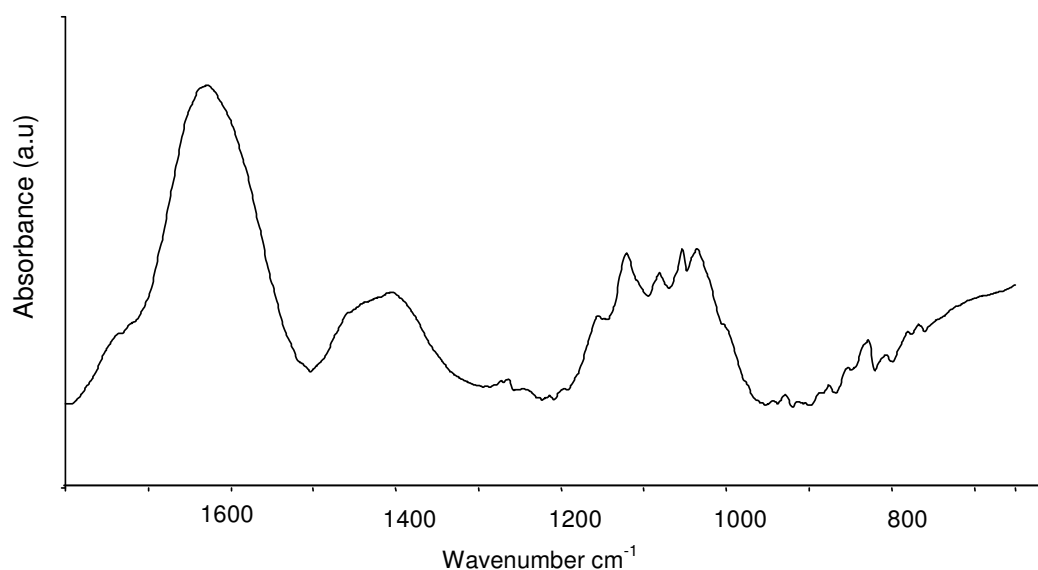


Figure 4.5 Infrared Spectrum of HiPco Carbon Nanotubes carried out in transmittance with a KBr disc.

Finally the two bands at 1400cm^{-1} and 1180cm^{-1} can be assigned to the C-C stretch, which are also part of the nanotube backbone, in the hexagonal array of the tube. The width of this feature may be attributable to the relative position of these bonds along the tube length.

4.5 Raman Analysis of Carbon Nanotubes.

Extensive studies have been carried out on the Raman effect in SWCNT (Brown *et al*, 2001; Chen *et al*, 1998; Dresselhaus *et al*, 2002; Jorio *et al*, 2002; Jorio *et al*, 2003; Kukovecz *et al*, 2002; Kuzmany *et al*, 2001; Pimenta *et al*, 2001; Yu *et al*, 2001). The preference for Raman spectroscopy over IR is a result of the strong Raman activity of the highly polarisable π – conjugated backbone; Figure 4.6 shows the Raman spectrum obtained for raw HiPco SWCNT at 514nm excitation. For the purpose of clarity the spectrum has been separated into three regions, namely low (below 500cm^{-1}), medium

(1200 – 1500 cm^{-1}) and high frequency (above 1500 cm^{-1}). The origins of the features present in each of the three regions will be discussed.

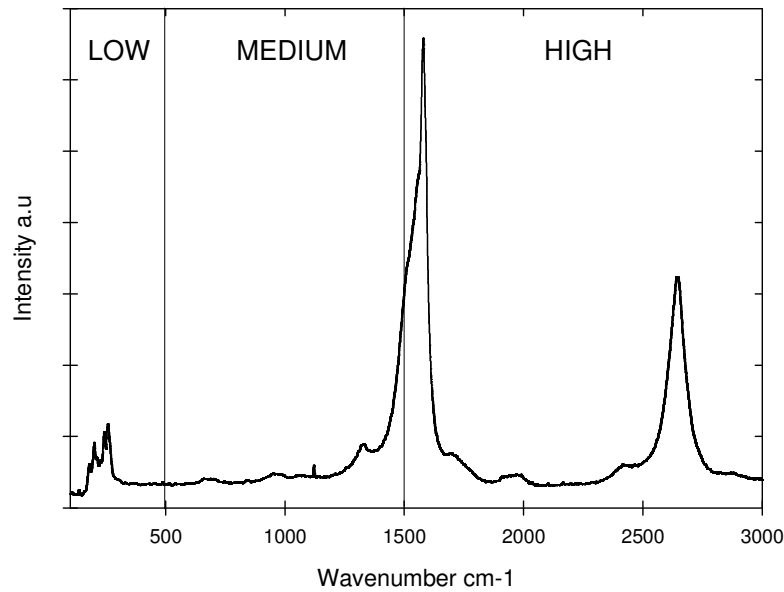


Figure 4.6 Raman Spectrum obtained for pristine HiPco SWCNT at 514nm excitation divided into characteristic Low, Medium and High Frequency Regions.

4.5.1 Low Frequency Raman Spectra.

In this region (below 500 cm^{-1}) the predominant feature is an in phase A_{1g} mode present between 116 and 192 cm^{-1} . This feature is termed the radial-breathing mode (RBM) in which all the atoms undergo an equal radial displacement. This mode is strongly diameter dependant (Dresselhaus *et al*, 2002; Kukovecz *et al*, 2002; Kuzmany *et al*, 2001).

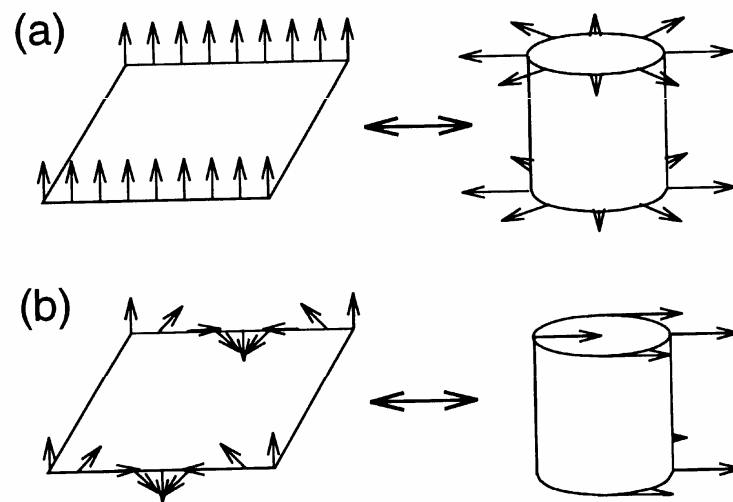


Figure 4.7 Schematic representations of RBM vibrations of SWCNT.

Using Raman spectroscopy, diameter distributions of samples can be evaluated from the RBM region (figure 4.8). Experimentation and calculation has confirmed a $1/d$ dependence of the mode frequency, where d is the tube diameter. The RBM frequency is known to be up shifted due to tube-tube interactions within a bundle and calculations have estimated this shift to be between 8 and 12% (Chen *et al*, 1998, Kuzmany *et al*, 2002). Further theoretical analysis confirmed that this up shift was dependent on the diameter and the number of tubes in the bundle.

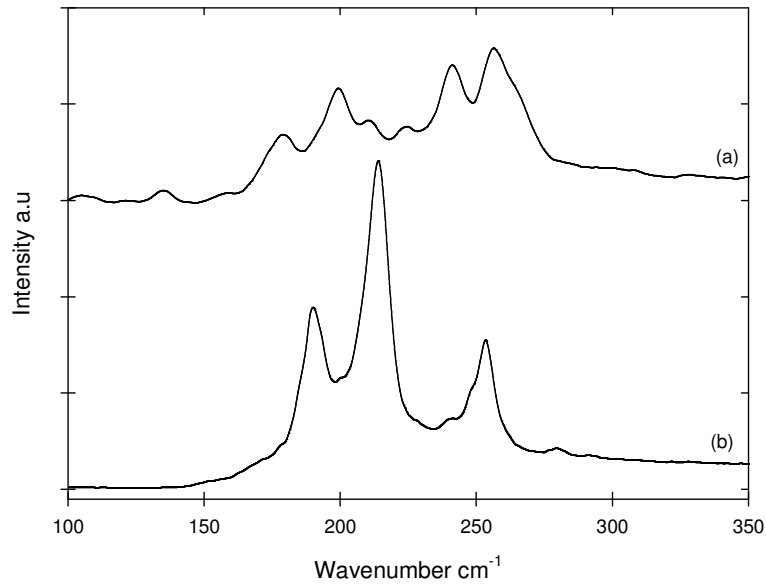


Figure 4.8 Raman Spectra of the RBM region of pristine HiPco SWCNT (a) 514 nm excitation and (b) 633nm excitation.

This relationship was modified to allow direct calculation of tube diameter ($d(nm)$) from the frequency of the RBM (ω_{RBM}) as follows:

$$\omega_{RBM} = \frac{c_1}{d(nm)} + c_2 = \frac{239}{d(nm)} + 8.5 \quad \text{Equation 4.5 (Kuzmany et al, 2002)}$$

where,

c_1 is a factor of proportionality

c_2 is a function that describes tube-tube (or other environmental) interactions

The values of c_1 and c_2 vary extensively in literature ($224 - 248 \text{ cm}^{-1}$ and $8 - 14 \text{ cm}^{-1}$).

In this study a c_1 value of 239 cm^{-1} and a c_2 value of 8.5 cm^{-1} was employed (Kuzmany et al, 2002).

4.5.2 Medium frequency Raman Spectra.

In the intermediate region of $1200 - 1500\text{cm}^{-1}$ calculated results show almost no intensity for Raman modes. Experiments on single walled nanotubes have shown weak features, which have been attributed to armchair modes (Pimenta *et al*, 1998). However calculation does not explain the appearance of these low intensity features. Experimentally peaks are observed at 1347cm^{-1} , which are known to be associated with symmetry lowering effects in graphite and carbon fibres for which a broad peak is observed at 1350cm^{-1} (Brown *et al*, 2001; Pimenta *et al*, 2001). The relative intensity of this peak in relation to a strong mode at 1582cm^{-1} is sensitive to the lowering of the crystal symmetry of graphite and it is therefore deduced that this feature is primarily associated with disorder in the sample and is termed the D-line (Brown *et al*, 2001).

4.5.3 High Frequency Raman Spectra.

In this region, otherwise known as known as the G-line region, strong Raman intensity modes from 1500 cm^{-1} to 1600cm^{-1} are seen (Bendiab *et al*, 2003; Jorio *et al*, 2001; Jorio *et al*, 2002;). The second feature in this region is termed the D*-line generally thought to be a second harmonic of the defect induced D-line found in the medium frequency region. The G-line region essentially consists of two A, two E_1 , and two E_2 phonon modes for chiral nanotubes and one A_{1g} , one E_{1g} and one E_{2g} mode for achiral nanotubes (Bendiab *et al*, 2003). Highly orientated pyrolytic graphite shows a peak at 1580cm^{-1} , which dominates the Raman spectrum and is attributed to the optical phonon E_{2g} mode. Nanotubes show multiple splitting of this peak, due to the dispersion curve of the optical phonon at 1580cm^{-1} where it splits into higher (longitudinal) and lower (transverse) energies, depending on curvature. Thus the allowed Raman lines appear as a series of doubly split peaks associated with the higher and lower energy sides of

1580cm^{-1} , as seen in figure 4.8. The Raman spectra for metallic nanotubes in bundles exhibit only two strong peaks, similar to isolated metallic nanotubes (Pimenta *et al*, 1998). In both tube types the peak frequency does not depend on the chirality of the tube, although the lower frequency mode is diameter dependant (Jorio *et al*, 2002). Using different excitation energies it is possible to study metallic and semiconducting nanotubes contained in both raw and composite materials (Hadjiev *et al*, 2001).

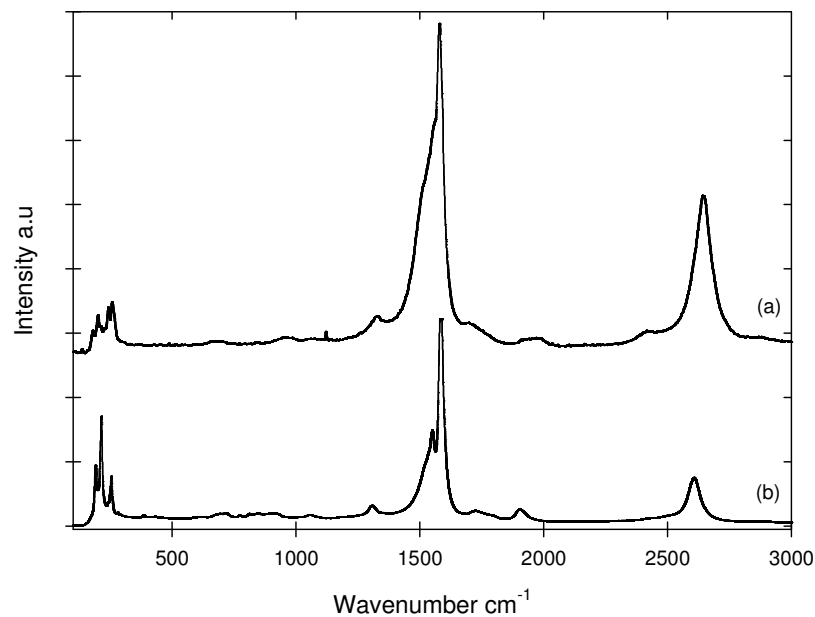


Figure 4.9 Raman Signal for Raw HiPco Carbon Nanotubes (a) 514.5nm Excitation and (b) 633nm Excitation.

Figure 4.9 shows the Raman signal obtained for the raw HiPco carbon nanotubes used in this study at two different excitation wavelengths namely 514 and 633nm. All the characteristic Raman modes, the Radial Breathing Modes (RBM), the D-line, the G-line and the D* -line are clearly visible. Another point of interest is the differences observed in the spectra due to the use of two different excitation energies (different excitation wavelength) (see also figure 4.8). This is in accordance with literature (Jorio *et al*, 2002; Jorio *et al*, 2003; Pimenta *et al*, 1998; Rao *et al*, 1997) In figure 4.9 the most obvious

difference between the two spectra is that of the G-line, clearly showing the different resonance effects due to excitation energy. There have been many reports on the dramatic effect of the Raman excitation wavelength on the distribution of the intensity and peak positions in the Raman spectrum. Figure 4.10 shows the Raman spectra of nanotubes (Rao *et al.*, 1997) produced in the laser vaporization generator at a number of different excitation wavelengths. These span from the near infrared to the visible. It should be noted that for even a small change in excitation wavelength there is a marked change in the spectrum. As the wavelength increases towards the infrared, the peaks near 1580 and 180 cm^{-1} are enhanced by an order of magnitude and many other peaks become observable. Resonant Raman scattering occurs when the energy of the incident photon matches the energy of the strong absorption causing electronic transitions. However, in the case of nanotubes with smaller diameters the situation changes dramatically. In many cases, there is a large apparent shift in the position of the Raman bands upon variation of the laser excitation. As the diameter decreases, the energy separation between the singularities increases. Hence, the Raman resonance condition thus selects the particular carbon nanotube (n, m) which has a singularity in its electronic density of states at a specific laser frequency. This is most apparent upon careful examination of the A_{1g} mode centred on 180 cm^{-1} .

frequencies predicted for (9,9) and (8,8) nanotubes, respectively. Thus the resonance effect is a quantum effect that can be explained in terms of both the electronic and phonon dispersion relations of the nanotubes. Since nominal single-wall carbon nanotubes samples consist of nanotubes with different diameters and chiralities, the resonant Raman effect may be seen in different nanotubes for different excitation frequencies.

5.5.4 Radial Breathing Mode (RBM) analysis of pristine HiPco carbon nanotubes

The radial breathing modes of carbon nanotubes are strongly diameter dependant (Dresselhaus *et al*, 2002; Kukovecz *et al*, 2002; Kuzmany *et al*, 2001), that is, their position (cm^{-1}) is inversely proportional to the diameter of the tube. A number of spectra were examined in this region and the RBM's were fitted with a combination of Lorentzian and Gaussian fits. An example of a fitted RBM region for the raw HiPco carbon nanotubes is given in figure 4.11, showing the individual fit components (dashed line) and the overall combined fit (grey line).

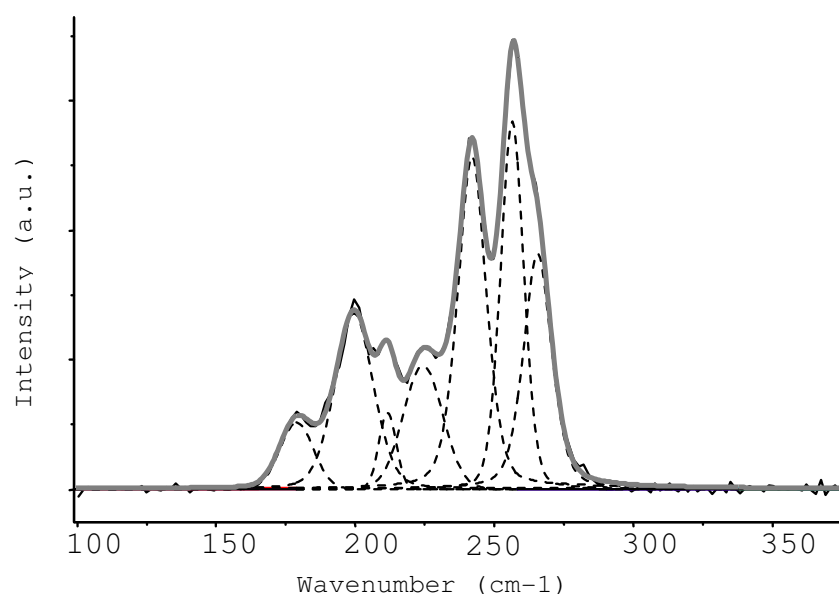


Figure 4.11 Fitted Radial Breathing Modes for Raw HiPco Carbon Nanotubes 514nm excitation.

Using the outlined relationship (Kuzmany *et al*, 2001) a diameter distribution for the raw HiPco used in this study (figure 4.12) was calculated based on the position of the RBM peaks from multiple spectra using 514 and 632 nm excitation.

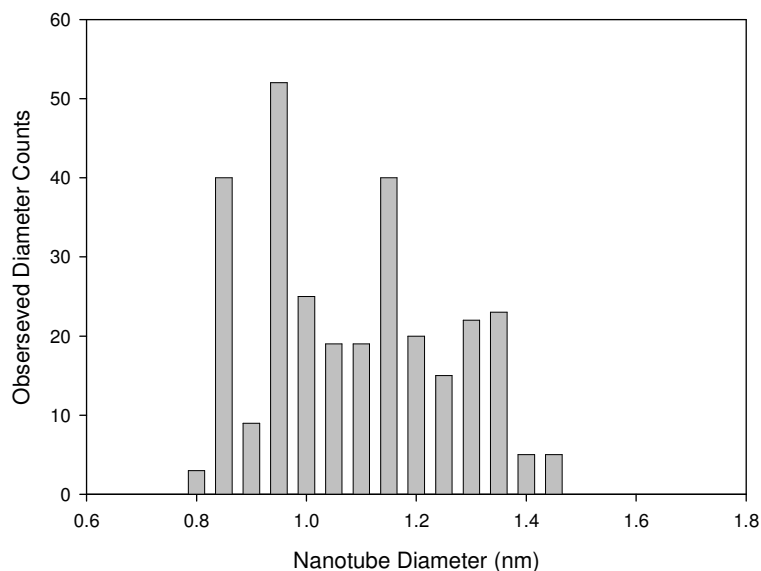


Figure 4.12 Diameter Distribution of pristine HiPco Carbon Nanotubes from RBM analysis at 514 and 632nm excitation.

Form this diameter distribution of 0.8 – 1.45nm was estimated which was in broad agreement with the distribution estimated from the UV/VIS/NIR spectrum as was seen in section 4.2.

The preceding sections have presented the spectroscopic characterisation of SWCNT, outlining the origins of the observed spectral features and giving details of the instrument employed. These instruments were used extensively through out the course of this study, in later sections they will be used to probe a variety of different systems assessing the physiochemical indicators of SWCNT toxicity.

4.6 Transmission Electron Microscopy (TEM) of pristine HiPco Carbon Nanotubes.

The TEM used to image the materials in this research was a Jeol 100 CX TEM, with an accelerating voltage of typically 100 keV applied. The substrates consisted of copper grids covered with an electron transparent polymer, 3 % Formvar resin in 1,2-dichloroethane. Formvar resin is a synthetic film containing polyvinyl acetyl and phenol resins.

To prepare the samples for imaging, 2 mg of untreated SWCNT were placed in 10 ml of ethanol and sonicated in the sonic bath (ULTRA sonick 57x, 230 V), for 30 minutes at medium power. The solution was then drop cast onto a copper grid with a 3% chloroform formvar polymer coating after which the samples were allowed to dry for approximately 24 hours.

Figure 4.13 shows the TEM image obtained for the raw HiPco nanotubes used in this study. In this image an area of what is termed high density tubes i.e. bundles of varying lengths and diameters, can be clearly seen. Of interest here is that using this technique, which has a much higher resolution than AFM microscopy, individual tubes can be clearly seen and tube length calculated. Furthermore catalytic iron particles remnant for the fabrication process can be clearly seen.

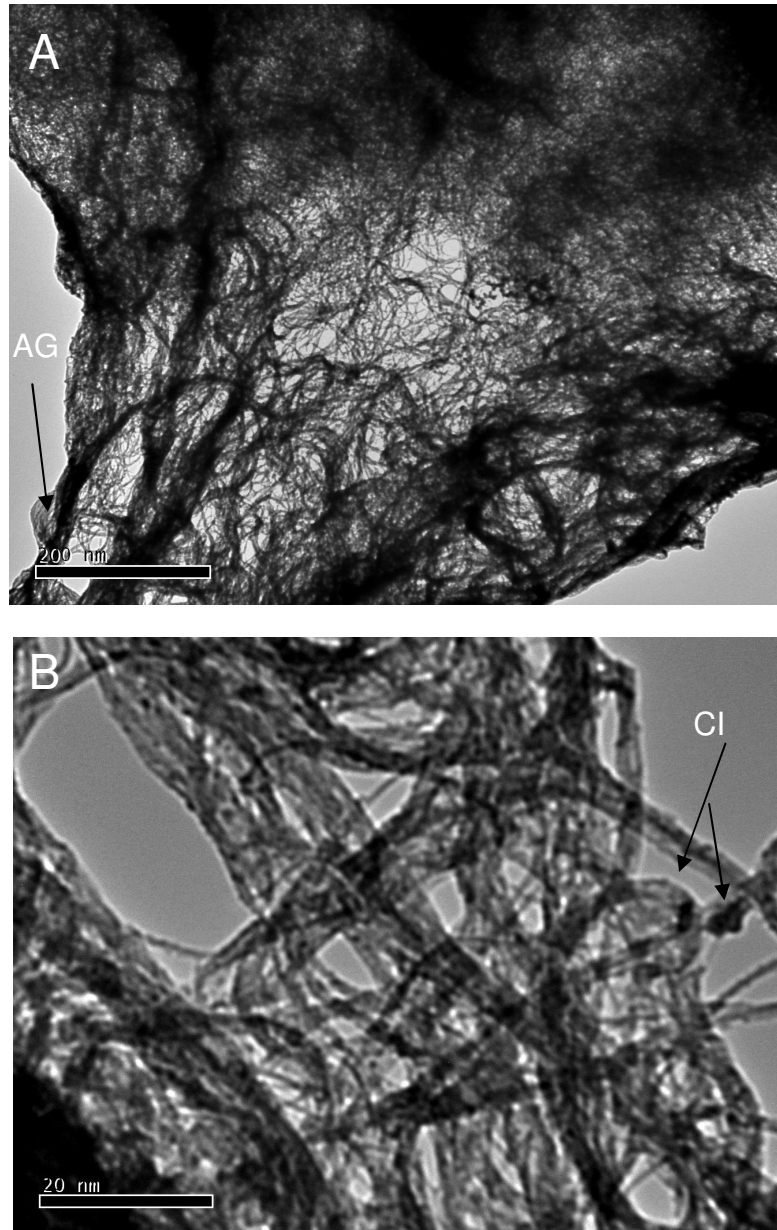


Figure 4.13 TEM of Raw as Purchased HiPco® SWCNT (A) 20000 times magnification showing large aggregates (AG) and high density tubes (B) 200000 times magnification showing individual tubes and remnant catalytic iron (CI) particles.

While microscopic studies of raw nanotube samples provide little information about the type of tubes (metallic or semiconducting) they do allow a visualisation of the morphology and aggregation state of the sample. Any changes in these which were incurred as a result of composite formation or sample processing can then be accessed. The average diameter noted for the batch of HiPco SWCNT used in this study

was 1.1nm which is in agreement with the spectroscopic estimation of SWCNT diameter in figure 4.12. Although it is difficult to assess the tube length from unprocessed samples, TEM imaging suggests tube length in excess of 50nm (figure 4.13B). In contrast, bundle diameter varies considerably from several nanometres up to tens of nanometres; rope lengths (figure 4.13A) appear to be in excess of 200nm. Variation in the bundle size and the tube distribution will be an important factor when considering the bio-integration or toxicity of SWCNT. It is expected that TEM will therefore be a useful tool in visualising the aggregation state of the tubes used in this study.

4.7 SWCNT characterisation summary.

This chapter has presented the characterisation of pristine SWCNT both spectroscopically and microscopically. Where applicable, the origins of observed spectral features were discussed. Electronic spectroscopy, namely absorption and emission, was shown to be dominated by the inter band transitions in the DOS of SWCNT, facilitating a diameter distribution of 0.8 – 1.36 nm for HiPco SWCNT employed in this study to be estimated. Infra red spectroscopy was seen to provide little information about the SWCNT present in the sample. Raman spectroscopy was seen to be a very useful tool in the analysis of SWCNT samples; it facilitated a diameter distribution to be estimated, by RBM analysis, of 0.8 – 1.45nm which was in broad agreement with that of the electronic spectroscopy. Transmission electron microscopy showed the aggregation state of the SWCNT sample, allowing bundle size to be estimated. The techniques presented in this chapter, and more precisely changes to the characteristic features observed, will be used to assess the interactions of SWCNT with

a variety of different molecules and biological systems; their implications for the quantitative evaluation of SWCNT cytotoxicity will be discussed later in chapters 5, 6 and 7 as well as the possible implications for nanoparticle cytotoxicity in general.

4.8 General Experimental.

The following subsections will give a brief account of the common experimental techniques carried out including details of the test materials used, dispersion of these materials, spectroscopic analysis and cell culture techniques which will be used throughout the upcoming chapters 5, 6 and 7. Where necessary additional experimental information will be given in the relevant chapters.

4.8.1 Test Materials and Reagents.

HiPco[®] SWCNT were purchased from Carbon Nanotechnologies, Inc. (Houston, TX). This material contained 10 wt % residual Fe catalyst particles. Arc Discharge SWCNT were purchased from Sigma Aldrich Ltd. (Dublin, Ireland). Printex 90 (Carbon Black) were received from Degussa AG (Frankfurt, Germany). The following cell viability dyes MTT, Commassie Brilliant Blue (COMMASSIE), Neutral Red (NR) were all purchased from Sigma Aldrich Ltd. (Dublin, Ireland). Alamar Blue[™] (AB) was purchased from Biosource (UK). The viability dye WST-1 was purchased from Roche (UK). Cell culture media and supplements and the trypsinisation solution were purchased from Biosciences (Dublin, Ireland).

4.8.2 Dispersion of SWCNT.

An ultrasonic tip (Ultra sonic processor VCX-750 watt) was employed to disperse the solutions prior to preparation of test concentrations. Minimal sample processing was employed to mimic exposure to raw nanotube powders as much as possible. The solutions were prepared by dispersing an initial concentration of 1 mg/ml of SWCNT in the solution under study by ultra sonication. Then by subsequent dilution and sonication, operating at 40% for a total time of 30 seconds carried out in 10 second sequential steps, the concentration of SWCNT was reduced over a wide range from the initial concentration down to a final concentration 9.7×10^{-4} mg/ml.

4.8.3 Spectroscopic Characterisation.

For cytotoxicity evaluation, fluorescence and absorbance were all quantified using a microplate reader (TECAN GENios, Grödig, Austria). Absorption and fluorescence spectroscopy were performed on the dispersions of nanotubes in all solutions after a 24 hour settling period after which they were characterised using the Perkin Elmer Lambda 900 Absorption and LS55B Luminescence spectrometers respectively. Raman Analysis was performed with the aid of the Instruments S.A. LabRam 1B Raman microscope using 514.5 nm laser excitation on drop cast samples.

4.8.4 Cell Culture.

The human alveolar carcinoma epithelial cell line A549 (ATCC, CCL-185) was employed for toxicity evaluation. Cells were grown in F-12K medium (Kaighn's Modification, Gibco) supplemented with 10% foetal calf serum (FCS), 45 IU ml⁻¹ penicillin and 45 µg ml⁻¹ streptomycin and grown in a humidified incubator at 37°C (5% CO₂). For testing cells were seeded at a density of 1×10^5 cells/ml for 24 hour

test, 7×10^4 cells/ml for 48 hour test, 3×10^4 cells/ml for 72 hour test and 2×10^4 cells/ml for 96 hour test in 96-well plates

4.8.5 Cytotoxicity Assays.

Five different assays were used through out the course of this research which were as follows: Alamer Blue (AB), Neutral Red (NR), Commassie Blue (COMMASSIE), MTT (3-(4,5-dimethylthiazol-2-yl)-2,5-diphenyltetrazolium bromide) and WST-1 (2-(4-iodophenyl)-3-(4-nitrophenyl)-5-(2,4-disulfophenyl)-2H-tetrazolium).

Cells were seeded at a density of 1×10^5 cells/ml in 96-well plates in at least 3 replicates. After 24 hours, the cells were treated with the material to be tested and left for another 24 hours whereupon they were assessed for cell viability using the five assays. The AB, NR and COMMASSIE assays were conducted subsequently on the same set of plates. The AB assay was performed first. The bioassay was carried out according to manufacturer's instructions. Briefly, control media or test exposures were removed, the cells were rinsed with PBS and 100 μ l of an AB/NR medium (5% [v/v] solution of AB and 1.25% [v/v] of NR dye) prepared in fresh media (without FBS or supplements) were added to each well. The plates were then incubated for 3 hours. The AB assay measures the innate metabolic activity of cells. The oxidised indigo blue, non-fluorescing form of this chromogenic indicator dye is reduced by cellular dehydrogenases to a reduced pink fluorescent form, which can be easily monitored spectrophotometrically. Following the 3 h incubation, AB fluorescence was quantified at the respective excitation and emission wavelength of 540 and 595 nm. Wells containing medium and AB without cells were used as blanks. The mean fluorescent

units for the six replicate cultures were calculated for each exposure treatment and the mean blank value was subtracted from these.

Viability and protein determination of the cells following exposure to each chemical were then subsequently investigated using the NR and Coomassie assays. The incorporation of the NR dye by the lysosomes of living cells and the quantification of the total amount of cellular proteins were performed according to Liebsch and Spielmann (1995) with the modification of Coomassie Brilliant Blue dye being employed in place of Kenacid Blue R dye. Briefly, after measurement of AB fluorescence, the AB/NR medium was discarded, the cells were washed with 100 μ l PBS and then the NR dye was extracted with 100 μ l of an acetic acid-ethanol solution (de-staining solution). The addition of the acetic acid-ethanol solution also acts as a cell fixative step so that protein determinations can be conducted subsequently. The plate was shaken at 240 rpm for 10 min and the fluorescence of NR was measured at excitation and emission values of 540 and 650 nm respectively with a microplate reader. Protein determinations were performed on the same plates immediately following NR determination. Excess NR dye was removed from the cells by washing with 100 μ l de-staining solution. COMMASSIE dye was added to each well and the plate agitated for 10 min. The dye was removed and the plate washed with an acetic acid-ethanol solution. The wash solution was discarded and the dye extracted with measuring solution (1M Potassium acetate). The plate was shaken at 240 rpm for 10 min and the absorbance of the extracted dye was read at 570 nm (reference filter 340 nm) using the microplate reader.

Using the MTT assay, cell viability was determined by measuring the reduction of yellow water-soluble MTT to a water-insoluble MTT-formazan. A MTT working concentration of 0.5 mg/ml was added to the cells and plates and incubated for 3h at 37°C (5% CO²). Cells were washed with 100 µl of PBS and 100 µl dimethylsulfoxide (DMSO) was then added to each well to extract the dye. The plate was shaken at 240 rpm for 10 min and absorbance was recorded at 550 nm. A second tetrazolium salt, WST-1, at a working concentration of 9.1 % was employed for measurement of cell viability after SWCNT treatment. For this assay, three replicate wells were used on each plate and cells were exposed to SWCNT concentrations of 0.00156 to 0.4 mg/ml. In contrast to the MTT assay, no extraction step was necessary due to the water solubility of the reduced form of WST-1 so that absorbance could be determined directly at 450 nm after conversion.

4.8.6 Statistical Analysis.

At least three independent experiments were conducted. Test results for each assay were expressed as percentage of the unexposed control \pm standard deviation (SD). Control values were set as 100%. Differences between samples and the control were evaluated using the statistical analysis package Minitab14. Statistical significant differences were set at $p < 0.05$. Normality of data was confirmed with Kolmogorov-Smirnov tests to validate the assumptions found in one-way analysis of variances (ANOVA) and Dunnett's multiple comparison tests.

References

Bachilo, S.M., Strano, M.S., Kittrell, C., Hauge, R.H., Smalley, R.E., Weisman, R.B. “Structure assigned optical spectra of single-walled carbon nanotubes”, *Science*, 2002, 298, 2361 – 2366.

Bendiab, N., Almairac, R., Paillet, M., Sauvajol, J.-L. “About the profile of the tangential modes in single-wall carbon nanotubes bundles”, *Chemical Physics Letters*. 2002, 372, 210-215.

Branca, C., Corsaro, F., Frusteri, F., Mangione, A., Migliardo, F., Wanderlingh, U. “Structural and vibrational properties of carbon nanotubes by TEM and infrared spectroscopy”, *Diamond and Related Materials*, 2004, 13, 1249-1253.

Brown, S.D.M., Jorio, A., Dresselhaus, M.S., Dresselhaus, G. “Observations of the D-band feature in the Raman spectra of carbon nanotubes”, *Physical Review B*. 2001, 64, 073403 -1 – 073403-4.

Coleman JN, Maier S, Fleming A, O’Flaherty S, Minett A, Ferreira MS, *et al.* “Binding kinetics and spontaneous single wall carbon nanotube bundle dissociation in low concentration polymer-nanotube solutions”. *Journal of Physical Chemistry B*. 2004; 108: 3446-50.

Curran SA, Ajayan PM, Blau WJ, Carroll DL, Coleman JN, Dalton AB, *et al.* “A composite from poly(m-phenylenevinylene-co-2,5-dioctoxy-p-phenylenevinylene) and carbon nanotubes: A novel material for molecular optoelectronics”. *Advanced Materials*. 1998; 10(14):1091-3.

Dalton AB, Stephan C, Coleman JN, McCarthy B, Ajayan PM, Lefrant S, *et al.* “Selective interaction of a semiconjugated organic polymer with single-wall nanotubes”. *Journal of Physical Chemistry B*. 2000; 104: 10012-16.

Dresselhaus MS, Jorio A, Souza Filho AG, Dresselhaus G, Saito R. Raman spectroscopy on one isolated nanotube. *Physica B*. 2002; 323:15-20.

Eklund, PC, Holden JM, Jishi, RA. “Vibrational modes of carbon nanotubes Spectroscopy and theory”. *Carbon*, 1995, 33, 7, 959-972

Giordani S, Bergin SD, Nicolosi V, Lebedkin S, Kappes MM, Blau WJ, *et al.* “Debundling of single-walled nanotubes by dilution: observation of large populations of individual nanotubes in amide solvent dispersions”. *Journal of Physical Chemistry B*. 110 (32): 15708-15718.

Hadjiev VG, Iliev MN, Arepalli S, Files PBS. Raman scattering test of single-wall carbon nanotube composites. *Applied Physics Letters*. 2001; 78: 3193-5.

Hedderman TG, Keogh SM, Chambers G, Byrne HJ, Solubilisation of Single walled carbon nanotubes with organic dye molecules. *Journal of Physical Chemistry B*. 2004; 108 (49): 18860-65.

Hedderman TG, Keogh SM, Chambers G, Byrne HJ. In-depth study into the interaction of single walled carbon nanotubes with anthracene and p-terphenyl. *Journal of Physical Chemistry B*. 2006; 110: 3895-901.

Iijima, S., Ichihashi, T. "Single shell nanotubes of 1-nm diameter", *Nature*, 1993, 363, 603-605.

Jorio, A., Saito, R., Hafner, J.H., Lieber, C.M., Hunter, M., McClure, T., Dresselhaus, G., Dresselhaus, M.S. "Structural (n,m) determination of isolated single-wall carbon nanotubes by resonant Raman scattering", *Physics Review Letters*. 2001, 86, 1118-1121.

Jorio, A., Filho, A.G.S., Dresselhaus, G., Dresselhaus, M.S., Swan, A.K., Unlu, M.S., Goldberg, B.B., Pimenta, M.A., Hafner, J.H., Lieber, C.M., Saito, R. "G-band resonant Raman study of 62 isolated single-wall carbon nanotubes", *Physical Review B*. 2002, 65, 155412-1 – 155412-9.

Jorio, A., Pimenta, M.A., Filho, A.G.S., Saito, R., Dresselhaus, G., Dresselhaus, M.S.
“Characterising carbon nanotube samples with resonance Raman scattering”, *New Journal of Physics*, 2002, 5, 139.1 – 139.17.

Kataura H, Kumazawa Y, Maniwa Y, Umezumi I, Suzuki S, Ohtsuka Y, *et al.* “Optical properties of single-wall carbon nanotubes”. *Synthetic Metals*. 1999; 103: 2555-8.

Keogh SM, Hedderman TG, Gregan E, Farrell GF, Chambers G, Byrne HJ.
Spectroscopic analysis of single walled carbon nanotube and semi-conjugated polymer composites. *Journal of Physical Chemistry B*. 2004; 108(20): 6233-41.

Keogh SM, Hedderman TG, Ruther MG, Lyng FM, Gregan E, Farrell GF, *et al.*
“Temperature induced nucleation of poly(m-phenylenevinylene-co-2,5-dioctoxy-p-phenylenevinylene) crystallization by HiPco single-walled carbon nanotubes”. *Journal of Physical Chemistry B*. 2005; 109 (12): 5600-7.

Kukovecz A, Kramberger C, Georgakilas V, Prato M, Kuzmany H. “A detailed Raman study on thin single-wall carbon nanotubes prepared by the HiPco process”. *European Physical Journal B*. 2002; 28: 223-30.

Kuhlmann, U., Jantoljak, H., Pfander, N., Bernier, P., Journet, C., Thomsen, C.
“Infrared active phonons in single-walled carbon nanotubes”. *Chemical Physics Letters*.
1998, 294, 237-240.

Kuzmany, H., Plank, W., Hulman, M., Kramberger, Ch., Gruneis, A., Pichler, Th.,
Peterlik, H., Kataura, H., Achiba, Y. “Determination of SWCNT diameters from the
Raman response of the radial breathing mode”, *The European Physical Journal B*.
2001, 32, 307-320.

Lian Y, Maeda Y, Wakahara T, Nakahodo T, Akasaka T, Kazaoui S, *et al.*
“Spectroscopic study on the centrifugal fractionation of soluble single-walled carbon
nanotubes”. *Carbon*, 2005; 43: 2750-59.

O’Connell M.J., Bachilo S.M., Huffman C.B., Moore V.C.; Strano M.S., Haroz E.H.,
Rialon, K.L., Boul P.J., Noon W.H., Kittrell C., Ma, J., Hauge, R.H., Weisman R.B.,
Smalley R.E. “Bandgap fluorescence from individual single-walled carbon nanotubes”
Science, 2002, 297, 593-6.

Pimenta, M.A., Jorio, A., Brown, S.D.M., Filho, A.G.S., Dresselhaus, G., Hafner, J.H.,
Lieber, C.M., Saito, R., Dresselhaus, M.S. “Diameter dependence of the Raman D-band
in isolated single-wall carbon nanotubes”, *Physical Review B*. 2001, 64, 041401-1 –
041401-4.

Pimenta, M.A., Marucci, A., Brown, S.D.M., Matthews, M.J., Rao, A.M., Eklund, P.C., Smalley, R.E., Dresselhaus, G., Dresselhaus, M.S. "Resonant Raman effect in single-wall carbon nanotubes", *Journal of Materials Research*.1998, 13, 2396-2404.

Rao, AM, Richter E, Bandow, S, Chase, B, Eklund, PC, Williams, KC, Fang, S, Subbaswamy, KR, Menon, M, Thess, A, Smalley, RE, Dresselhaus, G, Dresselhaus, MS. "Diameter-Selective Raman Scattering From Vibrational Modes in Carbon Nanotubes." *Science*, 1997, 275, 187-191.

Saito, R., Dresselhaus, G., Dresselhaus, M.S. "*Physical properties of carbon nanotubes.*" 1998, Imperial College Press, London.

Wayne, R.P. "Photochemistry", 1970, Butterworth and Co. Ltd., London, 59-100.

Yu Z, Brus J. "Rayleigh and Raman Scattering from individual carbon nanotube bundles." *Journal of Physical Chemistry B*, 2001, 105, 1123-34.

Chapter 5

“Nanotube medium interactions”

Adapted from

“Probing the interaction of single walled carbon nanotubes within cell culture medium as a precursor to toxicity testing.” Carbon 45, 34–40, 2007.

5.1 Introduction.

Understandably, for the area of bio-nanotechnology to advance, there has been a shift in current research towards more biologically compatible materials (Bandyopadhyaya *et al*, 2002; Chambers *et al*, 2003; Casey *et al*, 2005; Moulton *et al*, 2005; Salvador-Morales *et al*, 2006). The large surface area to volume ratio of nanoparticles renders them very attractive for a range of bio-related applications such as targeted drug delivery. SWCNT for example have been identified as potentially suitable candidates for targeted drug delivery as well as a range of bio sensing devices (Venkatestan *et al*, 2005). As a result of this drive to integrate nanotubes, in particular SWCNT, with biological systems, several calls have been made for a thorough assessment of the potential health risks of these materials to be carried out. Indeed there has been an increase in studies investigating the toxicity of SWCNT; however conflicting results seem to have emerged.

The *in vitro* cytotoxicity testing of SWCNT (Cui *et al*, 2005; Bottini *et al*, 2006) typically involves their dispersion within a cell culture medium, followed by their subsequent addition to a cell line of interest in the medium in which they have been dispersed. The degree of interaction between the SWCNT and the medium in which they are dispersed and the influence of such interactions on cell viability, however, has been completely uncharacterised in the literature. It is well established that SWCNT interact strongly with and can be made soluble by many molecular species including small organic molecules (Hedderman *et al*, 2004; Valeentini *et al*, 2006), organic polymers (Dalton *et al*, 2000; Keogh *et al*, 2004) polysaccharides (Bandyopadhyaya *et al*, 2002; Chambers *et al*, 2003; Casey *et al*, 2005), amino acids, proteins (Salvador-Morales *et al*, 2006) and DNA (Moulton *et al*, 2005). The mechanism is well understood as a reversible physisorption process (Keogh *et al*, 2004). It is thus suggested here that the potential for such interactions to occur may be one source of the disparity in the current literature.

This chapter will explore the interactions of SWCNT with the cell growth medium, which is a complex mixture of various different components vital for cellular growth (see appendix 2). Many of the components of the medium are known to interact with SWCNT to varying degrees. This chapter will use spectroscopic analysis to probe the interactions of SWCNT with the constituent components of the medium, highlighting the potential role that these interactions may play in the toxicity of these materials. UV/visible absorption and fluorescence spectroscopy were employed to examine the interactions and to differentiate between the effects on some of the constituent components of the medium, including the commonly employed foetal bovine serum growth supplement. Raman spectroscopy was employed to investigate whether the

SWCNT interactions with the constituent components resulted in debundling of the SWCNT aggregates (as produced) (Kukovecz *et al*, 2002), a critical consideration when evaluating the toxicity of these materials (Donaldson *et al*, 2006; Smart *et al*, 2006).

5.2 Experimental.

5.2.1 Dispersion of SWCNT.

Stock solutions of SWCNT were dispersed (see section 4.8.2) both in medium (F12K) containing 5% FBS, as is typical in cell culture experiments and medium without the addition of serum (0%). An initial concentration of 1 mg/ml of SWCNT was dispersed in both the medium containing the added serum (5%-FBS-F12K), and the serum free medium (0%-FBS-F12K). Then by subsequent dilution with medium the concentration of SWCNT was reduced over a wide range from the initial concentration down to a final concentration of 9.7×10^{-4} mg/ml.

5.3 Results and Discussion.

5.3.1 Initial Observations.

Initially, it was visually noted that in the higher concentration region above 0.2 mg/ml both media (5%-FBS-F12K and 0%-FBS-F12K) lost their characteristic pink colour (see appendix 3). This characteristic pink colour originates from the presence of the pH indicator phenol red within the medium. However, pH testing of the different concentrations did not show any change in their pH. A further visual difference could be observed between the different media in that the amount of SWCNT staying in suspension seemed to be greater in the presence of the serum. This indicated that the serum might be playing an active role in the dispersion of the SWCNT and so strongly interacts with the SWCNT. To further investigate this, UV/visible absorption analysis

was the first spectroscopic tool employed. Absorption spectroscopy was chosen as a starting point due to the aforementioned visual differences in the suspensions of SWCNT in the cell culture medium.

5.3.2 UV/Visible Absorption Spectroscopy.

The UV/visible absorption spectrum of 5%-FBS-F12K medium (figure 5.1.b) consists of four features at 270, 360, 410 and 560nm. The features at 270 and 410nm can be assigned to the added 5% FBS as they are not present in the serum free medium and indeed a spectrum of 5% (v/v) FBS in deionised water shows these features verifying that their origin is that of the FBS. Both the 5% and the 0% FBS-F12K share the features at 360 and 560nm. The feature at 360nm can be attributed to riboflavin (Posadz *et al.*, 2000, Zirak *et al.*, 2005), a vitamin present in the medium, whereas the feature at 560nm can be assigned to the phenol red indicator within the medium.

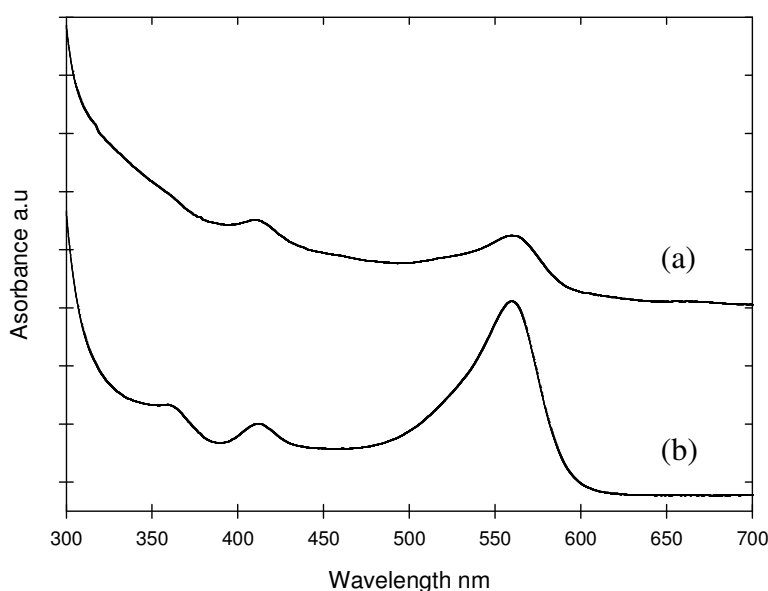


Figure 5.1. Absorption Spectra of (a) 5%-FBS-F12K containing 0.7 mg/ml SWCNT (b) 5%-FBS-F12K medium only.

Figure 5.1 compares the absorption spectrum of the 5%-FBS-F12K medium before (b) and after (a) the addition of 0.7 mg/ml SWCNT. The spectra have not been offset artificially and thus the increased baseline in (a) is a result of the addition of the SWCNT. As described in chapter 4, the absorption spectrum of SWCNT in water suspensions consists of three broad absorption features centred approximately at 1200nm, 800nm and 270nm. The peaks at 1200nm and 800nm are highly structured and are attributed to optical transitions between mirror image spikes in the diameter dependent density of states, with the feature at 270nm attributed to the π -plasma frequency of 5eV in π -conjugated carbon materials (Kataura *et al.*, 1999). At the concentrations used here, there is no evidence of these SWCNT features in the absorption spectrum. In the absence of centrifugation, the spectrum of SWCNT in water has a considerable contribution from a broad scattering background due to larger nanotubes aggregates (Yu *et al.*, 2001, Lian *et al.*, 2005). At concentrations of \sim 1g/L this scattering contribution can be up to 99% of the visible transmission losses in SWCNT solution (Giordani *et al.*, 2006). Although the SWCNT samples have been sonicated, allowed to settle for a 24 hour period and decanted, the addition of the SWCNT to the sample contributes to a significant background which can be attributed to scattering (Yu *et al.*, 2001, Lian *et al.*, 2005, Giordani *et al.*, 2006). The observed spectral changes thus do not derive from additional nanotube absorption.

Independent of this increase in scattering background, upon the addition of the SWCNT to the media the absorption spectrum undergoes significant changes. In both the medium based solutions (0% and 5% FBS-F12K) a reduction in the phenol red peak at 560nm (figure 5.1.a) is seen, which is as expected due to the colour change observed in the high SWCNT concentration region (above 0.2 mg/ml). However, as stated above, no

change in pH was registered. Organic dyes such as p-terphenyl and anthracene (Hedderman *et al.*, 2004, Hedderman *et al.*, 2006) are known to interact with SWCNT via a π - π stacking van der Waals interaction along the carbon nanotube backbone resulting in changes to their absorption and/or fluorescence spectrum and therefore this absorption reduction is not surprising. In SWCNT solutions of phenol red alone in water a similar colour change with no associated pH change is observable.

The feature at ~360nm attributed to the vitamin riboflavin is substantially reduced in both media solutions while the peak at ~ 410nm associated with the FBS serum is slightly reduced. The spectral changes indicate that the molecular components of the medium, both in the presence and absence of the serum, and indeed the serum itself, are interacting with the carbon nanotubes. Furthermore, the qualitatively different variations of the individual features indicate that the components are interacting to differing degrees. The next section will use fluorescent emission spectroscopy to complement the absorption spectroscopy and elicit further information about the interactions occurring between the individual components of the medium and the SWCNT.

5.3.3 Fluorescent Emission Spectroscopy.

Fluorescence studies have been shown to aid in the elucidation of the interaction of nanotubes with different molecular species (Hedderman *et al.*, 2006). Coleman *et al* (2004) constructed a model based on the adsorption/desorption of conjugated polymers in SWCNT composite solutions to explain the quenching of the fluorescence of the polymer when bound to the SWCNT. The analysis has more recently been extended to smaller organic molecules (Hedderman *et al.*, 2006). The ratio of the maximum fluorescence intensity of the composite solution, which contains bound and unbound

molecules, and the maximum fluorescence of the pristine molecular solution, which comprises solely of unbound molecules, was plotted as a function of concentration of SWCNT, C_{NT} . Equation 5.1 represents the dynamic equilibrium at which the adsorption rate equals the desorption rate, where N_F is the number of free molecules, N_B is the number of bound molecules, Fl_{comp} is the fluorescence of the composite and $Fl_{molecule}$ is the fluorescence of the pristine solution which gives the fraction of free molecules in solution. The model was derived for 1:1 ratios by mass and so for all concentrations the partial SWCNT concentration, C_{NT} , equals the partial molecular concentration, C_m .

$$\frac{N_F}{N_F + N_B} = \frac{1}{1 + C_{NT}/C_0} = \frac{Fl_{comp}}{Fl_{molecule}} \quad \text{Equation 5.1.}$$

C_0 is a characteristic concentration associated with the interaction and is described by

$$C_0 = \frac{\pi^2 \nu \rho_{Bun} A_{Bun} e^{-E_b/kT}}{48Df} \quad \text{Equation 5.2.}$$

where ν is a desorption pre-exponential frequency factor, ρ_{bun} is the bundle mass density, A_{bun} is the bundle surface area, E_b is the binding energy between the nanotube and the fluorescent molecule, D is a diffusion co-efficient for fluorescent molecule and f is a space integral. C_0 may be considered as a ratio of the desorption rate to the adsorption rate and thus equation 5.1 can be considered similar to that describing a Langmuir isotherm describing the adsorption of gases on a solid surface (Atkins *et al*). The system equates at equilibrium to the rate of adsorption of the molecules via van der Waals interaction onto a surface of area A_{bun} as it diffuses through the solvent, to the desorption rate which is largely determined by the binding energy. Applied to the experimental data of (Coleman *et al.*, 2004), deviation from the ideal behaviour was

shown to result from changes in the size of the SWCNT species, implying bundle size and as a result the model is able to elucidate concentration ranges in which the polymer interacts with the SWCNT individually and in bundles of varying diameter. For the purpose of this study this model will be employed to assess the degree of interaction between the SWCNT and a variety of different fluorophores. Where applicable their emission behaviour was monitored as a function of SWCNT concentration and fitted to the model proposed by Coleman *et al* (2005) allowing characteristic concentrations (C_0) to be estimated for the molecule under test. This C_0 value was then used to estimate the degree of interaction between the SWCNT and the relevant molecule. According to *equation 5.2* the C_0 value is inversely proportional to the binding energy (E_b) the nature of this relationship would imply that a low C_0 value would correspond to a higher E_b (higher degree of interaction) and similarly a high C_0 value would correspond to a lower E_b hence a lesser degree of interaction.

Concentration dependent fluorescent studies were thus employed to further elucidate the interaction between the medium (with and without serum) and the SWCNT. The 0% and 5%-FBS-F12K solutions have one absorption band in common, namely that of the riboflavin at 360nm, so this was chosen as the first excitation wavelength. Excitation at this wavelength yielded a broad emission spectrum centred at ~450nm in both serum free and containing medium (see appendix 4).

Figure 5.2 shows the ratios of the quenching of emission at 450nm by 360nm excitation of the medium as a function of SWCNT concentration in serum free medium (●) and 5% FBS (Δ) containing medium.

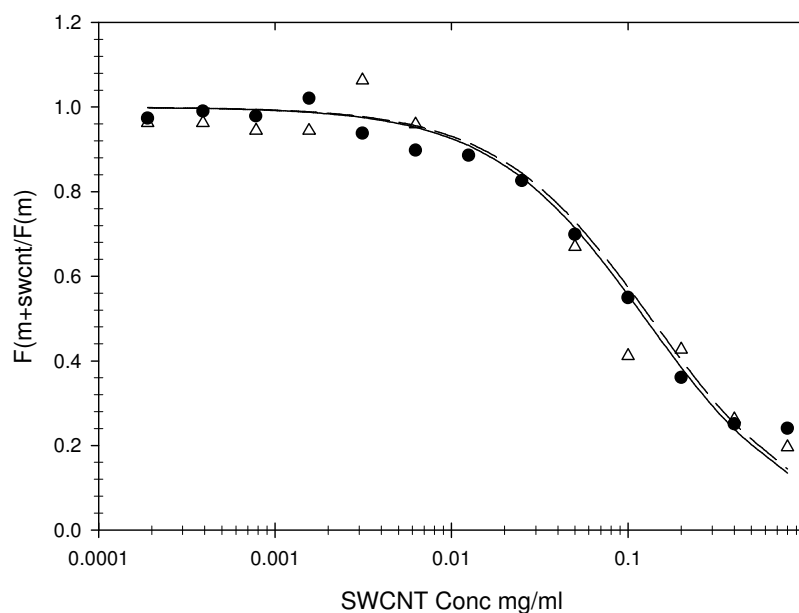


Figure 5.2. Plot of the emission ratios at 450nm by 360nm excitation of (●) 0%-FBS-F12K $C_0 = 0.135 \pm 0.020$ mg/ml and (Δ) 5%-FBS-F12K $C_0 = 0.125 \pm 0.020$ mg/ml.

A similar trend can be observed from the two plots, the ratio of fluorescence decreased as the concentration of SWCNT increased indicating an increased probability of adsorption of riboflavin onto the SWCNT surfaces with increased concentration. The plots were fitted with the model allowing a characteristic concentration value (C_0) to be evaluated. The fits yielded values of 0.135 ± 0.020 mg/ml (solid line) for the 0%-FBS-F12K and a marginally lower value of 0.125 ± 0.020 mg/ml (dashed line) for the 5%-FBS-F12K. Within the experimental accuracy, this indicates that the presence of the serum does not significantly influence the interaction of the riboflavin with the SWCNT.

Further fluorescence studies were carried out with the 5%-FBS-F12K, as the addition of the serum yielded new features in the spectrum at 268 and 410nm which were attributed

to the bovine serum. Both of these serum features gave rise to fluorescent emission, excitation by 268nm giving a maximum emission at 350nm (see appendix 5) and 410nm excitation giving a maximum emission at 470nm (see appendix 6). Figure 5.3 depicts the ratios between the intensity of emission at 350 nm (●) and 470 nm (Δ) for 268nm excitation and 410nm excitation respectively in 5%-FBS-F12K cell culture medium with varying SWCNT concentration. The solid and dashed lines show fits of equation 5.1. The quenching behaviour as a function of concentration is similar to that observed for 360nm excitation, yielding similar shaped curves and using the outlined model (Coleman et al., 2004) C_0 values were calculated to be $0.145 \pm 0.02\text{mg/ml}$ (solid line) and $0.2 \pm 0.02\text{mg/ml}$ (dashed line) for 268 and 410nm excitation respectively in 5%-FBS-F12K.

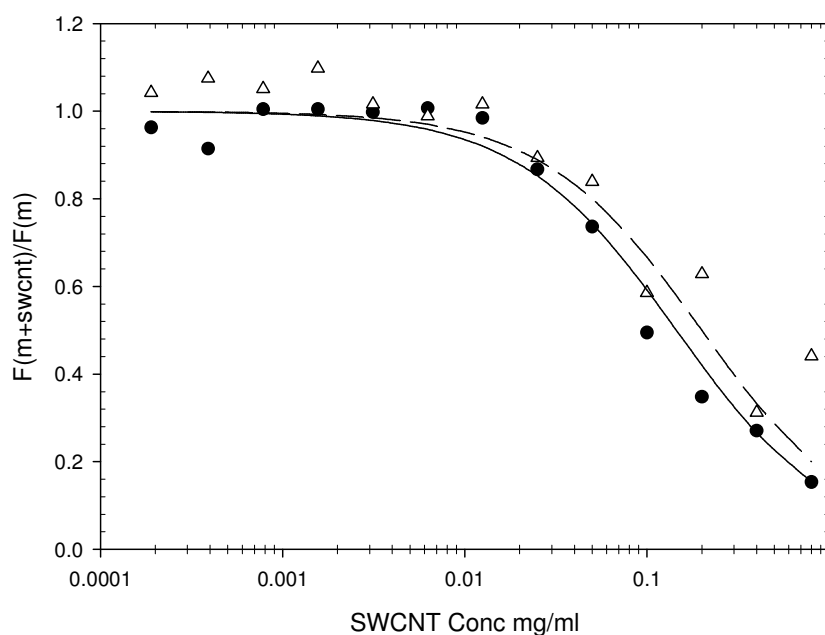


Figure 5.3. Plot of emission ratios against SWCNT concentration by (●) 268nm excitation $C_0 = 0.145 \pm 0.02\text{mg/ml}$ and (Δ) 410nm excitation $C_0 = 0.2 \pm 0.02\text{mg/ml}$ for 5%-FBS-F12K cell culture medium.

A similar concentration study of the FBS alone and the SWCNT was then carried out to further investigate the nature of this interaction. For this a concentration study was carried out by initially dispersing the SWCNT in 100% FBS at an initial concentration of 1000 mg/L which was then serially diluted with deionised water over the same SWCNT concentration range as used in the medium study. As the features at 268 and 410nm originate from the FBS, these excitation wavelengths were chosen for the study of the serum's interaction with the SWCNT. A similar trend was observed in the emission quenching ratio as for the medium (figure 5.4). C_0 values were evaluated for both the excitation wavelengths, 268nm yielding a C_0 value of $0.2 \pm 0.02\text{mg/ml}$ (solid line) and 410nm yielding a similar C_0 value of $0.275 \pm 0.02\text{mg/ml}$ (dashed line).

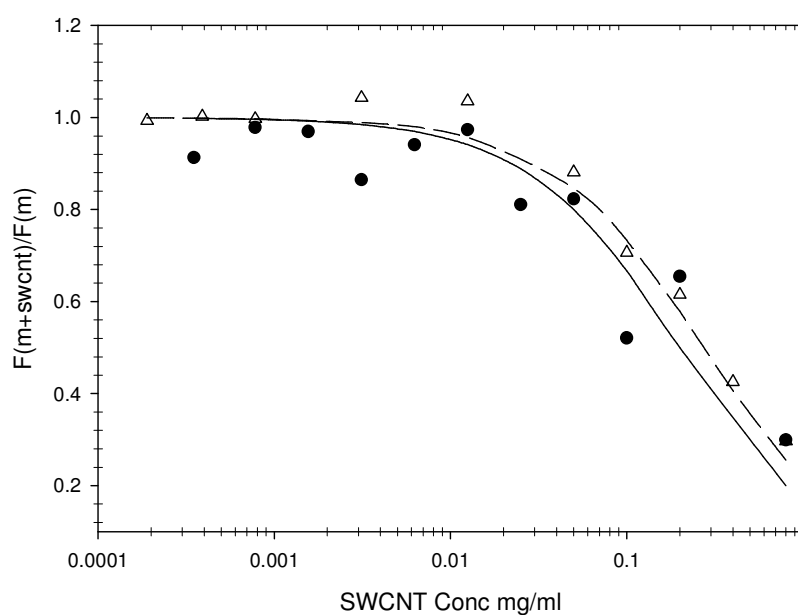


Figure 5.4. Plot of emission ratios against SWCNT concentration for a 1:1 ratio dilution of FBS at (●) 268nm excitation $C_0 = 0.2 \pm 0.02\text{mg/ml}$ and (Δ) 410nm excitation $C_0 = 0.275 \pm 0.02\text{mg/ml}$.

In comparison to other studies in which variations of C_0 over several orders of magnitude are observable for different molecules (Coleman *et al.*, 2004, Hedderman *et*

al., 2006), the C_0 values derived show little variation for all the features examined. The similarities of the values for the 360nm peak with and without serum indicate that the serum has little effect on the interaction between the riboflavin and the SWCNT. The values for the serum emission features are consistently higher however. Indeed the values for the 470nm emission are consistently higher than those for the 350nm emission both in the serum containing medium and the serum solution, potentially indicating that they have origin in different components of the serum. The characteristic concentration is essentially a ratio of desorption and adsorption rates (equation 5.2). Included in the desorption rate is the binding energy, a large binding energy reducing the desorption rate and consequently the C_0 value. The adsorption rate is critically dependant on the diffusion rate and thus the hydrodynamic radius of the adsorbing molecule. Large bulky molecules have slow diffusion rates and would be expected to yield large C_0 values. The indications are therefore, that the large protein molecules of the serum are relatively weakly bound and are slow to adsorb. Equally however, they are slow to diffuse once desorbed and so likely to play a stronger role in the solubilisation of the SWCNT which would give support to the visual observation of the serum based medium retaining more SWCNT in solution. The similarity of the C_0 values of all species may be an indication that the rates of adsorption and desorption are regulated by the complex composition of the medium. That the C_0 values of the serum-only solutions are higher may reflect a higher desorption rate in the purely water based solution. A direct comparison of the relative strengths of interactions should be through the calculated binding energies (Coleman *et al.*, 2004, Hedderman *et al.*, 2006). For such a comparison, however, parameters such as the hydrodynamic radius should be precisely known. In a complex mixture this may differ significantly from that in a

simple solution, measurements of the interaction of the individual will be discussed in section 5.4.

In terms of processing for potential applications, the ability to debundle the as produced SWCNT aggregates is critical. Similarly, whether SWCNT are presented to cells in large bundles or as isolated tubes is expected to significantly influence their toxicology. Indeed recent studies have noted decreased cytotoxicity of large aggregates of SWCNT in comparison to smaller bundles (Wick *et al*, 2007). The original study by Coleman *et al* demonstrated that changes in the composite concentration could affect the degree of SWCNT bundling. A constant value of C_0 , arising from a good fit to the behaviour predicted by equation 5.1 indicated that the degree of bundling (or debundling) was constant over the concentration range studied. That a good fit to the model is observed here would imply that the nanotube bundling (or de-bundling) is constant over the concentration range studied here. Over the range of concentrations therefore, the SWCNT are present in solution in a concentration dependent dynamic equilibrium between adsorption and desorption. It is noted that such species will contribute significantly to the scattering of incident light across the visible spectrum as is suggested by the offset of the absorption spectrum in figure 5.1.

5.3.4 Raman Spectroscopy.

Raman spectroscopy was employed to probe the effect on the SWCNT upon interaction with the medium. Raman analysis was carried out on all samples at 514.5 nm laser excitation. As described in chapter 4, the Raman spectrum of pristine nanotubes consists primarily of three main features, the radial breathing mode (RBM), the D line and the G line (Dresselhaus *et al.*, 2002). These modes are very sensitive to any perturbation to the

local environment of the nanotube and are therefore a good indication of complex formation and/or aggregate debundling (Curran *et al.*, 1998, Hadjiev *et al.*, 2001, Wise *et al.*, 2004, Keogh *et al.*, 2005).

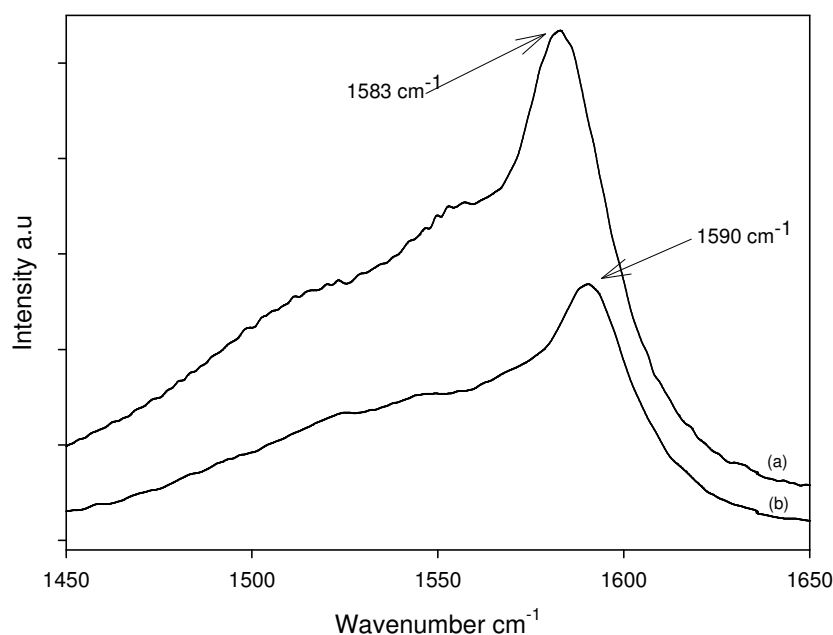


Figure 5.5 G-line region for 514.5nm excitation (a) Raw SWCNT Soot. (b) 5%-FBS-F12K containing 0.1 mg/ml SWCNT.

Firstly changes were observed in the G-line region of the spectrum positioned at ~ 1580 cm^{-1} (figure 5.5a). Similar shifts were observed in nanotube deposits from the serum free medium. This mode involves tangential C–C bond stretching motions and stems from the E_{2g} mode at 1580 cm^{-1} in graphite (Dresselhaus *et al.*, 2002). This mode exhibits a definite upward shift of ~ 7 cm^{-1} in the 5%-FBS-F12K (figure 5.5b). Similar up shifts in this mode have been reported before in SWCNT bundles and SWCNT/epoxy resin composites (Wise *et al.*, 2004) and with composites involving gamma cyclodextrins (Chambers *et al.*, 2003). In terms of the SWCNT/epoxy resin composites (Wise *et al.*, 2004) it was reported that the G-line up shifted by

approximately 3cm^{-1} when the SWCNT were embedded in 'Shell epoxy resin 862/EPI-CURE W' (Wise *et al.*, 2004). In such studies it was noted that changes in both the RBM and G-Line were observed with changes in pressure and significantly shifts of $\sim 14\text{cm}^{-1}$ were observed in the G-line region with respect to increasing pressure. It was further suggested that these shifts under the influence of hydrostatic pressure are in fact governed by van der Waals type interactions and may be the result of a lowering of the cylindrical symmetry of the tube (Wise *et al.*, 2004). The observed shifts are thus consistent with the coating of the SWCNT with molecular components of the medium and or the serum through van der Waals physisorption.

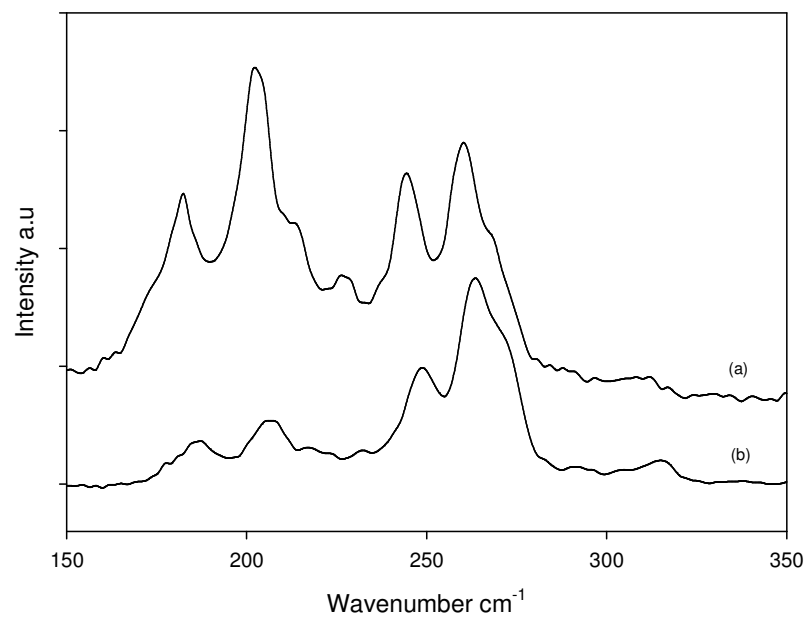


Figure 5.6 Radial breathing mode regions for 514nm excitation (a) Raw SWCNT Soot (b) 5%-FBS-F12K containing 0.1mg/ml SWCNT.

The frequency positioning of the RBM's of pristine nanotubes (figure 5.6a) are inversely related to the diameters of the nanotubes (Kukovecz *et al.*, 2002, Yu *et al.*, 2001) and using this relationship, a diameter range for the raw sample was calculated (Kukovecz *et al.*, 2002) to be from 0.8nm-1.4nm. The RBM spectrum is also significantly influenced

by the local environment and incurred changes can be employed to interpret such effects as de-bundling or selective solubilisation (Kataura *et al.*, 1999, Hedderman *et al.*, 2004, Keogh *et al.*, 2004.). Figure 5.6 depicts the radial breathing mode region at 514.5 nm excitation for (a) Raw SWCNT and (b) 5%-FBS-F12K with 0.1 mg/ml SWCNT, these RBM's were fitted with a combination of Lorentzian and Gaussian fits with Lab spec Version 4.1 (fits not shown). The concentration of 0.1 mg/ml shown above is well below the C_0 values estimated from the emission studies. As can be seen there are significant differences between the responses of the raw SWCNT (figure 5.6a) and that of the 0.1 mg/ml complex with the 5%-FBS-F12K (figure 5.6b). There is no significant change of the diameter distribution which would be indicative of selective solubilisation or de-bundling (Kukovecz *et al.*, 2002). However there is a reduction in the relative intensity of some of the modes at lower wavenumbers in comparison to that of the raw sample (figure 5.6a), but they are still present within the spectrum of the 0.1 mg/ml 5%-FBS-F12K media complex. This would suggest the SWCNT are present in the suspension as aggregates/bundles at all stages which would correlate well with conclusions drawn from the emission spectroscopy. Due to the nature of the quenching of emission observed, it was postulated that the same two species are interacting over the concentration range studied. It should be concluded therefore that the nanotubes, at all concentrations exist as bundles rather than individual tubes when dispersed in cell culture medium.

5.4 Individual Components.

To gain more information regarding the nature of the interactions of SWCNT within the cell culture medium the same spectroscopic techniques that were employed in section

5.3 will again be used, to assess the degree of interaction between the SWCNT and some of the medium's individual components. As a spectroscopic study of the interaction between the SWCNT and added protein was carried out and discussed earlier (*section 5.3.3*) it will not be discussed in this section. Three individual components of the medium were studied which were as follows the B vitamin riboflavin, phenylalanine and glutamic acid, two amino acids present in the medium.

In all tested components SWCNT containing solutions were prepared by dispersing, with the aid of a sonic tip, an initial concentration in a 1:1 mass ratio of the component under test, riboflavin/phenylalanine/glutamic acid and HiPco SWCNT in deionised water. The concentrations were then reduced over a wide range by serial dilution with deionised water and sonication. All solutions were then characterised spectroscopically after a 24 hour settling period.

5.4.1 Riboflavin.

Riboflavin, also known as vitamin B₂, is an easily absorbed micronutrient with a key role in maintaining health in animals. It is required for a wide variety of cellular processes. Like the other B vitamins, it plays a key role in energy metabolism, and is required for the metabolism of fats, carbohydrates, and proteins. Its presence in the medium hence is vital for healthy cellular growth.

Riboflavin is yellow or orange-yellow in colour and its absorption spectrum consists of a broad band centred at approximately 360nm (Posadaz *et al.*, 2000, Zirak *et al.*, 2005). Excitation by 360nm yields a broad emission feature centred at approximately 500nm. It is noted that the observed emission behaviour is different than that observed in the

medium study (*section 5.3.3*) which yielded an emission spectrum centred at approximately 450nm. The difference in emission may have resulted from the presence of the battery of different components present in the medium (see appendix 2) which may have resulted in a change in the emission behaviour of the riboflavin due to inter component interaction when in the medium, essentially a solvatochromatic shift.

As expected, upon the addition of SWCNT to the solution of riboflavin, the emission feature was reduced. This quenching of emission was then monitored as a function of SWCNT concentration and plotted as a ratio (figure 5.7) of the emission of a dispersion of riboflavin and SWCNT in equal mass concentration divided by the emission of riboflavin of the same mass concentration. This ratio was then fitted with the earlier described model proposed by Coleman *et al* (2005) (equation 5.1) facilitating a characteristic concentration for riboflavin to be evaluated.

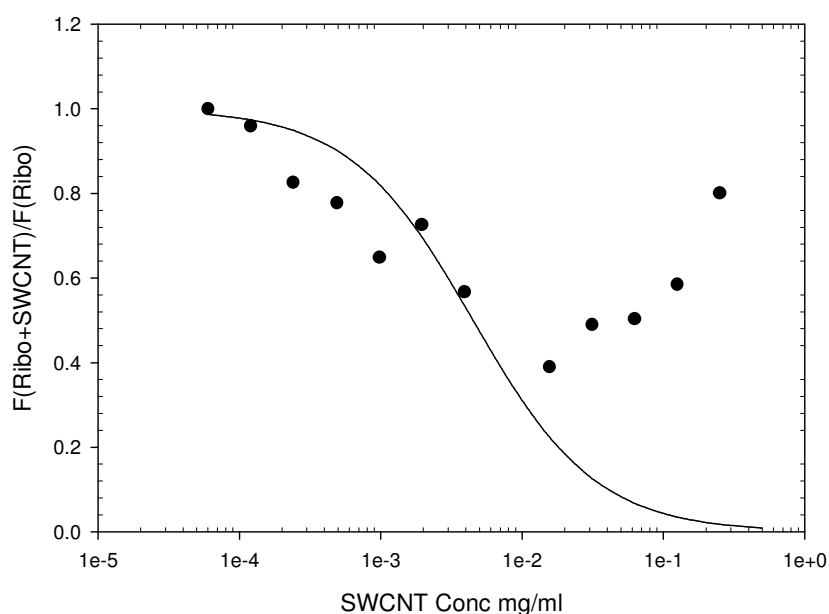


Figure 5.7 Plot of emission ratios at 500nm by 360nm excitation against concentration for a 1:1 mass ratio dilution of Riboflavin and SWCNT in deionised water. $C_0 = 0.0045 \pm 0.002$ mg/ml.

The ratio plot in figure 5.7 was fitted with the model allowing a characteristic concentration value (C_0) to be evaluated; the fit yielded a C_0 value of 0.0045 ± 0.002 mg/ml. The nature of the ratio plot (figure 5.7) is in very good agreement with the original plot presented by Coleman *et al* (2005) from which the model was derived. In the study, ratio points which correlated with the model fit (*equation 5.2*) were shown microscopically to be of constant size and deviation from the model in the higher concentration region was shown to be a result of changing aggregate size. Therefore the authors postulated that the use of the model could aid in the determination of concentration ranges in which individual tubes were present in the suspension and effectively with the visualisation of the concentration dependent debundling process. Deviation from the model fit seen here in the higher concentration region (figure 5.7) may give an indication that the aggregation state of the SWCNT is altered as a function of concentration by the riboflavin. The poor fit of the data to the model even at low concentrations indicates that even below the critical concentration the nanotubes are not fully debundled.

Upon examination of the RBM region of the Raman spectrum of the riboflavin SWCNT suspension (figure 5.8b) no differences were detectable in the diameter distribution from that of the raw (figure 5.8a). However there are differences in the relative intensities between the raw SWCNT and suspension this may indicate that a degree of debundling occurred which remained constant over the concentration range studied here.

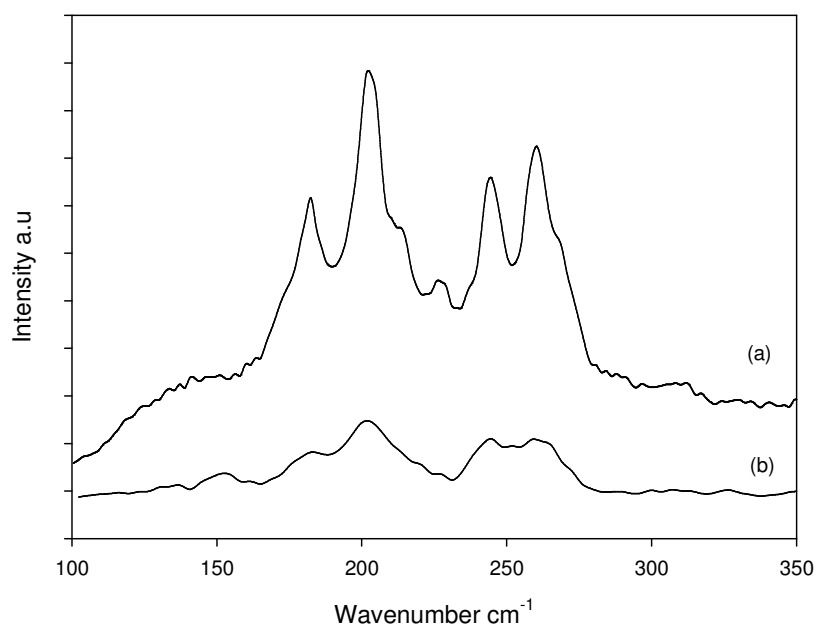


Figure 5.8 Radial breathing mode region for 514.5nm excitation (a) Raw SWCNT Soot (b) 0.125mg/ml SWCNT in 0.125mg/ml riboflavin taken from a drop cast sample.

When this vitamin was studied in the medium the fits yielded C_0 values of 0.135 ± 0.020 mg/ml for the 0%-FBS-F12K and a marginally lower value of 0.125 ± 0.02 mg/ml for the 5%-FBS-F12K (figure 5.2). The difference between these values and the value evaluated here for the individual vitamin ($C_0 = 0.0045 \pm 0.002$ mg/ml) may suggest that in the presence of the other components of the medium there are conflicting interactions between each component and the SWCNT resulting in the differing C_0 values being obtained.

5.4.2 Amino Acids (Phenylalanine and Glutamic Acid).

The amino acids phenylalanine and glutamic acid were examined in this study. They were chosen as they are present in the medium and, as amino acids are the basic structural building units of proteins, it was hoped their examination would provide further information into the interaction of the added protein supplement and the

SWCNT and the medium mixture itself. Amino acids form short polymer chains called peptides or longer chains either called polypeptides or proteins. In chemistry, an amino acid is a molecule that contains both amine and carboxyl functional groups. They can be divided into two classes; essential and standard amino acids. Essential cannot be synthesized by organisms whereas standard can be synthesized by organisms from other molecules and used to form proteins. Phenylalanine is an essential amino acid whereas glutamic acid is a standard amino acid.

Absorption spectroscopy revealed phenylalanine and glutamic acid to have absorption bands centred at 255nm and 260nm. 255nm excitation for phenylalanine yielded an emission band centred at 420nm whereas 260nm excitation for glutamic acid yielded an emission band centred at 425nm.

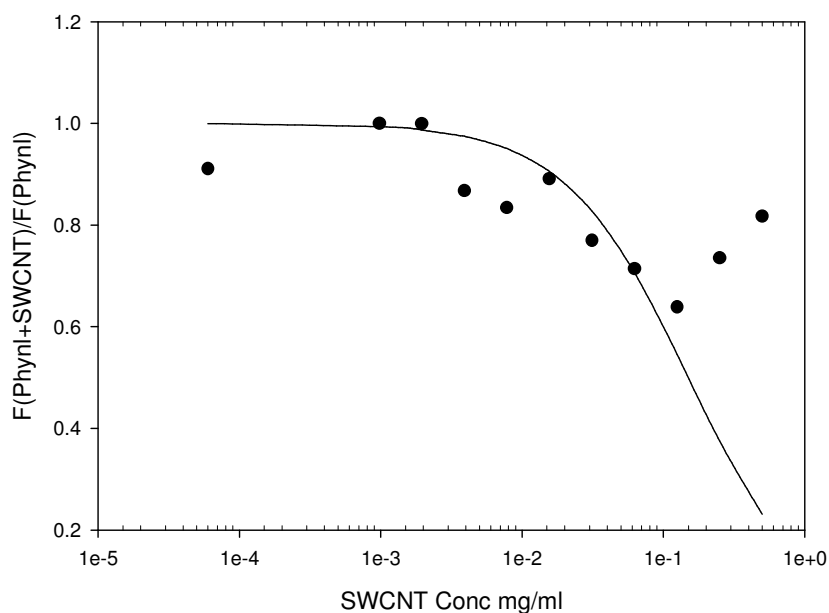


Figure 5.9 Plot of emission ratios at 420nm against SWCNT concentration for a 1:1 mass ratio dilution of Phenylalanine in deionised water. $C_0 = 0.15 \pm 0.02$ mg/ml.

These emission features were again seen to be quenched upon the addition of SWCNT. The quenching of emission was then monitored as a function of SWCNT concentration and plotted as a ratio as before (figure 5.9 and 5.10). A similar trend to that of the riboflavin was observed and fitting the ratio plots with the previously described model (Coleman *et al*, 2005) yielded C_0 values of 0.15 ± 0.02 mg/ml for phenylalanine and 0.008 ± 0.002 mg/ml for glutamic acid. These values were much lower than those obtained for the added FBS protein supplement when it was studied both in the medium and individually in section 5.3.3. Again, deviation from the model fit was noted in the higher concentration region for both amino acids tested, which as stated previously gives an indication that the aggregation state of the SWCNT present is changing as a function of concentration.

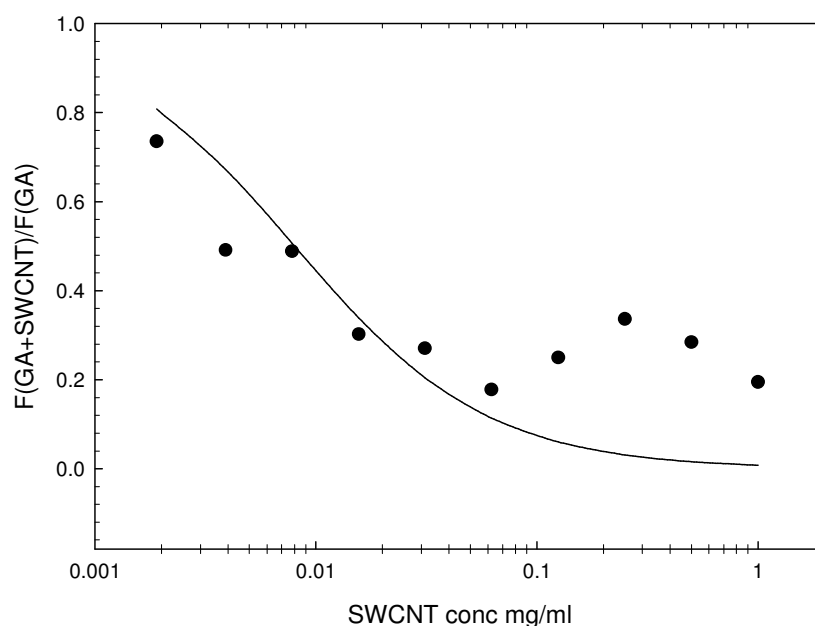


Figure 5.10 Plot of emission ratios at 425nm against SWCNT concentration for a 1:1 mass ratio dilution of Glutamic Acid in deionised water. $C_0 = 0.008 \pm 0.002$ mg/ml.

Raman spectroscopy was utilised to examine the RBM region of the SWCNT present in the sample. As can be seen in figure 5.11, differences are noted between the RBM of

the suspensions (figure 5.11 b and c) when compared to that of the pristine SWCNT (figure 5.11a). There is no reduction in the diameter distribution of the suspensions, based on the relationship between RBM position (cm^{-1}) and tube diameter, as described in section 4.5.1, to that of the pristine SWCNT. However as can be seen (figure 5.11), there are differences in the relative intensity of the RBM's present when compared to that of the pristine SWCNT sample. Furthermore a definite up shift in wavenumber position of the present RBM's can be observed when compared (see dashed lines on figure 5.11) to that of the pristine SWCNT spectrum. This decrease in relative intensity coupled with the observed up shift in RBM position is indicative of a debundling effect on the SWCNT samples (Heller *et al*, 2004, Lian *et al*, 2005) indicating that in the absence of the other medium components the two amino acids studied, phenylalanine and glutamic acid, have the capability to alter the aggregative state of the tested SWCNT samples.

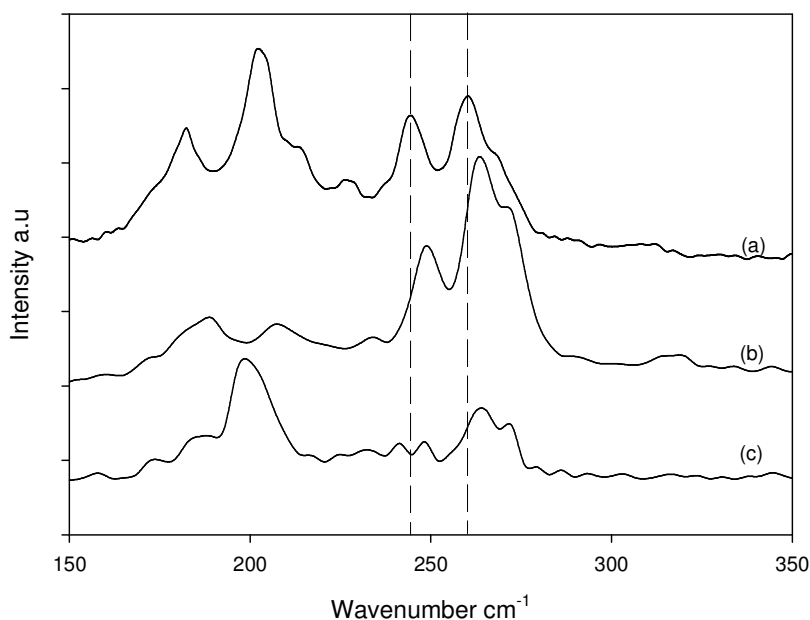


Figure 5.11 Radial breathing mode region for 514.5nm excitation (a) Raw SWCNT Soot (b) 0.125mg/ml SWCNT in equal concentration glutamic acid (c) 0.0315mg/mg SWCNT in equal concentration phenylalanine, taken from a drop cast sample.

While not giving any direct insight into the interaction occurring between the SWCNT and the added FBS protein in the medium the study has shown that amino acids, which combine to form proteins, unquestionably interact to varying degrees with SWCNT. The measurements give support to the data presented in section 5.3 that the various medium components and the added FBS protein supplement interact with SWCNT upon their dispersion. The potential implications of these, previously unrecognised interactions, for the *in vitro* toxicity of SWCNT will be discussed in chapter 6.

5.5 Chapter Summary.

This chapter has demonstrated clearly that upon the dispersion of nanotubes within a cell culture medium there are considerable interactions, which have been previously uncharacterised. The interaction is most likely a physisorption through van der Waals forces. Both the intrinsic components of the medium and the added FBS protein growth supplement are seen to interact with the SWCNT. The presence of the FBS serum was seen to aid the dispersion of the nanotubes.

Over the concentration range studied, the fluorescence quenching behaviour indicated that the aggregation state of the nanotubes did not vary and Raman spectroscopy verified that they are present as bundles similar to those of the as produced samples. Further spectroscopic studies were carried out with three of the individual components of the medium. Riboflavin, a vitamin found in the medium and the origin of the absorbance peak at 360nm in the medium, was shown to interact individually with the SWCNT. The characteristic concentration value (C_0) evaluated for riboflavin on its own was two orders of magnitudes lower than when studied in the medium and it was

postulated that this difference in C_0 values was a result of conflicting interactions between the medium components and SWCNT. Two standard amino acids, namely phenylalanine and glutamic acid, were examined to further elucidate information to the interaction of the added protein supplement and the SWCNT. These amino acids both yielded C_0 values two orders of magnitude less than that of the added protein supplement. The characteristic concentration is essentially a ratio of desorption and adsorption rates (equation 5.2). Included in the desorption rate is the binding energy, a large binding energy reducing the desorption rate and consequently the C_0 value. The adsorption rate is critically dependant on the diffusion rate and thus the hydrodynamic radius of the adsorbing molecule. Large bulky molecules, such as the added protein, have slow diffusion rates and would be expected to yield large C_0 values. The indications are therefore, that the large protein molecules of the serum are relatively weakly bound and are slow to adsorb, in contrast the amino acids which are smaller molecules and yield substantially lower C_0 values. According to the original model (Coleman *et al*, 2005) these molecules are expected to have a higher binding energies than that of the protein.

Minimal processing of the SWCNT samples was employed to mimic exposure to the raw, as-produced powder. This has shown that although the nanotubes are dispersed by the medium, they remain as larger diameter bundled aggregates. Thus, the likelihood of toxicity as a result of internalisation within the cell walls is reduced. More recent studies have shown a reduced toxicity for SWCNT aggregates (Wick *et al*, 2007) which is expected to originate from the decrease surface area in aggregates in comparison to individual tubes. A number of studies have shown that cellular internalization of various nanoparticles can occur (Stearns *et al.*, 2001, Monteiro-

Rivere *et al.*, 2005, Rouse *et al.*, 2006) with endocytosis being the most probable mechanism of uptake. However, transmission electron microscopy has confirmed that there was no intracellular localization of the tested SWCNT in A549 cells following 24 h exposure (Davoren *et al.*, 2007).

Finally it should be noted that although spectroscopic studies in this chapter indicated that the SWCNT remained as bundles when dispersed in the medium, if increased processing of the SWCNT samples to isolate the tubes was carried out, this would potentially result in an increased surface area per weight of SWCNT increasing the possibility for further interaction with the growth medium prior to cellular exposure. The interaction of these bundles with the growth medium and supplement, it is postulated, may result in a reduction in the availability of the constituents to the cells, potentially resulting in a secondary rather than primary toxicity of the SWCNT; this proposed notion of an indirect toxicity by medium depletion will be explored in chapter 6.

References.

Atkins P, De Paula J. Physical Chemistry, Eighth Edition, ISBN-10: 0-19-870072-5
Chapter 25, page 917.

Bandyopadhyaya R, Nativ-Roth E, Regev O, Yerushalmi-Rozen R. “Stabilization of individual carbon nanotubes in aqueous solutions.” *Nanoletters*. 2002; 2: 25-8.

Bottini M, Bruckner S, Nika K, Bottini N, Bellucci S, Magrini A, *et al.* . “Multi-walled carbon nanotubes induce T lymphocyte apoptosis.” *Toxicology Letters*. 2006; 160: 121-6.

Casey A, Farrell GF, McNamara M, Byrne HJ, Chambers G. “Interaction of carbon nanotubes with sugar complexes.” *Synthetic Metals*. 2005; 153: 357-60.

Chambers G, Carroll C, Farrell GF, Dalton AB, McNamara M, in het Panhuis M, *et al.* “Characterization of the interaction of gamma cyclodextrins with single walled carbon nanotubes.” *Nanoletters*. 2003; 3 (6): 843-6.

Coleman JN, Maier S, Fleming A, O’Flaherty S, Minett A, Ferreira MS, *et al.* “Binding kinetics and spontaneous single wall carbon nanotube bundle dissociation in

low concentration polymer-nanotube solution.” *Journal of Physical Chemistry B*. 2004; 108: 3446-50.

Cui D, Tian F, Ozkan CS, Wang M, Gao H. “Effect of single wall carbon nanotubes on human HEK293 cells.” *Toxicology Letters*. 2005; 155: 73-85.

Curran SA, Ajayan PM, Blau WJ, Carroll DL, Coleman JN, Dalton AB, *et al.* “A composite from poly(m-phenylenevinylene-co-2,5-dioctoxy-p-phenylenevinylene) and carbon nanotubes: A novel material for molecular optoelectronics.” *Advanced Materials* 1998; 10(14):1091-3.

Dalton AB, Stephan C, Coleman JN, McCarthy B, Ajayan PM, Lefrant S, *et al.* “Selective interaction of a semi conjugated organic polymer with single-wall nanotubes.” *Journal of Physical Chemistry B*. 2000; 104: 10012-16.

Davoren M, Herzog E, Casey A, Cottineau B, Chambers G, Byrne HJ, Lyng FM. “*In vitro* Toxicity Evaluation of Single Walled Carbon Nanotubes on human A549 lung cells.” *Toxicology in Vitro*. 2007, 21, 438-448.

Donaldson K, Aitken R, Tran L, Stone V, Duffin R, Forrest G, *et al.* “Toxicology of carbon nanotubes.” *Toxicology Science*. 2006; 92: 5-22.

Dresselhaus MS, Jorio A, Souza Filho AG, Dresselhaus G, Saito R. "Raman spectroscopy on one isolated nanotube." *Physica B* 2002; 323:15-20.

Giordani S, Bergin SD, Nicolosi V, Lebedkin S, Kappes MM, Blau WJ, *et al.* "Debundling of single-walled nanotubes by dilution: observation of large populations of individual nanotubes in amide solvent dispersions." *Journal of Physical Chemistry B*. 110 (32): 15708-15718.

Hadjiev VG, Iliev MN, Arepalli S, Files PBS. "Raman scattering test of single-wall carbon nanotube composites." *Applied Physics Letters*. 2001; 78: 3193-5.

Hedderman TG, Keogh SM, Chambers G, Byrne HJ, "Solubilisation of Single walled carbon nanotubes with organic dye molecules." *Journal of Physical Chemistry B*. 2004; 108 (49): 18860-65.

Hedderman TG, Keogh SM, Chambers G, Byrne HJ. "In-depth study into the interaction of single walled carbon nanotubes with anthracene and p-terphenyl." *Journal of Physical Chemistry B*. 2006; 110: 3895-901.

Heller DA, Barone PW, Swanson JP, Mayrhofer RM, Strano MS. "Using Raman spectroscopy to elucidate the aggregation state of single-walled carbon nanotubes". *Journal of Physical Chemistry B*. 2004; 108 (22): 6905-6909.

Hurt RH, Monthieux M, Kane A. "Toxicology of carbon nanomaterials: Status, trends, and perspectives on the special issue." *Carbon* 2006; 44: 1028-33.

Kataura H, Kumazawa Y, Maniwa Y, Umezumi I, Suzuki S, Ohtsuka Y, *et al.* "Optical properties of single-wall carbon nanotubes." *Synthetic Metals*. 1999; 103: 2555-8.

Keogh SM, Hedderman TG, Gregan E, Farrell GF, Chambers G, Byrne HJ. "Spectroscopic analysis of single walled carbon nanotube and semi-conjugated polymer composites." *Journal of Physical Chemistry B*. 2004; 108(20): 6233-41.

Keogh SM, Hedderman TG, Ruther MG, Lyng FM, Gregan E, Farrell GF, *et al.* "Temperature induced nucleation of poly(m-phenylenevinylene-co-2,5-dioctoxy-p-phenylenevinylene) crystallization by HiPco single-walled carbon nanotubes." *Journal of Physical Chemistry B*. 2005; 109 (12): 5600-7.

Kukovecz A, Kramberger C, Georgakilas V, Prato M, Kuzmany H. "A detailed Raman study on thin single-wall carbon nanotubes prepared by the HiPco process." *European Physics Journal B*. 2002; 28: 223-30.

Lian Y, Maeda Y, Wakahara T, Nakahodo T, Akasaka T, Kazaoui S, *et al.* "Spectroscopic study on the centrifugal fractionation of soluble single-walled carbon nanotubes." *Carbon* 2005; 43: 2750-59.

Monteiro-Riviere NA, Nemanich RJ, Inman AO, Wang YY, Riviere JE. "Multi-walled carbon nanotubes interactions with human epidermal keratinocytes." *Toxicology Letters*. 2005; 155: 377-84.

Monteiro-Riviere NA, Inman AO. "Challenges for assessing carbon nanomaterial toxicity to the skin." *Carbon* 2006; 44: 1070-78.

Moulton SE, Minett AI, Murphy R, Ryan KP, McCarthy D, Coleman JN, *et al.* "Bio molecules as selective dispersants for carbon nanotubes." *Carbon*, 2005; 43: 1879-84.

Posadaz A, Sanchez E, Gutierrez MI, Calderon M, Bertolotti S., Garcia NA, *et al.* "Riboflavin and rose Bengal sensitised photo-oxidation of sulfathiazole and succinylsulfathiazole kinetic study and microbiological implications." *Dyes and Pigments* 2000; 45: 219-28.

Rouse JG, Yang J, Barron AR, Monteiro-Riviere NA. "Fullerene-based amino acid nanoparticles interactions with human epidermal keratinocytes." *Toxicology in Vitro*. 2006; 20 (8): 1313-1320.

Salvador-Morales C, Flahaut E, Sim E, Sloan J, Green MLH, Sim RB. "Complement activation and protein adsorption by carbon nanotubes." *Molecular Immunology*. 2006; 43: 193-201.

Smart SK, Cassady AI, Lu GQ, Martin DJ. "The biocompatibility of carbon nanotubes." *Carbon* 2006; 44: 1034-47.

Stearns RC, Paulauskis JD, Godleski JJ. "Endocytosis of ultrafine particles by A549 cells." *American Journal of Respiratory Cell Molecular Biology*. 2001; 24: 108-15.

Valeentini L, Amentano I, Ricco L, Alongi J, Pennelli G, Mariani A, *et al.* "Selective interaction of single-walled carbon nanotubes with conducting dendrimer." *Diamond Related Materials*. 2006; 15: 95-9.

Venkatesan N, Yoshimitsu J, Ito Y, Shibata N, Takada K. "Liquid filled nanoparticles as a drug delivery tool for protein therapeutics." *Biomaterials* 2005; 26: 7154-63.

Wise KE, Park C, Siochi EJ, Harrison JS. "Stable dispersion of single wall carbon nanotubes in polyimide: the role of non-covalent interactions." *Chemical Physics Letters*. 2004; 391: 207-11.

Wörle-Knirsch JM, Pulskamp K, Krug HF. "Oops they did it again! Carbon nanotubes hoax scientists in viability assays." *Nanoletters*. 2006; 6: 1261-68.

Yu Z, Brus J. "Rayleigh and Raman Scattering from individual carbon nanotube bundles." *Journal of Physical Chemistry B*. 2001, 105, 1123-34.

Zirak P, Penzkofer A, Schiereis T, Hegemann P, Jung A, Schlichting I. "Absorption and fluorescence spectroscopic characterisation of BLUF domain of AppA from *Rhodobacter sphaeroides*." *Chemical Physics*. 2005; 315: 142-54.

Chapter 6

“Can interactions induce medium depletion?”

Adapted from

“Single walled carbon nanotubes induce indirect cytotoxicity by medium depletion in A549 lung cells”

Manuscript in Preparation

6.1 Introduction.

SWCNT interact strongly with a large range of molecular species from dyes to polysaccharides and bio-molecules (Bandypadhyaya *et al.*, 2002, Chambers *et al.*, 2003, Casey *et al.*, 2005; Dalton *et al.*, 2000; Hedderman *et al.*, 2004; Keogh *et al.*, 2004; Moulton *et al.*, 2005; Valeentini *et al.*, 2006; Salvador-Morales *et al.*, 2006). Close examination of a commercial cell culture medium, commonly used in toxicity studies, revealed significant interaction of the constituent components with SWCNT. It was shown in chapter 5 that on dispersal of in the cell culture medium significant colour changes were observed in the medium. These changes indicated a degree of molecular interaction between the SWCNT and the constituents of the medium. Spectroscopic analysis confirmed the presence of these interactions with a loss of the associated absorption and fluorescent emission of the medium components. The question is thus raised that if the SWCNT interact with the medium and its constituent nutrients, does the medium still have the same capability to maintain healthy cells? Furthermore, can the toxicological data collected on experiments performed in this way (dispersion of SWCNT in a cell culture medium) be affected? So it is postulated

that SWCNT may induce an indirect/secondary toxicity due to the reduction in the availability of the medium components to the cells due to interaction with the SWCNT.

This chapter will investigate this hypothesis of indirect/secondary toxicity by medium depletion. *In vitro* cytotoxicity studies were thus carried out on A549 lung cells with various carbon nanoparticles for comparative purposes, namely HiPco SWCNT, Arc Discharge (AD) SWCNT and Printex 90 (carbon black), which is made up of largely graphitic carbon nanoparticles of size ~14nm. Various concentrations of the carbon based nanoparticles were dispersed in cell culture medium and then removed by a process of centrifugation and filtration. Healthy confluent cells were then exposed to this filtered medium and cellular viability was estimated using two cytotoxic indicator dyes, namely Alamar Blue (AB) and Neutral Red (NR). Spectroscopic analysis was performed on all test media samples to firstly verify the complete removal of the nanoparticle in question from the suspension and secondly to investigate the effect of the removal of the nanoparticles on the constituents of the medium itself.

6.2 Experimental.

6.2.1 Preparation of test samples.

The solutions were prepared by dispersing an initial concentration of 0.8 mg/ml of both types of SWCNT and carbon black in 5% serum medium with an ultrasonic tip. Each stock concentration was then serially diluted with 5% serum medium and sonicated as before to prepare test concentrations. As discussed in chapter 5, the addition of the serum had an effect on the dispersion behaviour of the SWCNT and

the recommendation of working in the absence of serum in toxicity studies was made. Despite this, test concentrations were prepared in 5% serum media to facilitate the 72 and 96 hour exposure tests. After dispersion, the test concentrations were refrigerated for 24 hours and then underwent a process of centrifugation (3000RPM/1800G for 20 minutes) and filtering (using 0.2 μ m cellulose acetate filters) to remove the dispersed nanoparticles. Cells were then exposed to a concentration range (0.00156 - 0.8 mg/ml) of filtered medium.

6.2.2 Cytotoxicity Assay.

Cells were seeded at a density of 1×10^5 cells/ml for the 24 hour test, 7×10^4 cells/ml for the 48 hour test, 3×10^4 cells/ml for the 72 hour test and 2×10^4 cells/ml for the 96 hour test in 96-well plates in three replicates for AB and NR assays. After 24 hours, the cells were treated with centrifuged and filtered medium (previously containing test nanoparticle concentrations of 0.00156 to 0.8 mg/ml) and incubated for the required time period (24, 48, 72 and 96 hours) whereupon they were assessed for cell viability using the two assays. AB and NR assays were carried out sequentially on the same plate, as described in section 4.8.5.

6.3 Spectroscopic Analysis.

In this chapter spectroscopic techniques will be used to verify the removal of the SWCNT from the medium prior to cellular exposure. Secondly they will be used to show that upon interaction with the SWCNT the medium is altered as a result of the incorporation of SWCNT.

6.3.1 Initial Observations.

As seen in chapter 5, upon the dispersion of the SWCNT within the medium, there was a resultant colour change in the higher concentration regions (0.4 – 0.8 mg/ml). This colour change was observed again here in all test samples (HiPco SWCNT, AD SWCNT and Carbon Black). Visual differences were observed between the dispersion behaviour of the three test samples. Both type of nanotube suspensions (HiPco and AD) began to settle out of solution after a matter of hours. In contrast the carbon black remained completely dispersed after 24 hours. After centrifugation (3000RPM for 20 minutes) all SWCNT (both HiPco and Arc Discharge) had precipitated out of solution whereas the carbon black remained suspended. Upon filtration, the carbon black solution in the higher concentration region (above 0.1mg/ml) retained a light grey colour indicating that not all carbon black was removed. Filtration was repeated a number of times but this colour remained.

6.3.2 Raman Spectroscopy.

In order to investigate the proposed mechanism of a secondary rather than a direct toxicity of SWCNT, it is vital that the removal of the nanoparticle in question be carried out. For the purpose of this study Raman spectroscopy was employed to verify the removal of nanoparticles from the medium after centrifugation and filtration. Raman analysis was carried out on all samples at 514.5 nm laser excitation. As discussed in chapter 4, the Raman spectrum of pristine nanotubes consists primarily of three main features, the radial breathing mode (RBM), the D line and the G line (Brown *et al*, 2001; Chen *et al*, 1998; Dresselhaus *et al*, 2002; Jorio *et al*, 2001; Jorio *et al*, 2002; Kukovecz *et al*, 2002; Kuzmany *et al*, 2001; Pimenta *et al*, 2001; Yu *et al*, 2001). The dominant feature in the Raman signal of SWCNT is the G line situated between 1450

cm^{-1} and 1650cm^{-1} the absence of this feature from the recorded spectra would indicate that the SWCNT were successfully removed from the medium.

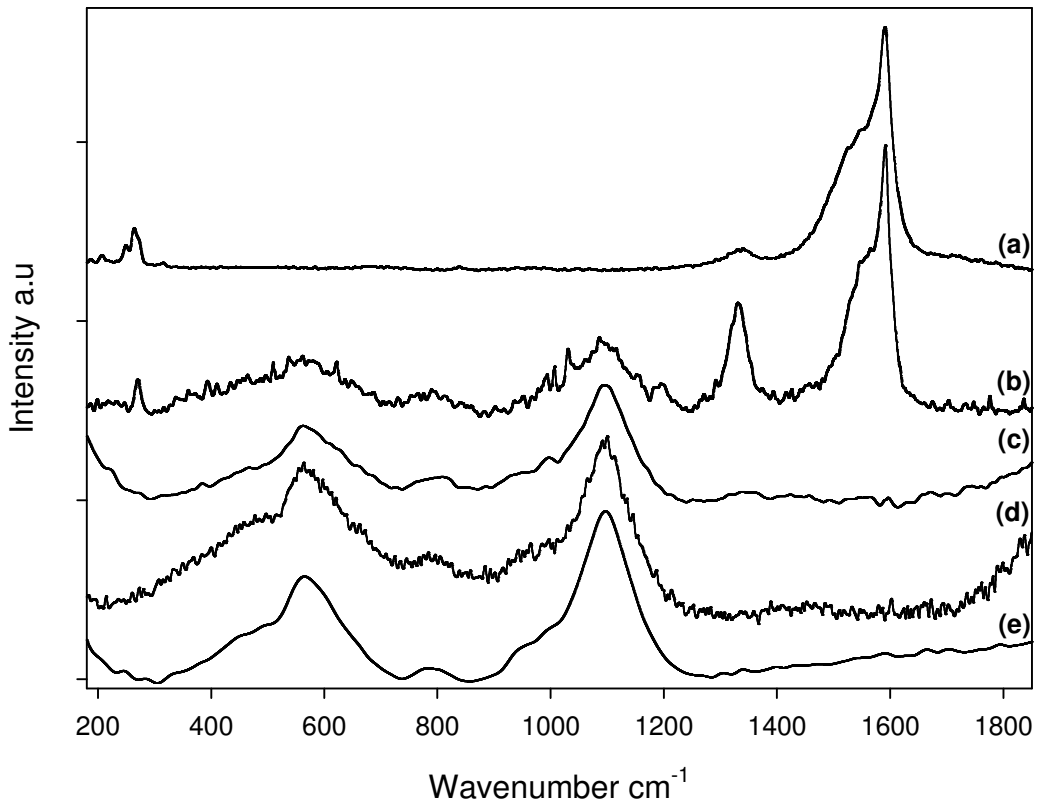


Figure 6.1 Raman Spectra by 514.5 nm excitation of (a) Unfiltered 5% FBS Medium containing HiPco SWCNT 0.8mg/ml (b) Unfiltered 5% FBS Medium containing HiPco SWCNT 0.00156 mg/ml (c) Arc Discharge SWCNT Filtrate 0.8mg/ml (d) Carbon Black Filtrate 0.8mg/ml (e) HiPco SWCNT Filtrate 0.8mg/ml.

Figure 6.1 displays the recorded spectra for unfiltered medium containing HiPco SWCNT (figure 6.1 a and b), and for all filtered media, HiPco SWCNT (figure 6.1 e), AD SWCNT (figure 6.1 c) and carbon black (figure 6.1 d). The pre-filtration spectra of HiPco SWCNT treated media suspensions (figure 6.1 a and b) were recorded from drop cast slides. In these spectra the dominant nanotube features can be clearly seen at both tested concentrations (0.1 (a) and 0.003 (b) SWCNT mg/ml). Close examination of

these spectra, in the RBM region; again shows that there was minimal alteration to the aggregative state of the SWCNT. This correlates well with the results present in chapter 5 that the tested SWCNT remained as bundles in all concentrations tested. Further more the difference in concentrations of these two samples gives a good representation of the fine quantities of SWCNT that can be detected spectrally by the Raman method. The absence of these features in the filtered samples would therefore provide a good indication of their removal by centrifugation and filtration. Figure 6.1 c to d displays the Raman spectra obtain by 514.5 nm excitation of the filtered samples (HiPco, AD SWCNT and Carbon Black) of the highest test concentrations (0.8 mg/ml) recorded from drop cast slides. As can be seen there is a complete absence of SWCNT and carbon black (see appendix 7) features from the spectra obtained. This is a strong indication that the nanoparticles have been essentially removed from the medium by centrifugation and filtration the proposed hypothesis of a secondary toxicity by medium depletion to be investigated.

6.3.3 UV-Vis Absorption Spectroscopy.

As discussed in chapter 5, the UV/visible absorption spectrum of 5%-FBS-F12K medium, consisting of four features at 270, 360, 410 and 560nm, was seen to undergo considerable changes upon the addition of SWCNT. The features at 270 and 410nm were assigned to the added 5% FBS, whereas the two remaining features at 360 and 560nm originate from the components of the medium itself. The feature at 360nm can be attributed to riboflavin (Posadaz *et al.*, 2000, Zirak *et al.*, 2005), a vitamin present in the medium whereas the feature at 560nm can be assigned to the phenol red indicator. The absorption spectrum of SWCNT in water suspensions, as previously described in chapter 4, consists of three broad absorption features centred approximately at 1200nm,

800nm and 270nm. The peaks at 1200nm and 800nm are highly structured and are attributed to optical transitions between mirror image spikes in the diameter dependent density of states, with the feature at 270nm attributed to the π -plasma frequency of $\sim 4.6\text{eV}$ in π -conjugated carbon materials (Kataura *et al.*, 1999).

In all test solutions, a reduction in the phenol red peak at 560nm was observed (figures 6.3, 6.4 and 6.5) which was as expected due to the colour change observed in the high SWCNT concentration region. However, as previously mentioned in chapter 5, no change in pH was registered. This was highlighted as evidence that the SWCNT altered the chemical “composition” of the medium by interaction. Further reductions were observed of the features attributed to the added FBS supplement, at 410 and 270nm, in all tested filtered samples (figures 6.3, 6.4 and 6.5).

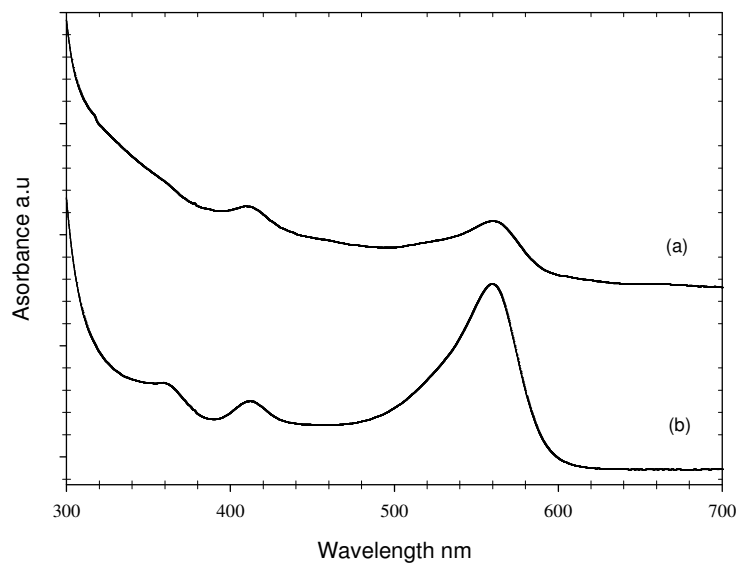


Figure 6.3 UV-Vis Absorption Spectra of (a) HiPco SWCNT Filtered medium 0.8mg/ml and (b) 5 % FBS medium.

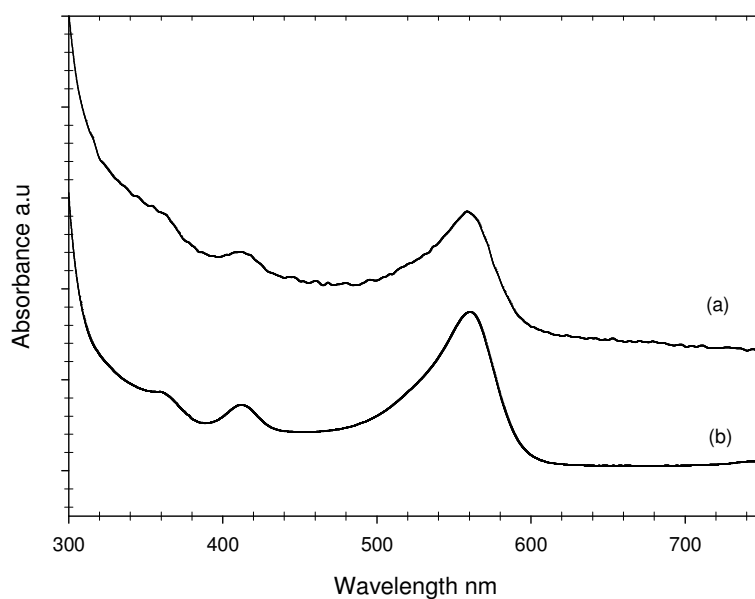


Figure 6.4 UV-Vis Absorption Spectra of (a) Arc Discharge SWCNT Filtered medium 0.8mg/ml and (b) 5 % FBS medium.

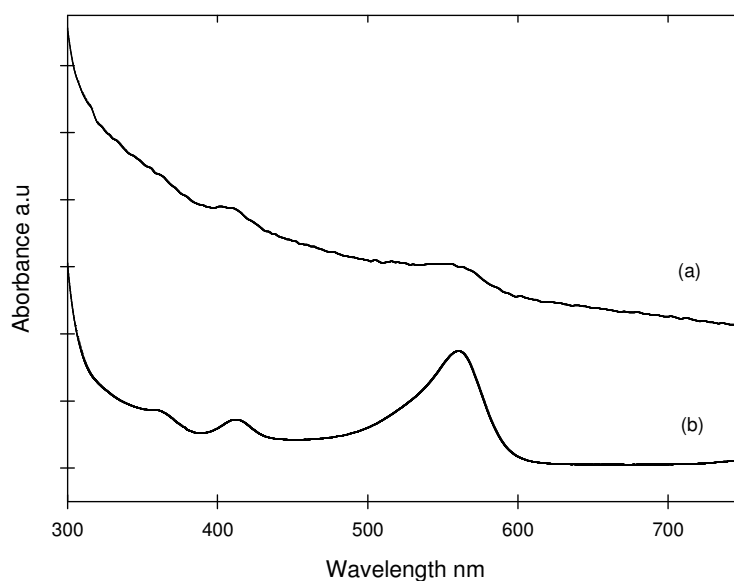


Figure 6.5 UV-Vis Absorption Spectra of (a) Carbon Black Filtered medium 0.8mg/ml and (b) 5 % FBS medium.

The feature at $\sim 360\text{nm}$, attributed to the vitamin riboflavin, was reduced in all tested filtered samples (figures 6.3, 6.4 and 6.5). The spectral changes correlate well to those observed in chapter 5. While again providing little insight into the type of interaction

between the SWCNT and the medium components, such reductions do give an indication that the molecular components of the medium and indeed the added serum are interacting with both types of SWCNT (HiPco and AD) and with the carbon black.

Finally it can be observed in all the absorption spectra obtained that there is considerably more scatter present, as evident by the increased absorbance baseline (figures 6.2a, 6.3a and 6.4a) when compared to the pristine medium (figures 6.2b, 6.3b and 6.4b). In SWCNT studies, increases of scatter of this nature are attributed to SWCNT being present in the suspension. As Raman spectroscopy yielded no spectral evidence of their presence in the sample it is justifiable to say that the observed increase in scatter here is not due to the presence of SWCNT. This raises questions about the origin of this increased scatter. One possible origin may be that the initial dispersion of the nanoparticles (Carbon Black, HiPco and AD SWCNT), which has been shown to interact with the various medium components in chapter 5, resulted in local aggregation of the components due to interaction with the dispersed SWCNT. Upon centrifuging and filtration these localised medium aggregates may have remained after the removal of the nanoparticles under test. It is of course plausible that impurities present in the samples upon their dispersion were not totally removed by centrifugation and filtration. Irrespective of the scatter, the observed spectral reductions in the absorption characteristics of the medium give supportive evidence to the alteration of the medium's composition by interaction with the SWCNT and indeed the carbon black. The effect of this on cellular growth will be explored in section 6.4.

6.3.4 Fluorescent Emission Spectroscopy.

As demonstrated in Chapter 5, fluorescence quenching studies have been shown to aid in the elucidation of the interaction of nanotubes with different molecular species (Coleman *et al*, 2005; Hedderman *et al.*, 2004; Keogh *et al.*, 2004). The model of Coleman *et al.* was described and employed to assess the degree of interaction between the SWCNT and the various components of cell culture medium and it will also be used here to assess the effect of the removal of the various carbon based nanoparticles from the medium post dispersion/interaction in the cell culture medium.

As described in section 6.3.3, reductions in absorbance were observed in the characteristic medium features so it was expected that there would be a reduction in their associated emission. As discussed in chapter 5, excitation of 5% FBS medium by three wavelengths, namely 268, 360 and 410 nm, each corresponding to the absorbance of an individual component of the medium, yielded emission spectra (see appendices 4, 5 and 6). These excitation wavelengths were again used here to study the filtered medium to assess the effect of SWCNT and carbon black removal. In all tested samples the emission, by excitation with the aforementioned wavelengths, was reduced. Again here the quenching of emission was monitored as a function of initial particle concentration, and plotted as a ratio (figure 6.6) as outlined in chapter 5.

As can be seen in figure 6.6 the emission ratio plots do not correlate with the model (Coleman *et al*, 2005) to the degree that was seen in chapter 5. Further examination of the model may provide an explanation for this deviation from the behaviour seen in chapter 5. Equation 5.1 represents the dynamic equilibrium at which the adsorption rate equals the desorption rate, in terms of N_F , the number of free molecules, and N_B , the

number of bound molecules. In essence the model is a ratio of the fluorescence of the free and bound molecules in the SWCNT containing solution, to that of the free molecules found in the pristine solution. The nature by which these samples were prepared for test, dispersion of SWCNT followed by their removal by centrifugation and filtration, would also remove any molecules bound to the SWCNT upon their initial dispersion. This would result in the ratio studied here becoming one between the remaining free molecules in the medium after SWCNT removal and the free molecules in the pristine solution explaining the deviation from the behaviour observed in chapter 5.

Despite the inability to reliably fit the data to the model proposed by Coleman *et al* (2005) it can be clearly seen in the ratio plots of figure 6.6 that the incorporation and removal of the carbon based nanoparticles into the medium altered its emission characteristics giving further supportive evidence for the alteration of the medium upon interaction with the SWCNT.

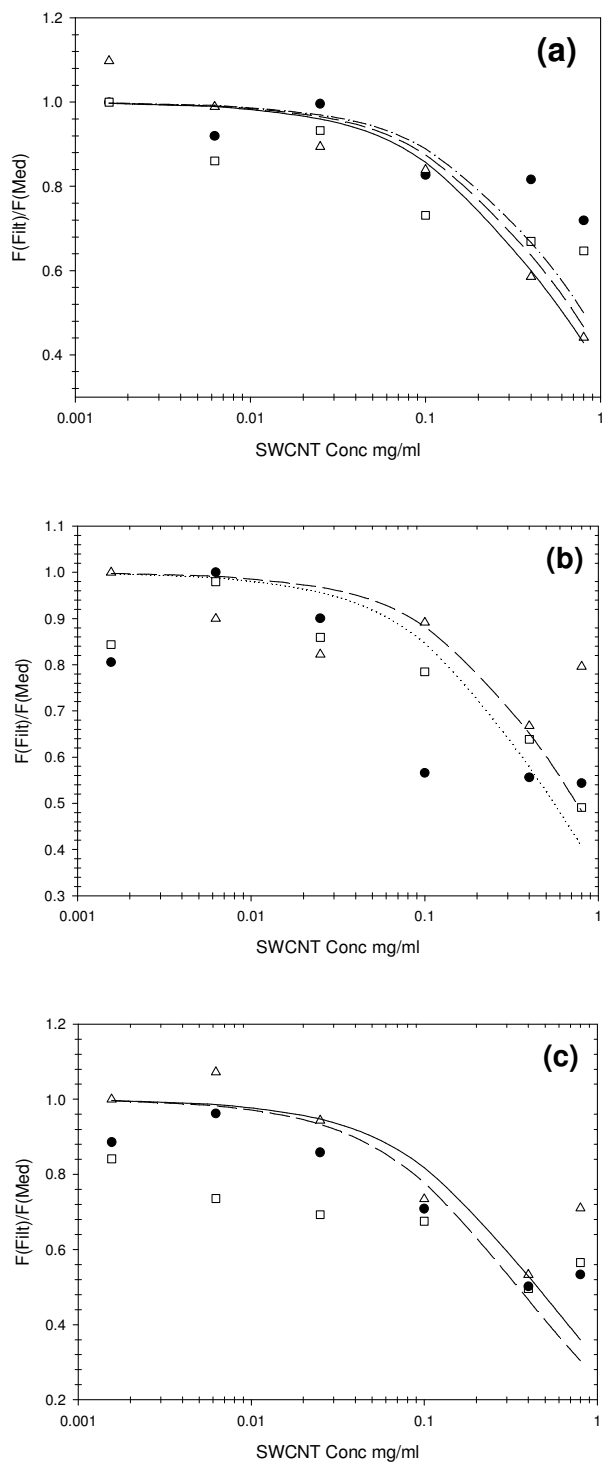


Figure 6.6 Plot of emission ratios of 5%-FBS-F12K filtered cell culture medium against (a) HiPco SWCNT (b) Arc Discharge SWCNT (c) Carbon black concentration (initial) by excitation at (\square) 268nm excitation, (\bullet) 360nm excitation and (Δ) 410nm excitation.

Differences were observed in the C_0 values estimated from the fits for each nanoparticle tested, which would suggest differing degrees of interaction between the medium and each of the nanoparticles. To study the indirect/secondary toxicity induced this could be interpreted as differing degrees of alteration of the medium which may play a significant role in the generation of any adverse effects observed. Both carbon black (0.35 – 0.45 mg/ml) and the AD SWCNT (0.45 – 0.55 mg/ml) were noted to yield lower C_0 values than that of the HiPco SWCNT (0.6 - 0.8 mg/ml). According to the original model (Coleman *et al*, 2005) a lower C_0 value would imply a higher binding energy between the SWCNT and the tested species, so here it would suggest a greater degree of interaction/alteration of the medium which may result in higher cytotoxicity being observed. This will be further explored in section 6.5.

6.3.5 Spectroscopic analysis summary.

The previous section has described the use of spectroscopic analysis to firstly verify nanoparticle removal from the medium prior to cellular exposure. Raman analysis of all samples showed no evidence of nanoparticle features suggesting they had been removed during centrifugation and filtration. Electronic spectroscopy, namely absorption and emission, were employed to assess the degree of alteration of the medium as a result of the removal of the nanoparticles. Reductions in the associated absorbance and emission verified that the medium was altered upon the dispersion and removal of the SWCNT. Fluorescent emission studies showed varying degrees of interaction between the medium and the various nanoparticles tested as could be seen by the different C_0 values estimated. The next section will investigate the notion of a secondary toxicity by medium depletion upon interaction with SWCNT as was proposed in chapter 5.

6.4 Indirect Cytotoxicity of SWCNT by medium depletion.

In this section an *in vitro* cytotoxicity study using the filtered medium for various exposure times (24, 48, 72 and 96 hours) to explore the concept of secondary or indirect toxicity due to medium depletion will be described. Two cytotoxicity indicator assays were employed, namely Alamar Blue and Neutral Red. The following sections will present the results for both cytotoxicity indicator dyes for HiPco and arc discharge SWCNT as well as carbon black.

6.4.1 Neutral Red (NR).

The first cytotoxicity endpoint that was employed was the Neutral Red, 3-amino-*m*-dimehtylamino-2-methyl-phenazine hydrochloride (NR) assay. The operation of this cytotoxicity assay is based on the ability of viable cells to incorporate and bind neutral red, a weak cationic dye that readily penetrates cell membranes by non-ionic diffusion. It accumulates in the lysosomes of cells where it binds to the sensitive lysosomal membrane. Cells damaged by xenobiotic action have a decreased ability to take up and bind NR, so that viable cells can be distinguished from damaged or dead cells. The dye can be extracted from intact cells using a solution of 1 % (v/v) acetic acid and 50 % (v/v) ethanol and the absorbance or fluorescence of solubilised dye can be determined. The test is very sensitive, specific, and readily quantifiable (Babich and Borenfreund, 1990) and has been extensively used in the literature as a cytotoxicity indicator.

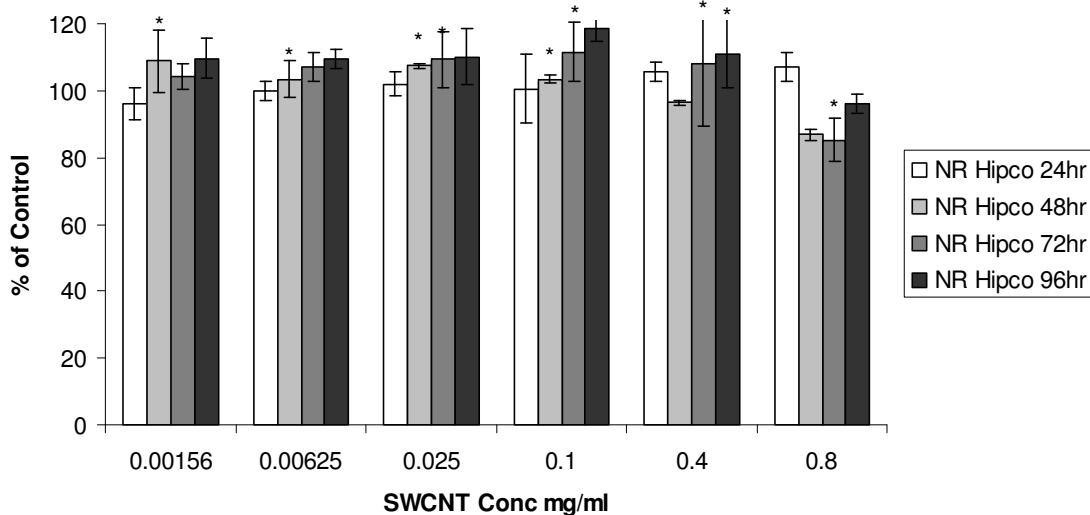


Figure 6.7 Cytotoxicity of HiPco SWCNT filtered medium to A549 cells after 24, 48, 72 and 96 hour exposures determined by the NR assay. Data are expressed as percent of control mean \pm SD of four independent experiments *Denotes significant difference from control ($P \leq 0.05$).

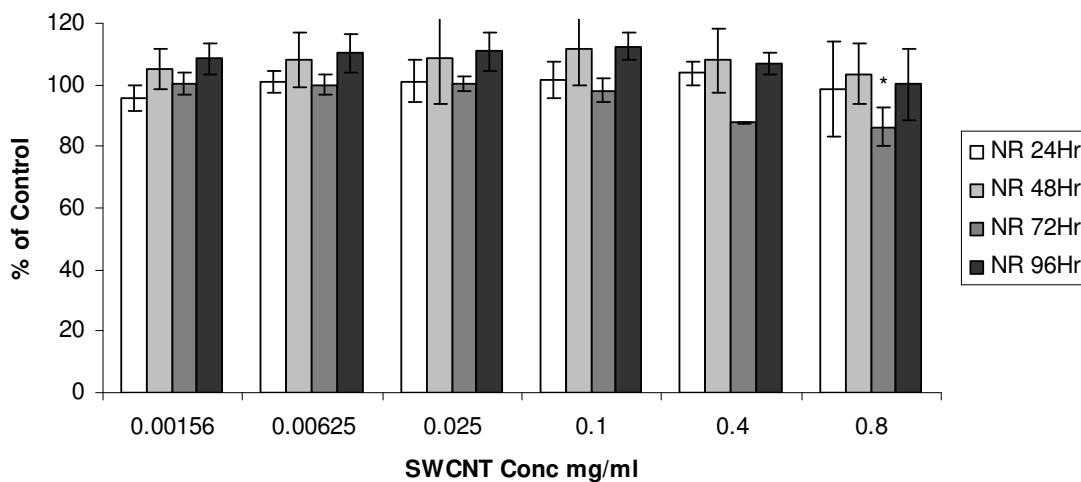


Figure 6.8 Cytotoxicity of Arc Discharge SWCNT filtered medium to A549 cells after 24, 48, 72 and 96 hour exposures determined by the NR assay. Data are expressed as percent of control mean \pm SD of three independent experiments *Denotes significant difference from control ($P \leq 0.05$).

Figures 6.7 and 6.8 display the obtained cytotoxicity response curves for HiPco and arc discharge SWCNT respectively using the NR assay. Concentrations in the aforementioned figures are those of the nanoparticles in the medium pre-filtration. Although significant cytotoxicity was observed for both types of SWCNT with this assay a number of difficulties were encountered as evidenced by the large error bars on the presented figures and the relative plateaux that can be seen in figures 6.7 and 6.9. The distinct lack of observed toxicity and the plateaux nature of the curves (figures 6.7 and 6.8) would seem to suggest that there is no decrease in the viability of the A549 cells upon exposure to the filtered medium which previously contained both types of SWCNT. In a study by Davoren *et al* (2007), upon the exposure of A549 cells to HiPco SWCNT, significantly more lamellar bodies were observed by TEM analysis post exposure, in comparison to the unexposed controls. In this study it was postulated that this increase in lamellar bodies was a defence mechanism of the cells in response to exposure to the SWCNT. In essence lamellar bodies are secondary lysosomes and as stated lysosomes are the region of the cell which incorporates the NR assay. It is possible that a similar effect, an increase of lamellar bodies upon exposure, is occurring here. This possible increase in lamellar bodies would account for the lack of observed toxicity upon exposure to the filtered medium. However TEM analysis would be required to verify this.

In the case of carbon black, significant toxicity was observed at the highest test concentration, 0.8mg/ml, after 48 hours and in 0.4mg/ml after 72 hour exposure (figure 6.9). This might suggest that carbon black has more potential to induce an indirect/secondary toxicity than both the tested SWCNT samples (HiPco and AD SWCNT) based on the use of the NR assay. However, the presence of residual carbon

black in the filtered medium, as evidenced by the residual grey colour, implies that a primary toxic mechanism cannot be ruled out.

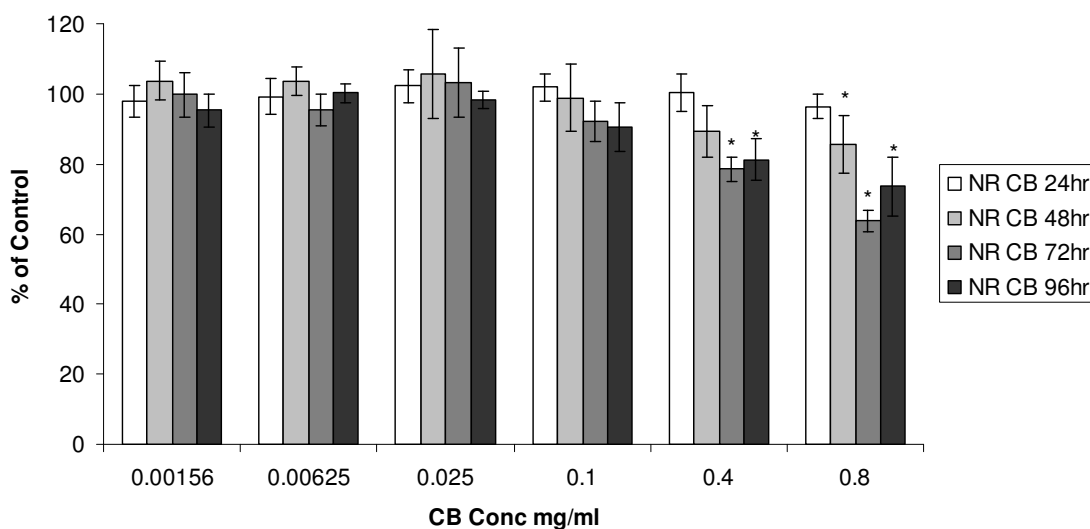


Figure 6.9 Cytotoxicity of Carbon Black filtered medium to A549 cells after 24, 48, 72 and 96 hour exposures determined by the NR assay. Data are expressed as percent of control mean \pm SD of three independent experiments *Denotes significant difference from control ($P \leq 0.05$).

Due to the inconsistencies observed between the nanoparticles tested here, the ability of the SWCNT samples to induce an indirect/secondary toxicity by means of medium depletion seems questionable. Examining the cytotoxic response curves of HiPco and AD SWCNT (figures 6.7 and 6.8) there would appear to be no change in cellular viability. For this reason a second cytotoxic endpoint was chosen to further study the effect of the filtered medium, namely the AB assay. This assay is known to be a more sensitive cytotoxic endpoint than that of the NR.

6.4.2 Alamar Blue (AB).

The Alamar Blue™ (AB) assay is a relatively new method to measure cell viability. The internal environment of viable, proliferating cells is more reduced than that of

damaged, necrotic or apoptotic cells, resulting in higher ratios of NADPH/NADP, FADH/FAD, FMNH/FMN, and NDH/NAD. The oxidation-reduction potential of AB, E_0 is +380 mV at pH 7.0 and 25 °C. Therefore, NADPH ($E_0 = - 320$ mV), FADH ($E_0 = - 220$ mV), FMNH ($E_0 = - 210$ mV), NADH ($E_0 = - 320$ mV), and cytochromes ($E_0 = - 290$ mV to + 80 mV) can reduce the dye. AB reduction is accompanied by a measurable colour shift from non-fluorescing indigo blue to fluorescent pink. Measurements may be made by absorption spectroscopic monitoring of AB supplemented culture media, or alternatively, fluorometric analysis. The absorption spectra of the oxidized and the reduced forms of AB overlap. Therefore absorption has to be measured at the two absorption maxima, 570 nm and 600 nm respectively. Fluorescence measurements can be made by exciting at 530 to 560 nm and measuring emission at 590 nm (Biosource, 2006).

In contrast to the other cytotoxic indicator dyes where conversion by healthy cells occurs, such as the MTT assay, the AB dye has the advantage of being water soluble, stable in the culture medium and non-toxic, so that continuous monitoring of cell cultures is permitted, and viability of cells is not altered. The MTT assay's oxidation-reduction potential is only + 10 mV, so can only be reduced by NADPH, FADH, FMNH, and NADH, and not by cytochromes. Thus, MTT does not substitute for molecular oxygen as an electron acceptor, while AB does. At present, the actual site of AB reduction has not been evaluated. Mitochondria have been suggested as one site of AB reduction, but cell cytoplasm has been reported to be another possible site where the reaction may take place (Biosource, 2006). It further has been suggested that there may actually be multiple sites of conversion of this assay by the cells (Biosource,

2006), which is not the case with the NR assay which only probes lysosomal activity, a more decisive impression of general cellular health when the AB assay is employed.

Figures 6.10, 6.11 and 6.12 display the cytotoxicity response curves obtained for HiPco SWCNT (figure 6.10), arc discharge SWCNT (figure 6.11) and carbon black (figure 6.12) using the AB assay following exposure to the filtered medium. Again concentrations in the aforementioned figures are those of the nanoparticles in the medium pre-filtration.

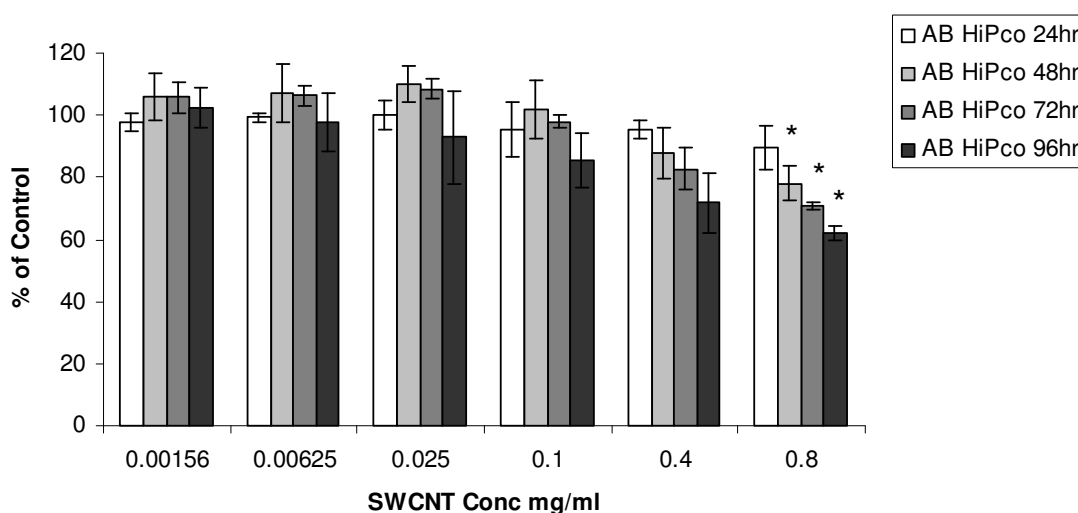


Figure 6.10 Cytotoxicity of HiPco SWCNT filtered medium to A549 cells after 24, 48, 72 and 96 hour exposures determined by the AB assay. Data are expressed as percent of control mean \pm SD of four independent experiments *Denotes significant difference from control ($P \leq 0.05$).

Figure 6.11 displays the cytotoxicity response curve obtained for filtered medium which previously contained HiPco SWCNT. As can be seen, from a concentration of 0.4mg/ml upwards after 48 hours, toxicity can be noted. However significant toxicity was only observed after 48 hours for the highest concentration tested, namely 0.8mg/ml. This would suggest that SWCNT can induce an indirect toxicity by means of medium

alteration at high concentrations after 48 hours, which was not observed with the NR assay in section 6.4.1.

A slightly different behaviour was observed for the arc discharge SWCNT filtered medium (figure 6.11). Significant toxicity was observed at a concentration, lower than that of the HiPco, of 0.4 mg/ml upwards after 48 hours, significant toxicity being observed after 24 hours for the highest test concentration of 0.8 mg/ml. Although arc discharge SWCNT are similar to HiPco in terms of physical attributes such as size, electronic properties and length, the fabrication method does result in differences between the bulk samples. Arc discharges SWCNT are typically less pure and contain a higher percentage impurity level containing substantially more amorphous carbon than HiPco SWCNT.

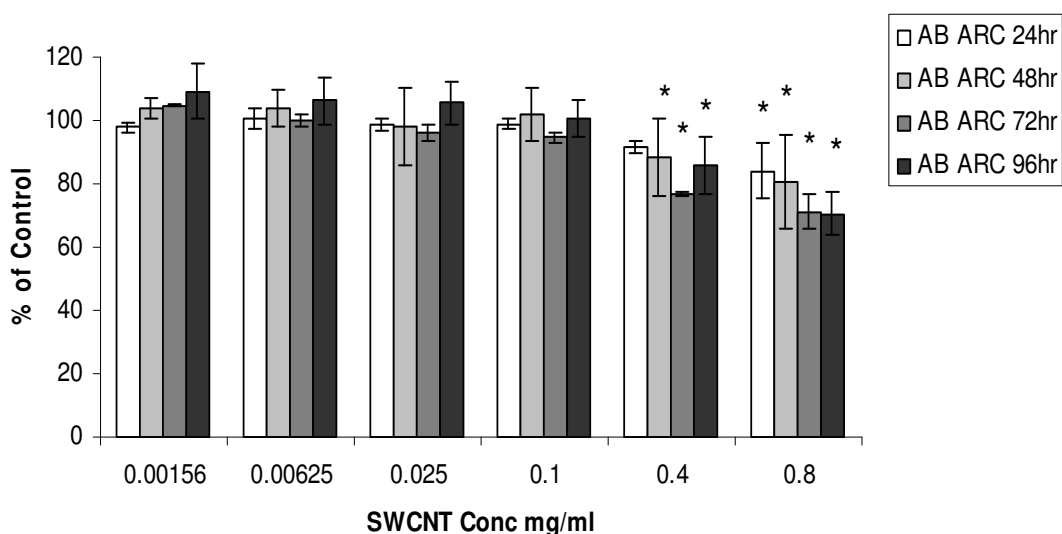


Figure 6.11 Cytotoxicity of Arc Discharge SWCNT filtered medium to A549 cells after 24, 48, 72 and 96 hour exposures determined by the AB assay. Data are expressed as percent of control mean \pm SD of three independent experiments *Denotes significant difference from control ($P \leq 0.05$)

As stated in section 6.3.4 differences were noted between the emission characteristics of the medium after filtration, dependant on the nanoparticle which had originally been dispersed. By modelling the emission properties of the filtered media, C_0 values were estimated, for each nanoparticle tested a different C_0 value was obtained, AD SWCNT yielded a slightly lower C_0 value (0.45 – 0.55 mg/ml) than that of the HiPco SWCNT (0.6 - 0.8 mg/ml). According to the original model (Coleman *et al*, 2004) and other studies which have employed it to study the interaction with various fluorescent species (Hedderman *et al*, 2004; Keogh *et al*, 2006) a lower C_0 value would indicate a higher degree of interaction between the two species under study. In a study of this nature this could be interpreted as a higher degree of alteration of the medium by interaction with the nanoparticles dispersed. The differing C_0 values from section 6.3.4 undoubtedly indicate that the medium was altered to varying degrees and resulted in a higher level of indirect/secondary toxicity being observed as can be seen in figures 6.10.and 6.11 where, AD SWCNT (with a lower C_0 value of 0.45 – 0.55 mg/ml) showed increased indirect/secondary toxicity when compared to that of the HiPco SWCNT (with a higher C_0 value of 0.6 - 0.8 mg/ml). Supportive evidence for this can be seen in figure 6.12 which displays the obtained cytotoxicity response curve, using the AB assay, for carbon black.

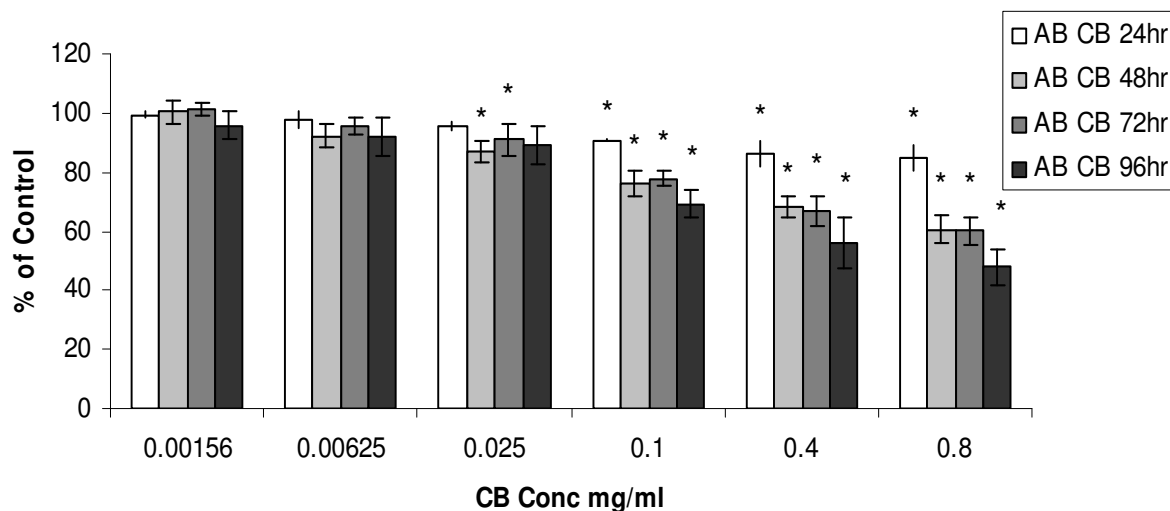


Figure 6.12 Cytotoxicity of Carbon Black filtered medium to A549 cells after 24, 48, 72 and 96 hour exposures determined by the AB assay. Data are expressed as percent of control mean \pm SD of three independent experiments *Denotes significant difference from control ($P \leq 0.05$).

For the carbon black filtered medium significant toxicity was observed at concentrations of 0.1mg/ml upwards after 24 hours (figure 6.12). In section 6.3.4 carbon black was seen to yield the lowest C_0 value based on the fluorescent emission of the medium post filtration. This suggests that the medium was altered to a greater degree by carbon black when compared to that of the two tested SWCNT samples (HiPco and AD) and resulted to the increased indirect/secondary toxicity observed in figure 6.12. This result is of great significance as several studies evaluating the toxicity of carbon based nanoparticles have employed carbon black as a reference material. This study has shown that like nanotubes, carbon black has the potential to induce an indirect/secondary toxicity by the alteration of the medium making its usage as a reference material questionable.

6.5 Chapter Summary.

This chapter has used spectroscopic analysis and cytotoxicity analysis to verify the proposed notion of an indirect or secondary toxicity as a result of the interaction of SWCNT, within cell culture medium as described in chapter 5. To confirm this effect, spectroscopic analysis was performed to verify the removal of the SWCNT from the medium by centrifugation and filtration. Raman spectroscopy gave no indication of the presence of SWCNT or carbon black in the filtered samples suggesting they were sufficiently removed during the test sample preparation process. Reductions in the associated absorbance and emission verified that the medium was altered upon the dispersion and removal of the SWCNT. By modelling the emission characteristics of the filtered media differing degrees of alteration were noted as evident by the different C_0 values estimated. According to these C_0 values it was suggested that carbon black with the lowest C_0 value resulted in the greatest degree of alteration followed by the AD SWCNT and HiPco with the highest C_0 value altered the medium to a lesser extent than the carbon black and the AD SWCNT.

Cytotoxicity studies were thus conducted with the altered medium, using two cytotoxicity end points namely the NR and AB assays. The assays showed that SWCNT did induce an indirect/secondary toxicity by means of medium depletion as seen in figures 6.7 to 6.11,. Differences were noted in the cytotoxicity responses of the different nanoparticles tested. Carbon black was seen to induce significant indirect/secondary toxicity after 24 hours at a pre-filtration concentration of 0.1 mg/ml upwards, followed by AD SWCNT with significant indirect/secondary toxicity observed after 48 hours at 0.4 mg/l upwards, determined by the AB assay. In the HiPco filtered medium

significant indirect/secondary toxicity was observed after 48 hours only at a pre-filtration concentration of 0.8 mg/ml. This was in agreement with the fluorescent emission studies in which the degree of alteration of the medium was seen to follow the same trend. The AB was noted to be more sensitive than that of the NR assay. Indeed literature does indicate that the AB assay is a more sensitive and reproducible cytotoxic endpoint when compared to that of the NR assay (Davoren *et al*, 2005; Davoren and Fogarty, 2006).

The two assays used to evaluate the indirect toxicity in essence are a measure of cellular viability but the mechanisms by which this is evaluated is different for both assays. The NR assay is only incorporated into the lysosomes of viable cells and gives a good indication of general cellular viability post exposure. The AB assay's operation is more complicated and its conversion is expected to be an indicator of a number of contributing factors (proliferation, metabolic and mitochondrial activity and also the cell cytoplasm have all been suggested as possible converters) (Biosource, 2006). Indeed studies have employed this assay to monitor the proliferative capacity of cells following a variety of cell treatments (Ahmed *et al*, 1994; Abuodeh *et al*, 1996; Qureshi *et al*; 2001). If this assay is a potential measure of cellular proliferation it may be an indication that, in the presence of the filtered medium, cellular proliferation is reduced as apparent by the cytotoxicity response curves of the AB assay (figures 6.10, 6.11 and 6.12) and cellular viability is retained, as evident by the plateau cytotoxic response curves of the NR assay (figures 6.7, 6.8 and 6.9). However further experimental studies would be required to verify this hypothesis. A recent study carried out by Herzog *et al.*,(2007) to develop a clonogenic assay to evaluate SWCNT cytotoxicity directly, has shown that upon exposure colony number remains largely unaltered but colony size is

greatly reduced which would support the hypothesis that the proliferation rate is reduced but cellular viability is retained in the presence of the depleted medium.

Nevertheless it is without question that upon their dispersion and subsequent removal all the nanoparticles tested in this chapter did alter the composition of the medium, as evidenced by the spectroscopic analysis. This in turn did result in an adverse effect on cellular growth as verified by the cytotoxic data presented for the AB assay and may contribute to a false positive toxic effect being observed in the evaluation of the direct cytotoxicity of SWCNT due to medium depletion by interaction.

As literature has recently noted adsorptive interferences between SWCNT and some standard cytotoxicity endpoints (Hurt *et al.*, 2006; Montiero-Riviere *et al.*, 2006) resulting in both false positive and negative toxic effects being evaluated in the presence of SWCNT, the next chapter will evaluate the direct cytotoxicity of SWCNT with a battery of cytotoxicity assays. This will facilitate an estimate of the direct toxicity of SWCNT. The validity of the evaluated cytotoxicity data will be then assessed by spectroscopic analysis of the cytotoxicity assays interactions with the tested SWCNT.

References

Abuodeh RO, Wilson V and Scalarone GM. “ Induction and detection of cell mediated reactions with different *Blastomyces dermatitidis* antigenic preparation” *Mycoses*, 1996; 39; 85-89.

Ahemed SA, Gogal RM and Walsh JE. “A new rapid and non-radioactive assay to monitor and determine the proliferation of lymphocytes: and alternative to [³H] thymide incorporation assay. *Journal of Immunology Methods*. 1994; 170; 211-224.

Alamar Blue[™] Product information pamphlet. BioSource International, Inc., USA

Bandyopadhyaya R, Nativ-Roth E, Regev O, Yerushalmi-Rozen R. “Stabilization of individual carbon nanotubes in aqueous solutions.” *Nanoletters*. 2002; 2: 25-8.

Borenfreund E, Babich H, Martin- Alguacil N. “Comparisons of two *in vitro* cytotoxicity assays – The neutral red (NR) and tetrazolium MTT tests.” *Toxicology in Vitro*. 1988; 2: 1-6.

Brown, S.D.M., Jorio, A., Dresselhaus, M.S., Desselhaus, G. “Observations of the D-band feature in the Raman spectra of carbon nanotubes”, *Physical Review B*. 2001, 64, 073403 -1 – 073403-4.

Casey A, Farrell GF, McNamara M, Byrne HJ, Chambers G. "Interaction of carbon nanotubes with sugar complexes." *Synthetic Metals*. 2005; 153: 357-60.

Chambers G, Carroll C, Farrell GF, Dalton AB, McNamara M, in het Panhuis M, *et al.* "Characterization of the interaction of gamma cyclodextrins with single walled carbon nanotubes." *Nanoletters*. 2003; 3 (6): 843-6.

Coleman JN, Maier S, Fleming A, O'Flaherty S, Minett A, Ferreira MS, *et al.* "Binding kinetics and spontaneous single wall carbon nanotube bundle dissociation in low concentration polymer-nanotube solution." *Journal of Physical Chemistry B*. 2004; 108: 3446-50.

Dalton AB, Stephan C, Coleman JN, McCarthy B, Ajayan PM, Lefrant S, *et al.* "Selective interaction of a semi conjugated organic polymer with single-wall nanotubes." *Journal of Physical Chemistry B*. 2000; 104: 10012-16.

Davoren M, Ni-Shuilleabhain S, Hartl MGJ, Sheehan D, O'Brien NM, O'Halloran J, Van Pelt F, Mothersill C. "Assessing the potential of fish cell lines as tools for the cytotoxicity testing of estuarine sediment aqueous elutriates" *Toxicology in vitro*, 2005; 19; 421-431.

Davoren M and Fogarty AM. "In vitro cytotoxicity assessment of the biocidal agents sodium o-phenylphenol, sodium o-benzyl-p-chlorophenol, and sodium p-tertiary amylphenol using established fish cell lines" *Toxicology in vitro*, 2006; 20; 1190-1201.

Dresselhaus MS, Jorio A, Souza Filho AG, Dresselhaus G, Saito R. "Raman spectroscopy on one isolated nanotube." *Physica B* 2002; 323:15-20.

Hedderman TG, Keogh SM, Chambers G, Byrne HJ, "Solubilisation of Single walled carbon nanotubes with organic dye molecules." *Journal of Physical Chemistry B*. 2004; 108 (49): 18860-65.

Hurt RH, Monthieux M, Kane A. "Toxicology of carbon nanomaterials: Status, trends, and perspectives on the special issue." *Carbon* 2006; 44: 1028-33.

Jorio, A., Saito, R., Hafner, J.H., Lieber, C.M., Hunter, M., McClure, T., Dresselhaus, G., Dresselhaus, M.S. "Structural (n,m) determination of isolated single-wall carbon nanotubes by resonant Raman scattering", *Physical Review Letters*. 2001, 86, 1118-1121.

Jorio, A., Filho, A.G.S., Dresselhaus, G., Dresselhaus, M.S., Swan, A.K., Unlu, M.S., Goldberg, B.B., Pimenta, M.A., Hafner, J.H., Lieber, C.M., Saito, R. "G-band resonant

Raman study of 62 isolated single-wall carbon nanotubes”, *Physical Review B*. 2002, 65, 155412-1 – 155412-9.

Kataura H, Kumazawa Y, Maniwa Y, Umezumi I, Suzuki S, Ohtsuka Y, *et al.* Optical properties of single-wall carbon nanotubes. *Synthetic Metals*. 1999; 103: 2555-8.

Keogh SM, Hedderman TG, Gregan E, Farrell GF, Chambers G, Byrne HJ. “Spectroscopic analysis of single walled carbon nanotube and semi-conjugated polymer composites.” *Journal of Physical Chemistry B*. 2004; 108(20): 6233-41.

Keogh SM, Hedderman TG, Ruther MG, Lyng FM, Gregan E, Farrell GF, *et al.* “Temperature induced nucleation of poly(m-phenylenevinylene-co-2,5-dioctoxy-p-phenylenevinylene) crystallization by HiPco single-walled carbon nanotubes.” *Journal of Physical Chemistry B*. 2005; 109 (12): 5600-7.

Kukovecz A, Kramberger C, Georgakilas V, Prato M, Kuzmany H. “A detailed Raman study on thin single-wall carbon nanotubes prepared by the HiPco process.” *European Physical Journal B*. 2002; 28: 223-30.

Kuzmany, H., Plank, W., Hulman, M., Kramberger, Ch., Gruneis, A., Pichler, Th., Peterlik, H., Kataura, H., Achiba, Y. “Determination of SWCNT diameters from the Raman response of the radial breathing mode”, *European Physical Journal B*. 2001, 32, 307-320.

Moulton SE, Minett AI, Murphy R, Ryan KP, McCarthy D, Coleman JN, *et al.* “Biomolecules as selective dispersants for carbon nanotubes.” *Carbon*, 2005; 43: 1879-84.

Monteiro-Riviere NA, Inman AO. “Challenges for assessing carbon nanomaterial toxicity to the skin.” *Carbon* 2006; 44: 1070-78.

Pimenta, M.A., Jorio, A., Brown, S.D.M., Filho, A.G.S., Dresselhaus, G., Hafner, J.H., Lieber, C.M., Saito, R., Dresselhaus, M.S. “Diameter dependence of the Raman D-band in isolated single-wall carbon nanotubes”, *Physical Review B*. 2001, 64, 041401-1 – 041401-4.

Posadaz A, Sanchez E, Gutierrez MI, Calderon M, Bertolotti S., Garcia NA, *et al.* “Riboflavin and rose Bengal sensitised photo-oxidation of sulfathiazole and succinylsulfathiazole kinetic study and microbiological implications.” *Dyes and Pigments*. 2000; 45: 219-28.

Qureshi MH and Garvy BA. “Neonatal T cells in adult lung environment are competent to resolve *Pneumocystis carinii* pneumonia.” *Journal of Immunology Methods*. 2001; 166; 5704-5711.

Valeentini L, Amentano I, Ricco L, Alongi J, Pennelli G, Mariani A, *et al.* “Selective interaction of single-walled carbon nanotubes with conducting dendrimer.” *Diamond Related Materials*. 2006; 15: 95-9.

Salvador-Morales C, Flahaut E, Sim E, Sloan J, Green MLH, Sim RB. "Complement activation and protein adsorption by carbon nanotubes." *Molecular Immunology*. 2006; 43: 193-201.

Yu Z, Brus J. "Rayleigh and Raman Scattering from individual carbon nanotube bundles." *Journal of Physical Chemistry B*. 2001, 105, 1123-34.

Zirak P, Penzkofer A, Schiereis T, Hegemann P, Jung A, Schlichting I. "Absorption and fluorescence spectroscopic characterisation of BLUF domain of AppA from *Rhodobacter sphaeroides*." *Chemical Physics* 2005; 315: 142-54.

Chapter 7

“SWCNT interfere with cytotoxicity endpoints”

Adapted from

“Spectroscopic analysis confirms the interactions between single walled carbon nanotubes and various dyes commonly used to assess cytotoxicity”

Carbon 45, 1425-1432, 2007.

7.1 Introduction.

While there have been great advances in the technological research of SWCNT (Pantarotto *et al.*, 2004; Venkatestan *et al.*, 2005; Singh *et al.*, 2006; Harrison *et al.*, 2007), direct toxicological evaluations lag somewhat behind in comparison. Several studies both *in vivo* and *in vitro* have been carried out on refined and raw SWCNT (Cui *et al.*, 2005; Donaldson *et al.*, 2006; Muller *et al.*, 2006; Warheit *et al.*, 2006). In both the *in vivo* and *in vitro* studies, differences in SWCNT toxicity and biocompatibility have been observed. These discrepancies have been attributed to the varying percentages of remnant catalytic particles and other impurities in the samples tested and the different dispersion methods of the SWCNT (Cui *et al.*, 2005; Donaldson *et al.*, 2006; Muller *et al.*, 2006; Warheit *et al.*, 2006). Furthermore, as is evident from chapters 5 and 6, the interaction of SWCNT with the medium and any added protein supplements may have also contributed to these inconsistencies.

Recent literature has indicated that the interactions of SWCNT and other carbon based nanomaterials with various commonly used cytotoxicity assays results in interference with absorption/fluorescence data used to evaluate cytotoxicity (Hurt *et al.*, 2006; Montiero-Riviere *et al.*, 2006; Worle-Knirsch *et al.*, 2006). While these studies highlighted the interference of SWCNT and other carbon based materials with cytotoxicity dyes, namely MTT and Neutral Red, no attempts to quantify these interferences have been realised to date although recommendations involving the use of various other cytotoxicity dyes have been made (Worle-Knirsch *et al.*, 2006).

Chapter 6 explored the ability of SWCNT to induce an indirect/secondary toxicity by means of medium alteration. This chapter will present a direct cytotoxic evaluation of HiPco SWCNT, evaluated after 24 hour exposure using the following assays, Commassie Blue (COMMASSIE), Alamar Blue™ (AB), Neutral Red (NR), 3-(4,5-dimethylthiazol-2-yl)-2,5-diphenyltetrazolium bromide (MTT) and 2-(4-iodophenyl)-3-(4-nitrophenyl)-5-(2,4-disulfophenyl)-2H-tetrazolium (WST-1). A corresponding spectroscopic study will be carried out with the aforementioned assays and the tested SWCNT to assess any interactions occurring between the two species. The results from the spectroscopic analysis will be used to estimate the validity of the cytotoxicity data presented. Finally the spectroscopic analysis will be used to make recommendations for the use of cytotoxicity indicator dyes in the quantitative evaluation, in this and future studies of SWCNT toxicity.

7.2 Experimental.

7.2.1 Dispersion of SWCNT.

The test solutions were prepared by dispersing an initial concentration of 0.8 mg/ml of HiPco SWCNT in serum free medium, no FBS (protein supplement) was used in test concentrations as in chapter 5 strong interactions with the serum were highlighted. Each stock concentration was then serially diluted on a 96-well plate with each type of medium to prepare test concentrations. Cells were then exposed to a concentration range (0.00156 - 0.8 mg/ml) of SWCNT.

7.2.2 Cytotoxicity Assays.

Cells were seeded at a density of 1×10^5 cells/ml in 96-well plates in six replicates (for AB, NR, COMMASSIE, MTT assays) or triplicate (for the WST-1 assay). After 24 h, the cells were treated with SWCNT suspensions in concentrations of 0-00156 to 0.8 mg/ml (0.00156 to 0.4 mg/ml for WST-1 assay) and left for another 24 hours whereupon they were assessed for cell viability using five assays AB, NR, COMMASSIE, MTT and WST-1. All assays were performed according to the manufacturer's instructions as detailed in section 4.8.5. Cytotoxicity data was recorded using a microplate reader (TECAN GENios, Grödig, Austria).

7.3 Results and Discussion.

In the following subsections, for each cytotoxicity assay employed, the direct cytotoxicity of SWCNT based on the use of the aforementioned assays will be estimated. Secondly, spectroscopic analysis will be presented to assess the degree of

interaction between the SWCNT and the dye under test, thus evaluating the validity of cytotoxicity data evaluated.

7.3.1 COMMASSIE Blue.

The protein content of cells after exposure to a suspected toxicant is often used as a measure of cytotoxic effects *in vitro*. Different spectroscopic methods are routinely available for determination of protein concentrations, including measurement of protein intrinsic UV absorbance, namely the Lowry assay, and methods generating a protein-dependent colour change, the Smith copper/bicinchoninic assay. The simplest and most sensitive is the Bradford assay (Bradford, 1976), introduced in the mid 1970s, and based on the equilibrium between three forms of Coomassie Brilliant Blue-G250 (COMMASSIE) dye, which bind specifically to tyrosine side chains of protein molecules but not to other cellular constituents. Under strongly acidic conditions, the dye is most stable in its double protonated red state. When bound to protein, the unprotonated blue form becomes more stable. Within the linear range of the assay (approximately 5 to 25 µg/ml), the more protein present, the more Coomassie binds due to hydrophobic and ionic interactions (Bradford, 1976).

The main disadvantage concerning this assay is the possibility to record some protein based material although no viable cells are present. The assay is very prone to influences from non protein sources, particularly detergents, and becomes progressively more non-linear at high protein concentrations (Borenfreund, 2006). The main advantage for multi-endpoint cytotoxicity studies is that after the absorbance/fluorescence of another dye has been established, total cell protein can be measured on the same test cells using COMMASSIE dye.

A concentration response cytotoxicity (figure 7.1a) curve for the COMMASSIE assay was obtained and significant toxicity was observed at concentrations at and above 0.4 mg/ml. A spectroscopic study was carried out to investigate if there was an interaction between the SWCNT and the COMMASSIE dye. For this, an absorbance concentration study was carried out with two sets of samples, the first containing only the COMMASSIE dye and the other containing the COMMASSIE dye and SWCNT in equal concentrations, starting with an initial concentration of 0.4 mg/ml which was then serially diluted by half with an acetic acid buffer solution to a final concentration of 2.34×10^{-3} mg/ml. These solutions were allowed to settle for 24 hours and then decanted before any spectroscopic analysis was carried out.

The COMMASSIE absorbance was then plotted as a function of concentration with and without SWCNT and as expected, a linear relationship was observed in both cases (figure 7.1b). However, noticeable differences existed between the two linear plots. A reduction in the COMMASSIE associated absorbance was noted at all SWCNT concentrations. Furthermore the associated slope of concentration versus absorbance was seen to be reduced, from 2.5 to 1.4 upon the addition of SWCNT to the COMMASSIE.

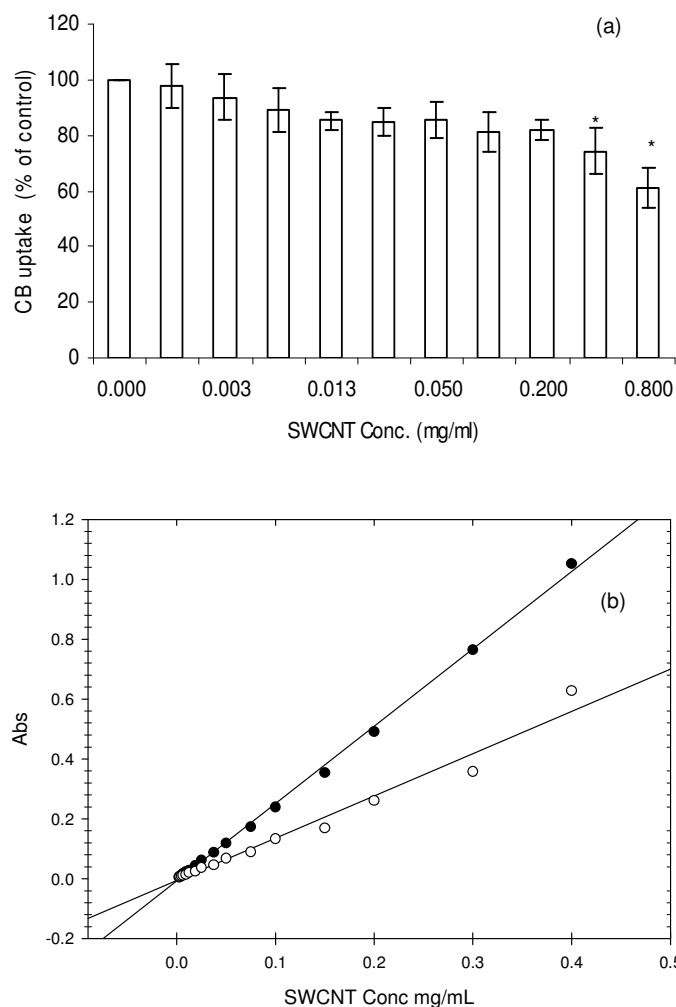


Figure 7.1 (a) Cytotoxicity of SWCNT to A549 cells after 24 hour exposure determined by the COMMASSIE assay. Data are expressed as percent of control mean \pm SD of six independent experiments. *Denotes a significant difference from the control ($P \leq 0.05$); (b) Plots of COMMASSIE absorbance at 615nm versus concentration mg/ml (●) COMMASSIE and (○) COMMASSIE and SWCNT in a 1:1 mass ratio.

While the reduction in an absorbance feature of this nature provides little information about the type of the interaction between the two species, it undoubtedly verifies the existence of an interaction. In the spectroscopic studies it should be noted that a reduction in absorbance of the COMMASSIE was observed at all SWCNT concentrations, with significant reductions being observed at concentrations above 0.025 mg/ml. Given that it has been demonstrated that significant numbers of SWCNT

remain adhered to the cells even after washing this interaction could potentially have an adverse effect on the evaluation of toxicity of the SWCNT based on the absorbance of protein bound COMMASSIE.

7.3.2 Alamar Blue™ .

The Alamar Blue™ (AB) assay is designed to quantify the proliferation of various cell lines and is as stated widely utilized to measure cytotoxicity. Viable proliferating cells cause a reduction of the dye causing a colour change from a non-fluorescing indigo blue (oxidised) to a fluorescent pink species (reduced). One main advantage of this assay lies in its water solubility. It therefore requires no solvent extraction step and hence cellular viability is unaffected allowing multiple tests to be carried out on the cells. Measurements may be made by absorbance monitoring of AB supplemented cell culture medium or alternatively fluorescent measurements can be made (Biosource Inc, O'Brien *et al.*, 2000). The absorbance spectra of the oxidised and the reduced forms overlap. Therefore the absorbance measurements must be made at the absorbance maxima of each form, namely 570 nm and 600 nm. Fluorescent measurements can be made by exciting from 530 to 560 nm and recording emission at 590 nm (Biosource Inc, O'Brien *et al.*, 2000). A concentration response cytotoxicity (figure 7.2a) curve for the AB dye was obtained and again, as with the COMMASSIE dye, significant toxicity was observed at concentrations above 0.4mg/ml.

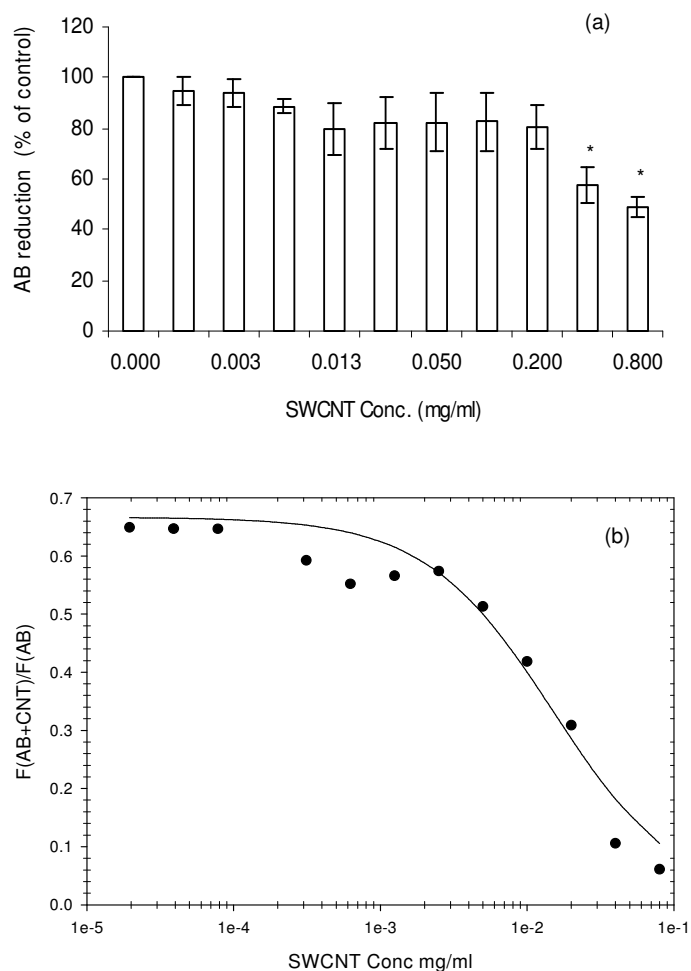


Figure 7.2 (a) Cytotoxicity of SWCNT to A549 cells after 24 hour exposure determined by the AB assay. Data are expressed as percent of control mean \pm SD of six independent experiments. *Denotes a significant difference from the control ($P \leq 0.05$); (b) Plot of emission ratios at 595nm by 540nm excitation for the AB assay against SWCNT concentration mg/ml.

To study the interaction of the reduced form of AB, confluent cells were exposed to an AB solution and it was allowed to undergo the oxidation process to the fluorescent pink species. This was then decanted off the cells and centrifuged to remove any remaining cells. SWCNT were then added to the solution at an initial concentration of 0.4 mg/ml and serially diluted down. The pink AB solution immediately lost its characteristic colour (see appendix 8) and total quenching of fluorescent emission at 595nm by 540nm

excitation was observed. The procedure was then repeated and a much lower initial SWCNT concentration of 0.08 mg/ml (10 % of highest toxicity test concentration) and serially diluted with the reduced form of AB to a final SWCNT concentration of 3.9×10^{-5} mg/ml. Fluorescent measurements of all solutions were then recorded after a 24 hour settling period. At the initial concentration of 0.08 mg/ml the solution again lost its characteristic pink colour and became transparent and a total quenching of emission at 595nm was observed. This quenching was then monitored as a function of SWCNT concentration and plotted as a ratio of the SWCNT free AB solution's emission by 540nm excitation, figure 7.2b depicts this ratio.

As described in Chapter 5, fluorescence studies have shown to aid in the elucidation of the interaction of nanotubes with different molecular species. SWCNT are known to interact with a wide variety of different molecular species. These interactions have been extensively documented, (Moulton *et al.*, 2005; Zhou *et al.*, 2001; Georgakilas *et al.*, 2002; Valeentini *et al.*, 2006; Keogh *et al.*, 2005) are well understood and are known to result in quenching of the emission of many fluorescent species (Hedderman *et al.*, 2004; Keogh *et al.*, 2004). Coleman *et al* constructed a model based on the adsorption/desorption of conjugated polymers in SWCNT composite solutions to explain the quenching of the fluorescence of the polymer when bound to the SWCNT (Coleman *et al.*, 2004). In chapter 5 this model was employed to assess the degree of interaction between the SWCNT and the various components of cell culture medium and will be also used here to assess the interaction between the SWCNT and the fluorescent dyes used to measure cytotoxicity.

The model described by equation 5.1 was applied to the data of figure 7.2b and a characteristic concentration value (C_0) was evaluated yielding a value of 0.015 ± 0.002

mg/ml. In a study of this nature the ability to use this value to estimate a binding energy, for which the model was originally derived is limited. This is primarily due to the nature of the dilution process, in which the AB concentration was kept constant and it was assumed 100% of the initial AB concentration exposed to the cells was reduced to the pink fluorescent form. However that the experimental data fits well to this model and that the AB emission is quenched would indicate that the two species are undoubtedly interacting to a degree. It should be noted that at the lowest SWCNT concentration of 3.9×10^{-5} mg/ml, fluorescent quenching was observed with a reduction to approximately 68% from AB solution to that containing SWCNT. This has severe implications for toxicity evaluations using this assay, potentially resulting in false positive toxicity evaluations being made as a result of the interaction of the SWCNT with the AB assay itself, as it has been previously noted that bundle residues of SWCNT irreversibly bind to cell surfaces during exposures so that SWCNT are present during all steps of the AB assay and therefore are able to interact with the dye even after cell washing steps (Davoren *et al.*, 2007).

7.3.3 Neutral Red.

The NR cytotoxicity assay is based on the ability of viable cells to incorporate and bind neutral red, a weak cationic dye that readily penetrates cell membranes by non-ionic diffusion (Borenfreund *et al.*, 1984, Borenfreund *et al.*, 1988). It accumulates in the lysosomes of cells where it binds to the sensitive lysosomal membrane. Cells damaged by xenobiotic action have decreased ability of taking up and binding NR, so that viable cells can be distinguished from damaged or dead cells. The dye can be extracted from intact cells using a solution of 1 % (v/v) acetic acid and 50 % (v/v) ethanol and the absorbance or fluorescence of solubilised dye can be determined (Borenfreund *et al.*,

1984; Borenfreund *et al.*, 1988). The test is very sensitive, specific, and readily quantifiable. Recent literature has highlighted absorptive interferences between carbon black and cellular viability markers such as NR resulting in false readings (Montiero-Riviero *et al.*, 2006) as in the absence of human epidermal keratinocytes, a false negative signal was generated, inaccurately indicting the presence of viable cells. The carbon black was found to adsorb to the NR dye and trigger a signal in the dye implying high cell viability when in fact the cells were not even present.

Throughout the toxicity studies carried out here, inconsistent fluorescent readings were acquired when using the NR dye suggesting an interaction between the SWCNT and the NR dye. Figure 7.3a depicts the concentration response cytotoxicity curve obtained for the NR dye. Large variations were experienced throughout the study, as can be seen from the error bars in the data presented. A curve of this nature could be interpreted as a hormesis effect but more likely as a false negative effect caused by interference by the SWCNT with the NR dye, similar to that reported by Monteiro-Riviere *et al.* In a study by Davoren *et al.* (2007) to evaluate the cytotoxicity of SWCNT, TEM analysis of A549 cells post exposure to SWCNT showed a discernible increase in lamellar bodies in the exposed cells in comparison to unexposed controls. It was postulated that the increase of lamellar bodies may have been a defence mechanism of the cells upon exposure to the SWCNT; it is also plausible that this increase in lamellar bodies contributed to the inconsistencies shown here with the NR dye, as secretion vacuoles like lamellar bodies are secondary lysosomes (Achterrath *et al.*, 2005).

To elucidate the extent of this interaction a concentration fluorescent study was carried out. SWCNT were dispersed in a NR deionised water solution in an initial 1:1

concentration ratio of 0.0625 mg/ml and were then serially diluted down with deionised water, to reduce both the NR and the SWCNT concentration equally to a final concentration of 9.5×10^{-7} mg/ml. Fluorescent measurements were recorded, the quenching of the NR emission was monitored as a function of SWCNT concentration and this quenching was then plotted as a ratio between the SWCNT containing solution and SWCNT-free solutions (figure 7.3b). Using the model described above, a C_0 value was estimated to be 0.0095 ± 0.002 mg/ml. The ability to fit the data to this model and evaluate a C_0 value coupled with the inconsistent cytotoxicity data obtained, verifies that there is an interaction occurring between the two species and severely limits its potential use in toxicity studies involving SWCNT.

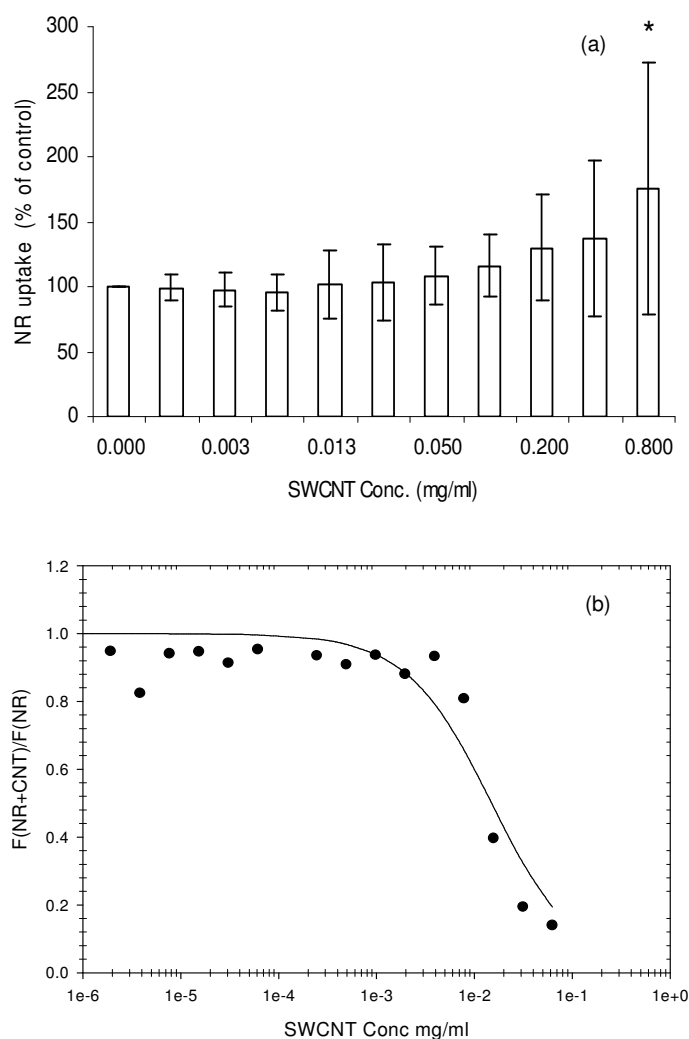


Figure 7.3(a) Cytotoxicity of SWCNT to A549 cells after 24 hour exposure determined by the NR assay. Data are expressed as percent of control mean \pm SD of six independent experiments.

*Denotes a significant difference from the control ($P \leq 0.05$); (b) Plot of emission ratios for the NR assay against SWCNT concentration mg/ml.

7.3.4 MTT (3-(4,5-dimethylthiazol-2-yl)-2,5-diphenyltetrazolium bromide).

The MTT colorimetric assay determines the ability of viable cells to reduce the soluble, yellow tetrazolium salt [3-(4,5-dimethylthiazol-2-yl)-2,5-diphenyltetrazolium bromide] (MTT) into an insoluble, purple formazan precipitate which can be solubilised by the

addition of an organic solvent and quantified spectroscopically. Tetrazolium salts accept electrons from oxidized substrates or enzymes, such as NADH and NADPH. Reduction of MTT takes place at the ubiquinone and cytochrome b and c sites of the mitochondrial electron transport chain due to succinate dehydrogenase activity (Mosmann, 1983).

Applications for the MTT assay include drug sensitivity and cytotoxicity. The assay is considered as rapid, safe, versatile, quantitative, and highly reproducible with an intra-test variation between data points of only +/- 15 percent. For each cell type, a linear relationship between cell number and absorbance can be established, enabling accurate quantification (Supino, 1998). The main disadvantage to the use of tetrazolium salts are their cytotoxicity. To solubilise the formazan crystals, solvents such as dimethylsulfoxide (DMSO) or HCl/isopropanol have to be used. This treatment results in destruction of investigated cells, allowing only a single time point measurement (Biosource, 2006). Addition of DMSO destroys the cell membrane and results in liberation and solubilisation of the crystals. The number of viable cells is thus directly proportional to the level of the initial formazan product created and can be quantified by measuring the absorbance at 570 nm (Magrez *et al.*, 2006).

Recent literature has demonstrated that the reduced formazan precipitate binds to the SWCNT and the resultant decrease in absorbance is due to interference of the dye with the SWCNT and not toxicity as had previously been reported when using the MTT assay (Worle-Knirsch *et al.*, 2006). The likelihood of the curve shown here being a true representation of SWCNT toxicity is therefore questionable and could originate from adsorptive interferences caused by the interaction of the SWCNT with the MTT assay.

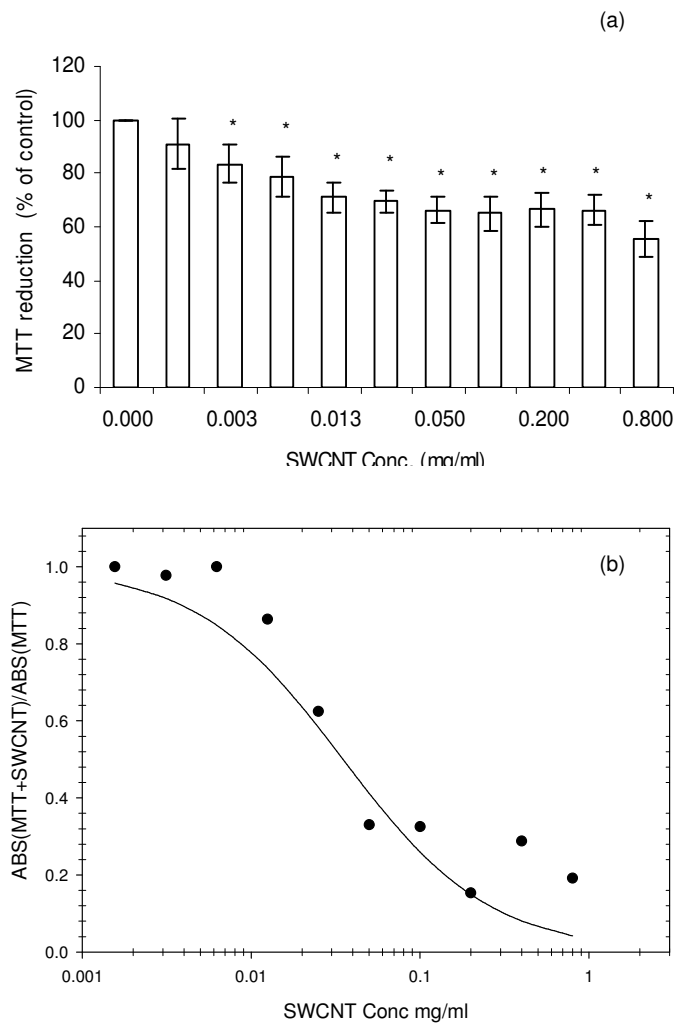


Figure 7.4 (a) Cytotoxicity of SWCNT to A549 cells after 24 hour exposure determined by the MTT assay. Data are expressed as percent of control mean \pm SD of six independent experiments. *Denotes a significant difference from the control ($P \leq 0.05$); (b) Plot of the absorbance ratio of the converted MTT formazan against SWCNT concentration mg/ml.

To verify that the MTT assay was potentially giving a false positive toxicity for the SWCNT, confluent cells were exposed to an MTT solution (0.5 mg/ml) and the system was allowed to undergo the reduction process to form the purple formazan precipitate. This was then extracted with 0.04N HCl prepared in isopropanol and then decanted and centrifuged to remove any remaining cells. SWCNT containing solutions were then prepared with this at an initial concentration of 0.8 mg/ml and serially diluted down to

reduce the SWCNT concentration. The samples had to be allowed to settle for 48 hours (double the sedimentation period of all other assays tested) before they were characterised spectroscopically. Visual differences were observed between the solutions; at SWCNT concentrations above 0.05 mg/ml the solutions underwent a colour change from the characteristic purple of the converted form of MTT to a pale yellow similar to that of the unconverted MTT. This colour change may indicate the presence of unconverted MTT, which was not converted by the cells and did not interact with the SWCNT. Wörle Knirsch *et al*, (2006) showed microscopically that the converted formazan crystals bound to the nanotubes and resulted in a false positive toxic effect being concluded.

In this study, absorbance spectra were recorded and the reduction of the formazan feature at 570nm was monitored as a function of SWCNT concentration. This was then plotted as a ratio (figure 7.4b). There were no noticeable spectroscopic differences at concentrations below 0.00625 mg/ml. Above this, a reduction in absorption was observed and this reduction was seen to increase with increasing SWCNT concentration. The reduction in the MTT associated absorbance combined with the visual differences observed at concentrations above 0.05 mg/ml (colour change from purple to pale yellow) undoubtedly verified the presence of an interaction between the two species. This supports the notion proposed by Wörle Knirsch *et al*, (2006) that the formazan precipitate of the MTT assay binds to the SWCNT. Figure 7.4b shows spectroscopically that this proposed binding process induces a reduction in the associated absorbance resulting in a false positive toxic effect being evaluated as was observed in the cytotoxicity curve presented.

7.3.5 WST-1 (2-(4-iodophenyl)-3-(4-nitrophenyl)-5-(2,4-disulfophenyl)-2H-tetrazolium).

The WST-1 assay is very similar to the MTT assay. The tetrazolium salt WST-1 is reduced by cellular mitochondrial hydrogenases at the same structural position when compared to MTT (Tan *et al.*, 2000, Ranke *et al.*, 2004). The resulting product, in contrast to the MTT assay, is water-soluble and can be spectroscopically quantified at 450 nm without any required extraction step (Tan *et al.*, 2000, Ranke *et al.*, 2004). Its water-solubility is also the reason why this dye was recommended by Wörle Knirsch *et al.* as no binding of crystals to SWCNT could be observed microscopically so the authors concluded no interaction would take place. A concentration response cytotoxicity (figure 7.5a) curve for the WST-1 assay was obtained in our study and significant toxicity was observed at 0.4 mg/ml.

A similar spectroscopic study was carried out on the WST-1 dye as performed with the AB and MTT dyes. The WST-1 dye was allowed to undergo the conversion process by exposing it to confluent cells for a period of three hours followed by decanting and centrifugation to remove any remaining cells. This was then used to form SWCNT containing solutions by dispersing an initial concentration of 0.4 mg/ml SWCNT. The SWCNT concentration was sequentially reduced by serial dilution with the converted WST-1 dye. Upon examination of the absorbance spectra of the solutions, differences were observed. A reduction in the WST-1 associated absorbance was noted at concentrations above 0.0125 mg/ml. This reduction was then seen to increase with increasing SWCNT concentration. The absorbance of the WST-1 dye was then monitored as a function of SWCNT concentration and again plotted as a ratio (figure 7.5b). This plot was then fitted with the described model (Coleman *et al.*, 2004) and a

C_0 value of 0.185 mg/ml was obtained. The original model was derived for emission quenching of a fluorescent species and that a good fit is observed here confirms the presence of an interaction between the WST-1 dye and the SWCNT. This therefore has implications for the use of this assay in the evaluation of toxicity as the interaction between the WST-1 dye and the SWCNT may result in a false positive toxic effect being observed similar to that of the MTT assay.

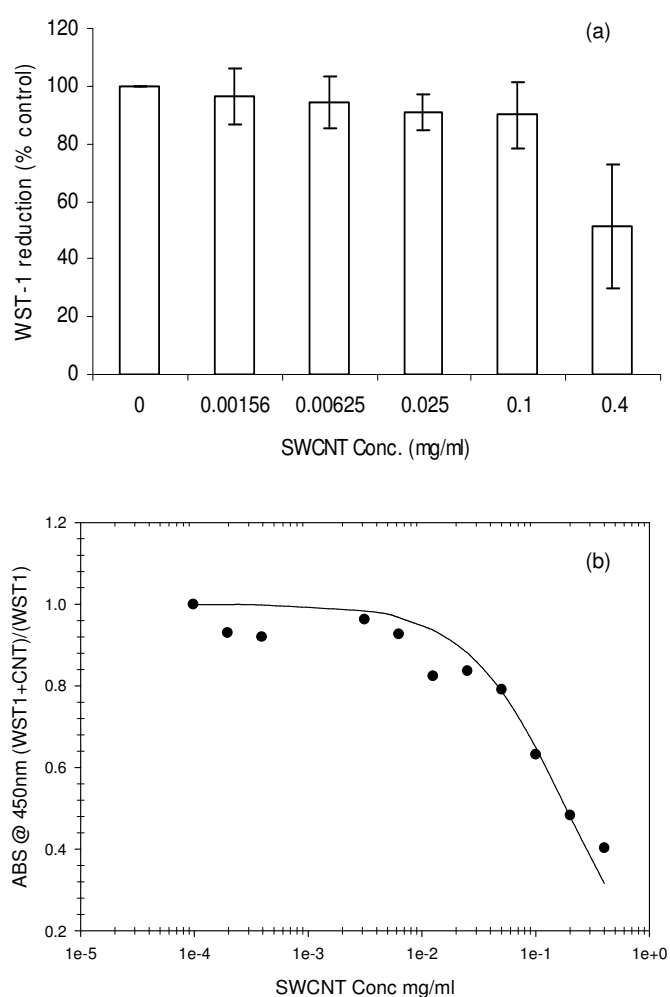


Figure 7.5 (a) Cytotoxicity of SWCNT to A549 cells after 24 hour exposure determined by the WST-1 assay. Data are expressed as percent of control mean \pm SD of three independent experiments. *Denotes a significant difference from the control ($P \leq 0.05$); (b) Plot of the absorbance ratios for the WST-1 assay against SWCNT concentration mg/ml.

7.4 Chapter Summary.

This chapter has highlighted difficulties encountered in the evaluation of the *in vitro* cytotoxicity of SWCNT. The spectroscopic characterisation revealed interactions of varying degrees between the SWCNT and all the tested indicator dyes employed in this study to assess particle toxicity as evident by the differing C_0 values determined for each assay. This undoubtedly raises questions about the validity of the cytotoxicity data presented in this chapter and other studies based on the absorption/fluorescent emission of these dyes.

Table 7.1 displays a list of all cytotoxic dyes tested, the spectroscopic property from which cytotoxicity data is evaluated, the SWCNT concentration at which toxicity was observed and the lowest SWCNT concentration at which absorptive interferences were detected.

| Indicator Dye | Property | Toxicity Observed Conc. mg/ml | Interference Observed Conc. mg/ml |
|----------------------|-----------------|--|--|
| Comassie | Absorption | 0.4 | 2.25×10^{-2} |
| NR | Fluorescence | 0.8 | 1.95×10^{-2} |
| AB | Fluorescence | 0.4 | 3.9×10^{-5} |
| MTT | Absorption | 0.003 | 6.25×10^{-3} |
| WST-1 | Absorption | 0.4 | 1.25×10^{-2} |

Examining the data presented in table 7.1 it can be clearly seen that in the presence of fine quantities of SWCNT absorptive interferences were noted, this raises questions about the validity of the cytotoxicity data presented. In a study by Davoren *et al*, (2007) it was noted that SWCNT remain bound to the surface of the cells post exposure after

several washes with PBS. Their presence and the possibility of interference with the tested assays is therefore a realistic scenario when carrying out *in vitro* cytotoxicity studies of this nature. With the exception of the NR assay the interferences noted, by spectroscopic analysis, would undoubtedly contribute to a false positive toxic effect being evaluated in the presence of fine quantities of SWCNT. The ideal test for *in vitro* cell cytotoxicity must not interfere with the compound to be tested. The results presented in this chapter therefore have comprehensively confirmed that the indicator dyes used here namely, Commassie Blue, AB, NR, MTT and WST-1 were not appropriate for the quantitative toxicity assessment of carbon nanotubes.

References

Achterrath U, Blumcke S. "Electron-histochemical investigations on Clara cells and type II pneumocytes of normal rat lungs." *Lung*, 2005; 152: 123-129.

Alamar Blue™ Product information pamphlet. BioSource International, Inc., USA

Bradford MM. "A rapid and sensitive method for the quantitation of microgram quantities of proteins utilizing the principle of protein dye binding." *Analytical Biochemistry*. 1976; 72:248-254.

Borenfreund E, Puerner JA. "A simple quantitative procedure using monolayer cultures for cytotoxicity assays (HTD/NR-90)." *Journal of Tissue Culture Methods* 1984; 9:1.

Borenfreund E, Babich H, Martin- Alguacil N. "Comparisons of two *in vitro* cytotoxicity assays – The neutral red (NR) and tetrazolium MTT tests." *Toxicology in Vitro* 1988; 2: 1-6.

Casey A, Farrell GF, McNamara M, Byrne HJ, Chambers G. "Interaction of carbon nanotubes with sugar complexes." *Synthetic Metals*. 2005; 153: 357-60.

Casey A, Davoren M, Herzog E, Lyng FM, Byrne HJ, Chambers G. "Probing the interaction of single walled carbon nanotubes within cell culture medium as a precursor to toxicity testing." *Carbon*, 2007, 45, 34-40.

Coleman JN, Maier S, Fleming A, O'Flaherty S, Minett A, Ferreira MS, *et al.* "Binding kinetics and spontaneous single wall carbon nanotube bundle dissociation in low concentration polymer-nanotube solutions." *Journal of Physical Chemistry B*. 2004; 108: 3446-50.

Cui D, Tian F, Ozkan CS, Wang M, Gao H. "Effect of single wall carbon nanotubes on human HEK293 cells." *Toxicology Letters*. 2005; 155: 73-85.

Davoren M, Herzog E, Casey A, Cottineau B, Chambers G, Byrne HJ, Lyng FM. "*In vitro* Toxicity Evaluation of Single Walled Carbon Nanotubes on human A549 lung cells." *Toxicology in Vitro*, 2007, 21, 438-448.

Donaldson K, Aitken R, Tran L, Stone V, Duffin R, Forrest G, *et al.* "Toxicology of carbon nanotubes." *Toxicology Science*. 2006; 92: 5-22.

Georgakilas V, Tagmatarchis N, Pantarotto D, Bianco A, Brian JP, Prato M. "Amino acid functionalisation of water soluble carbon nanotubes." *Chemical Communications*. 2002; 3050-51.

Giordani S, Bergin SD, Nicolosi V, Lebedkin S, Kappes MM, Blau WJ, *et al.* "Debundling of single-walled nanotubes by dilution: observation of large populations of individual nanotubes in amide solvent dispersions." *Journal of Physical Chemistry B*. 2006; 110: 15708-18.

Hurt RH, Monthieux M, Kane A. "Toxicology of carbon nanomaterials: Status, trends, and perspectives on the special issue." *Carbon*. 2006; 44: 1028-33.

Harrison BS, Atala A. "Carbon nanotube applications for tissue engineering." *Biomaterials* 2007; 28:344-53.

Hedderman TG, Keogh SM, Chambers G, Byrne HJ. "Solubilisation of Single walled carbon nanotubes with organic dye molecules." *Journal of Physical Chemistry B*. 2004; 108 (49): 18860-65.

Hedderman TG, Keogh SM, Chambers G, Byrne HJ. "In-depth study into the interaction of single walled carbon nanotubes with anthracene and p-terphenyl." *Journal of Physical Chemistry B*. 2006; 110: 3895-901.

Kawamoto H, Uchida T, Kojima K, Tachibana M. "Raman study of DNA-wrapped single walled carbon nanotube hybrids under various humidity conditions." *Chemical Physics Letters*. 2006; 431: 118-120.

Keogh SM, Hedderman TG, Ruther MG, Lyng FM, Gregan E, Farrell GF, *et al.* "Temperature induced nucleation of poly(m-phenylenevinylene-co-2,5-dioctoxy-p-phenylenevinylene) crystallization by HiPco single-walled carbon nanotubes." *Journal of Physical Chemistry B*. 2005; 109 (12): 5600-7.

Keogh SM, Hedderman TG, Gregan E, Farrell GF, Chambers G, Byrne HJ. "Spectroscopic analysis of single walled carbon nanotube and semi-conjugated polymer composites." *Journal of Physical Chemistry B*. 2004; 108(20): 6233-41.

Matejovicova M, Mubagwa K, Flameng W. "Effect of vanadate on protein determination by the comassie brilliant blue microassay procedure." *Analytical Biochemistry*. 1997; 245: 252-54.

Monteiro-Riviere NA, Inman AO. "Challenges for assessing carbon nanomaterial toxicity to the skin." *Carbon*. 2006; 44: 1070-78.

Mosmann T. "Rapid colorimetric assay for cellular growth and survival: Application to proliferation and cytotoxicity assays." *Journal of Immunology Methods*. 1983; 65: 55-63.

Moulton SE, Minett AI, Murphy R, Ryan KP, McCarthy D, Coleman JN, *et al.* "Biomolecules as selective dispersants for carbon nanotubes." *Carbon*. 2005; 43: 1879-84.

Muller J, Huaux L, Lison D. "Respiratory toxicity of carbon nanotubes: How worried should we be?" *Carbon*. 2006; 44: 1048-56.

O'Brien J, Wilson I, Orton T, Pognan F. "Investigation of alamar blue (resazurin) fluorescent dye for the assessment of mammalian cell cytotoxicity." *European Journal of Biochemistry*. 2000; 267: 5421-5426.

Pantarotto D, Singh R, McCarthy D, Erhardt M, Briand JP, Prato M, *et al.*
“Functionalized carbon nanotubes for plasmid DNA gene delivery.” *Angewandte Chemie International* 2004; 43: 5242-46.

Ranke J, Mölter K, Stock F, Bottin-Weber U, Poczobutt J, Hoffmann J, *et al.*
“Biological effects of imidazolium ionic liquids with varying chain lengths in acute *Vibrio fischeri* and WST-1 cell viability assays.” *Ecotoxicology and Environmental Safety*. 2004; 58: 396-404.

Salvador-Morales C, Flahaut E, Sim E, Sloan J, Green MLH, Sim RB. “Complement activation and protein adsorption by carbon nanotubes.” *Molecular Immunology*. 2006; 43: 193-201.

Singh KV, Pandey RR, Wang X, Lake R, Ozkan CS, Wang K, *et al.* “Covalent functionalization of single walled carbon nanotubes with peptide nucleic acid: Nanocomponents for molecular level electronics.” *Carbon*. 2006; 44: 1730-39.

Supino R. MTT assays. 1998; In: O’Hare, S., Atterwill C.K. (Eds), *Methods in Molecular Biology, In Vitro Toxicity Testing Protocols* 43. Humana Press Inc. N.J, pp. 137-149.

Tan AS, Berridge MV. “Superoxide produced by activated neutrophils efficiently reduces the tetrazolium salt, WST-1 to produce a soluble formazan: a simple

colorimetric assay for measuring respiratory burst activation and for screening anti-inflammatory agents.” *Journal of Immunology Methods*. 2000; 238: 59-68.

Warheit DB. “What is currently known about the health risks related to carbon nanotube exposure?” *Carbon*. 2006; 44: 1064-69.

Wörle-Knirsch JM, Pulskamp K, Krug HF. “Oops they did it again! Carbon nanotubes hoax scientists in viability assays.” *Nanoletters*. 2006; 6: 1261-68.

Valeentini L, Amentano I, Ricco L, Alongi J, Pennelli G, Mariani A, *et al.* “Selective interaction of single-walled carbon nanotubes with conducting dendrimer.” *Diamond and Related Materials*. 2006; 15: 95-9

Venkatesan N, Yoshimitsu J, Ito Y, Shibata N, Takada K. “Liquid filled nanoparticles as a drug delivery tool for protein therapeutics.” *Biomaterials* 2005; 26: 7154-63.

Yu X, Chattopadhyay D, Galeska I, Papadimitrakopoulos F, Rusling JF. “Peroxidase activity of enzymes bound to the ends of single-wall carbon nanotube forest electrodes.” *Electrochemistry Communications* 2003; 5:408–11.

Zhou W, Ooi YH, Russo R, Papanek P, Luzzi DE, Fischer JE, *et al.* “Structural characterization and diameter-dependant oxidative stability of single wall carbon nanotubes synthesized by the catalytic decomposition of CO.” *Chemical Physics Letters*. 2001; 350: 6-14.

Chapter 8

“Conclusions”

8.1 Summary of findings.

Over the course of this thesis, a number of issues previously unaddressed in the literature, relating to the evaluation of SWCNT toxicity *in vitro* have been highlighted. In chapter 5 it was shown that upon the dispersion of SWCNT within commercial cell culture medium, considerable previously uncharacterised interactions occurred. The origins of these interactions were determined spectroscopically. Absorption spectroscopy revealed that the observed colour change in the higher SWCNT concentration regions was attributed to an interaction of the SWCNT with the phenol red component of the medium. The function of the phenol red is as a pH indicator within the medium. However no significant change in pH was noted as a function of SWCNT concentration. Furthermore absorption spectroscopy revealed reductions in the associated absorbance of the components of the medium and the added FBS protein supplement.

SWCNT concentration dependant fluorescent studies were then employed to assess the degree of interaction occurring between the SWCNT and the medium components. This was done by excitation of the SWCNT medium suspensions by three wavelengths, namely 268, 360 and 410nm, each corresponding to a medium component. The emission characteristics of each of these components were then monitored as a function

of SWCNT concentration. Using a model (Coleman *et al*, 2004) originally derived to study the interactions and aggregation state of SWCNT within a polymer matrix; characteristic concentrations were calculated for each medium component. In the original study these values were used to further calculate the binding energy between the SWCNT and the polymer. In this study it was not feasible to do this due to the nature in which the suspensions were prepared. Despite the inability to estimate binding energy the ability to fit the data to such a model and calculate different characteristic concentrations for each medium components interaction with the SWCNT, undoubtedly verifies the presence of considerable interactions upon the dispersion of SWCNT within cell culture medium.

The model was also used to monitor the aggregation state of SWCNT as a function of concentration. In this study the nature of the obtained emission ratio plots presented in chapter 5 would imply that the aggregation state of the SWCNT remained constant over the concentration range studied, Raman spectroscopy and TEM analysis (see appendix 9) verified this. It was therefore shown that the SWCNT tested remained as aggregates rather than individual tubes. Thus, the likelihood of toxicity as a result of internalisation within the cell walls would be reduced. A number of studies have shown that cellular internalization of various nanoparticles can occur (Stearns *et al.*, 2001, Monteiro-Riviere *et al.*, 2005, Rouse *et al.*, 2006) with endocytosis being the most probable mechanism of uptake. However, transmission electron microscopy in a study performed by Davoren *et al.*, (2007) confirmed that there was no intracellular localization of the tested SWCNT bundles in A549 cells following 24 hour exposure.

The addition of the FBS protein supplement was noted to visually affect the dispersion behaviour of the SWCNT in the medium. Using fluorescent emission spectroscopy the interaction of the FBS was studied and a characteristic concentration for the added protein calculated. It was postulated that the large bulky protein molecules would be relatively slow to adsorb onto the surface of the nanotube aggregates but subsequently would also be slow to desorb off the surface. Hence they played an active role in retaining the SWCNT in the medium suspension. Recommendations were made that future toxicity studies evaluating the direct cytotoxicity of SWCNT should culture and expose cells in the absence of an added protein supplement. Its presence is expected to have adverse effects in the evaluation of SWCNT cytotoxicity. This was verified in a study by Davoren *et al*, (2007) evaluating the direct cytotoxicity of SWCNT in which it was noted that in the absence of the added protein supplement increased cytotoxicity was observed.

As a result of these interactions it was postulated that SWCNT may induce an indirect/secondary toxicity by means of medium depletion due to interaction with the SWCNT. This proposed notion was investigated and verified in chapter 6. Spectroscopic analysis confirmed that all SWCNT dispersed within the cell culture medium were removed by centrifugation and filtration, as no evidence of their presence could be detected spectroscopically. Absorption and emission spectroscopy confirmed that the composition of the medium had been altered due to the dispersion and removal of the SWCNT, as evidenced by reduction in the associated absorbance and emission of the medium components.

The human alveolar carcinoma epithelial cell line A549 was then employed for toxicity evaluation. The indirect cytotoxicity of SWCNT was then evaluated by 24, 48, 72 and 96 hour exposures to the filtered medium and evaluated using two cytotoxic indicator dyes namely Alamar Blue and Neutral Red. These cytotoxicity studies did show that SWCNT could induce significant toxicity indirectly at high concentrations after a period of 48 hours. Differences in the observed cytotoxicity were noted between the different fabrication methods of SWCNT as determined by the AB assay. Differences in the observed cytotoxicity between the two cytotoxic assays employed were also noted. Alamar blue appeared more sensitive than the neutral red, as the obtained cytotoxicity data for neutral red was not as consistent when compared to that of the alamar blue. It was postulated that these differences may have arisen from a reduction of the proliferative capacity of the A549 cells in the filtered medium as determined by the AB assay but with little or no effect on cellular viability as determined by the neutral red assay. However the results of this chapter did conclusively confirm that SWCNT could induce an indirect/secondary toxicity by means of medium depletion and this mechanism could therefore contribute to a false positive toxic effect being observed when evaluating SWCNT toxicity.

Chapter 7 employed standard techniques to evaluate the direct cytotoxicity of SWCNT with a battery of cytotoxicity indicator dyes which had been used in the literature to previously evaluate SWCNT cytotoxicity. A549 lung cells were again used and were cultured and exposed to SWCNT in serum free medium. The validity of this cytotoxicity data was then tested using spectroscopic analysis to investigate the effect of SWCNT on the effective operation of each cytotoxicity indicator dye employed. The spectroscopic characterisation revealed interactions of varying degrees between the

SWCNT and all the tested indicator dyes employed in this study to assess particle toxicity which was evident by the differing C_0 values determined for each assay. While the calculation of a characteristic concentration provides very relevant information about the degree of interaction between the assays and the SWCNT in terms of cellular laboratory practice it could be difficult to interpret.

This undoubtedly raises questions about the validity of the cytotoxicity data presented in this and other studies based on the absorption/fluorescent emission of these dyes. The ideal test for *in vitro* cell cytotoxicity must not interfere with the compound to be tested. The results in this thesis therefore comprehensively confirmed that the indicator dyes used in this study (CB, AB, NR, MTT and WST-1) were not appropriate for the quantitative toxicity assessment of carbon nanotubes. The question of how toxic are SWCNT remains unanswered and will remain questionable until new screening techniques are developed which do not involve the uses of such indicator dyes that interfere with the carbon nanomaterial.

8.2 Further work.

The additional or continual research in this area should focus predominately on the development of an alternative interdisciplinary screening technique. However there are some other issues which need to be addressed.

Due to the various fabrication techniques there are a large amount of SWCNT with differing properties (diameter, length, and surface reactivity, impurity level, metallic or semi-conducting) and indeed there can also be substantial differences between samples produced from the same process batch to batch. This leads to a large range of materials

which can have differing properties classified as SWCNT. It is therefore vital that key contributing factors that could induce toxicity be evaluated and classified in order of their toxicological importance specifically for SWCNT. If this type of mechanistic approach was taken in future studies it is plausible that the key contributing factors of SWCNT toxicity would be applicable to a much wider range of engineered nanoparticles and be of great benefit to the research area.

In chapter 6 differences were noted between the AB and NR assays and it was postulated that these differences may have arisen due to a reduction in proliferation and retention in cellular viability in the depleted medium. As such this is an area which could be further explored. By using a more basic approach involving cell counts and clonogenic studies this hypothesis could be verified and could further contribute to elucidating the origins of the inconsistent cytotoxicity data that exists in current literature.

Recent studies have employed the use of trans-scriptomics and proteomics as a way to “fingerprint” cellular responses to perturbation, for example by the presence of nanoparticles. The principle is that all cells have a characteristic mRNA and protein expression profile, which can be mapped. The introduction of nanoparticles (or other stimuli or perturbation) will result in changes to these characteristic expression profiles. The up- and down- regulation of mRNA and proteins can thus be used to “fingerprint” the response of the cells to the presence of the nanoparticles.

Raman and infra red spectroscopy can also be used to “fingerprint” cells, and this technique been shown to be able to monitor changes in cellular behaviour, such as cell

proliferation. Thus, vibrational spectroscopy could be used to fingerprint responses of cells to nanoparticles, and the results could be correlated with the trans-scriptomic and proteomic data to provide the fullest description of the effects of interaction with nanoparticles on cells.

Such data would feed directly into the development of a risk assessment method for nano-safety, as well as helping to validate alternative toxicity screening methodologies which could reduce the cost and complexity of nanoparticle safety screening, reducing the reliance on animal tests and enabling high-throughput screens to emerge.

8.3 Concluding remarks.

Over the course of this thesis a number of contributing factors, which have hindered the development of the toxicological profile of SWCNT, have been highlighted. SWCNT were shown to interact with a commercial cell culture medium, these interactions were seen to affect the evaluation of SWCNT toxicity, in the case of the serum reducing the observed direct cytotoxicity of SWCNT resulting in a false negative toxic response. These interactions were further shown to induce an indirect toxicity which would contribute to a false positive toxic response being observed. Finally absorptive interferences were shown for all the cytotoxic dyes tested again creating a false positive toxic response. The presented studies have effectively shown that classical *in vitro* protocols and endpoints need to be adapted if the potential health risks of SWCNT are to be truly assessed. As a result of this the development of an alternative screening technique is of paramount importance.

The results presented have raised a very important question; does nanotoxicology necessitate a new toxicological science? The answer to this question undoubtedly, like nanotoxicology, is complicated. It is the general consensus of researchers in the field of nanotoxicology, that if it is to move forward as a discipline and reach the overall goal of providing reliable toxicological data on the ever increasing range of engineered nanoparticles then it will rely heavily on the collaboration of materials and biological scientists. Collaborations of this manner should facilitate all contributing factors, from both physical/chemical and biological viewpoints, to be identified and classified in order of toxicological relevance. Nanotoxicology does not necessitate a new toxicological science as such but it does demand the communication between different disciplines of science as was seen through out this thesis which employed both physical/chemical and biological techniques to assess contributing factors to SWCNT toxicity.

References

Coleman JN, Maier S, Fleming A, O'Flaherty S, Minett A, Ferreira MS, *et al.* "Binding kinetics and spontaneous single wall carbon nanotube bundle dissociation in low concentration polymer-nanotube solution." *Journal of Physical Chemistry B*. 2004; 108: 3446-50.

Davoren M, Herzog E, Casey A, Cottineau B, Chambers G, Byrne HJ, Lyng FM. "*In vitro* Toxicity Evaluation of Single Walled Carbon Nanotubes on human A549 lung cells." *Toxicology in Vitro*. 2007, 21, 438-448.

Monteiro-Riviere NA, Nemanich RJ, Inman AO, Wang YY, Riviere JE. "Multi-walled carbon nanotubes interactions with human epidermal keratinocytes." *Toxicology Letters*. 2005; 155: 377-84.

Rouse JG, Yang J, Barron AR, Monteiro-Riviere NA. "Fullerene-based amino acid nanoparticles interactions with human epidermal keratinocytes." *Toxicology in Vitro*. 2006; 20 (8): 1313-1320.

Stearns RC, Paulauskis JD, Godleski JJ. "Endocytosis of ultrafine particles by A549 cells." *American Journal of Respiratory Cell Molecular Biology*. 2001; 24: 108-15.

Appendices

Appendix 1

The appended paper details research carried out in the initial stages of my PhD research in composite SWCNT systems with saccharides. Inclusion complexes of starch were utilised to create aqueous dispersions of SWCNT these suspensions were then subsequently characterised spectroscopically.

Appendix 2

| COMPONENTS | Molecular Weight | Concentration (mg/L) | Molarity (mM) |
|--|------------------|----------------------|---------------|
| Amino Acids | | | |
| Glycine | 75 | 15 | 0.200 |
| L-Alanine | 89 | 18 | 0.202 |
| L-Arginine hydrochloride | 211 | 422 | 2.00 |
| L-Asparagine-H ₂ O | 150 | 30 | 0.200 |
| L-Aspartic acid | 133 | 26.6 | 0.200 |
| L-Cysteine hydrochloride-H ₂ O | 176 | 70 | 0.398 |
| L-Glutamic Acid | 147 | 29 | 0.197 |
| L-Glutamine | 146 | 292 | 2.00 |
| L-Histidine hydrochloride-H ₂ O | 210 | 45.8 | 0.218 |
| L-Isoleucine | 131 | 7.88 | 0.0602 |
| L-Leucine | 131 | 26.2 | 0.200 |
| L-Lysine hydrochloride | 183 | 73 | 0.399 |
| L-Methionine | 149 | 8.96 | 0.0601 |
| L-Phenylalanine | 165 | 9.92 | 0.0601 |
| L-Proline | 115 | 69 | 0.600 |
| L-Serine | 105 | 21 | 0.200 |
| L-Threonine | 119 | 23 | 0.193 |
| L-Tryptophan | 204 | 4.1 | 0.0201 |
| L-Tyrosine disodium salt dihydrate | 181 | 13.5 | 0.0746 |
| L-Valine | 117 | 23 | 0.197 |
| Vitamins | | | |
| Biotin | 244 | 0.07 | 0.000287 |
| Choline chloride | 140 | 14 | 0.1000 |
| D-Calcium pantothenate | 477 | 0.5 | 0.00105 |
| Folic Acid | 441 | 1.3 | 0.00295 |
| i-Inositol | 180 | 18 | 0.1000 |
| Niacinamide | 122 | 0.037 | 0.000303 |
| Pyridoxine hydrochloride | 206 | 0.06 | 0.000291 |
| Riboflavin | 376 | 0.04 | 0.000106 |
| Thiamine hydrochloride | 337 | 0.3 | 0.000890 |
| Vitamin B12 | 1355 | 1.4 | 0.00103 |
| Inorganic Salts | | | |
| Calcium Chloride (CaCl ₂) (anhyd.) | 111 | 102 | 0.919 |
| Cupric sulfate (CuSO ₄ ·5H ₂ O) | 250 | 0.002 | 0.000080 |
| Ferric sulfate (FeSO ₄ ·7H ₂ O) | 278 | 0.8 | 0.00288 |
| Magnesium Chloride (anhydrous) | 95 | 49.7 | 0.523 |
| Magnesium Sulfate (MgSO ₄) (anhyd.) | 120 | 192 | 1.60 |
| Potassium Chloride (KCl) | 75 | 285 | 3.80 |
| Sodium Bicarbonate (NaHCO ₃) | 84 | 2500 | 29.76 |
| Sodium Chloride (NaCl) | 58 | 7530 | 129.83 |
| Sodium Phosphate dibasic (Na ₂ HPO ₄) anhydrous | 142 | 115.5 | 0.813 |
| Sodium Phosphate monobasic (NaH ₂ PO ₄) anhydrous | 139 | 59 | 0.424 |

| | | | |
|---|-------|-------|----------|
| Zinc sulfate (ZnSO ₄ -7H ₂ O) | 288 | 0.144 | 0.000500 |
| Other Components | | | |
| D-Glucose (Dextrose) | 180 | 1260 | 7.00 |
| Hypoxanthine Na | 131 | 4 | 0.0305 |
| Lipoic Acid | 206 | 0.21 | 0.00102 |
| Phenol Red | 376.4 | 3 | 0.00797 |
| Putrescine 2HCl | 161 | 0.32 | 0.00199 |
| Sodium Pyruvate | 110 | 220 | 2.00 |
| Thymidine | 242 | 0.7 | 0.00289 |

Technical Resources - Media Formulations

F-12K Nutrient Mixture Kaighn's Modification (1X) liquid
Contains L-glutamine.

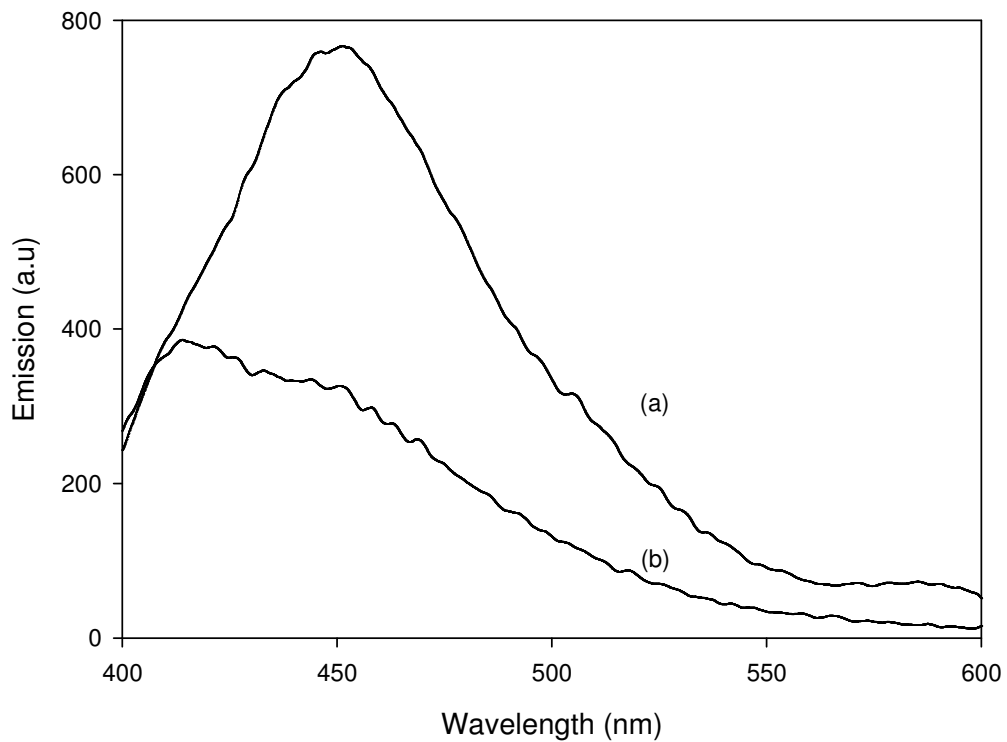
Catalogue Number: [21127022](#)

Appendix 3



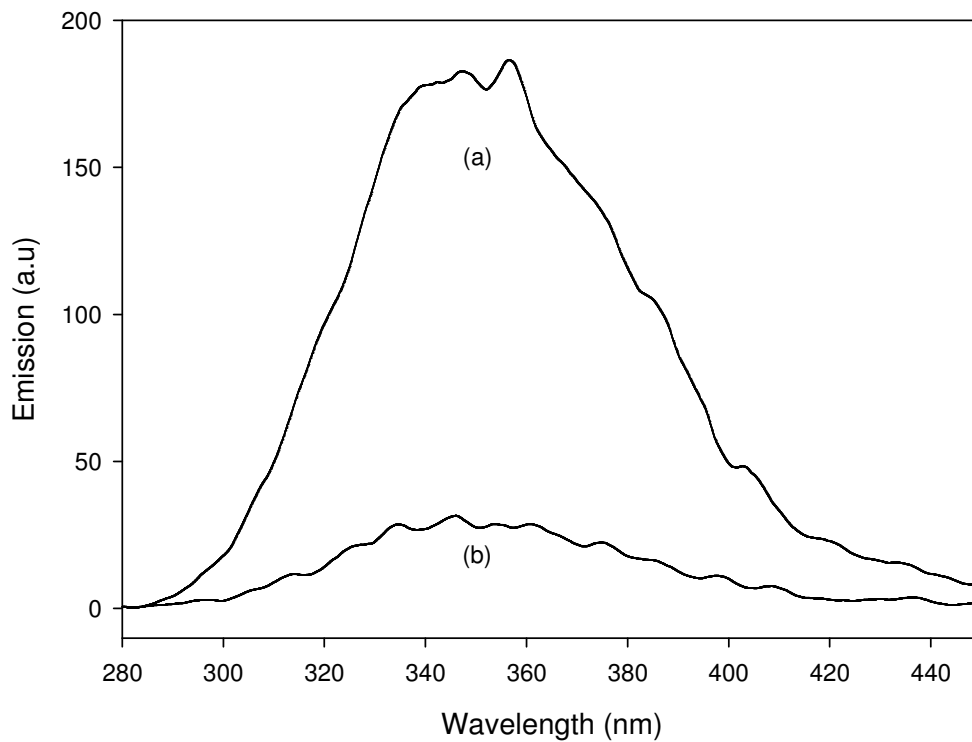
Appendix 3 displays a photograph showing the observed colour change in the medium upon the dispersion of SWCNT (0.4 mg/ml) following a 24 hour settling period. This observed colour change was attributed to the interactions of SWCNT with a phenol red pH indicator within the medium.

Appendix 4



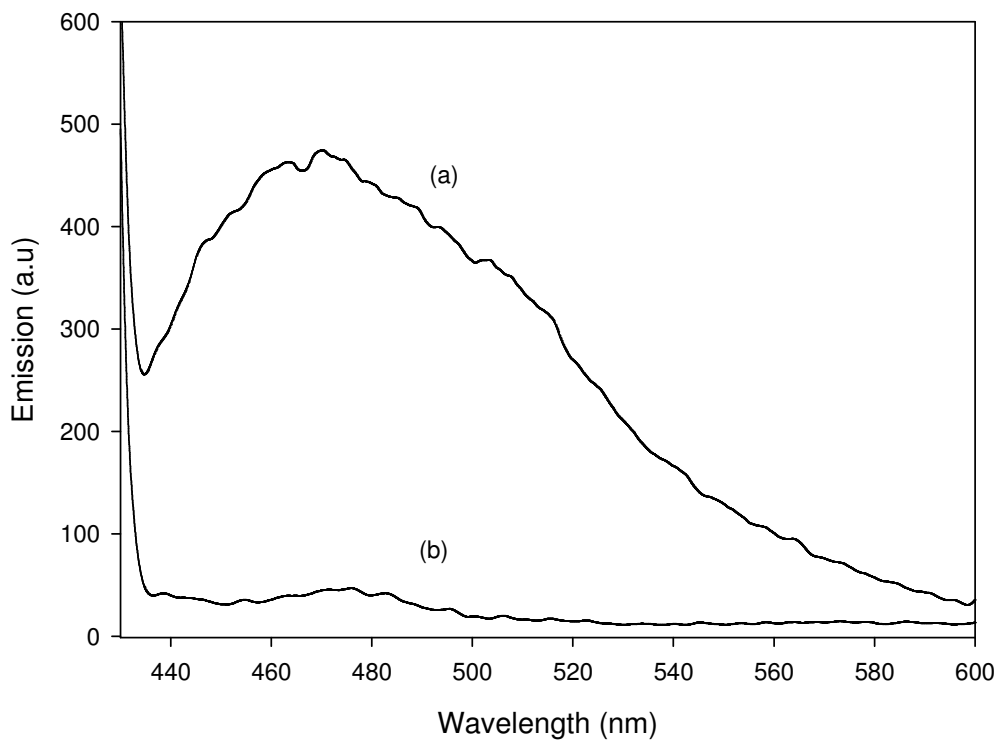
Appendix 4 displays the emission spectra obtained for (a) the tested cell culture medium by 360nm excitation (b) the quenched emission of this feature upon the addition of SWCNT. As was discussed in chapter 5 excitation of the medium by 360nm yielded an emission spectrum centred at 450nm. The origin of this feature was attributed to that of riboflavin a B vitamin found in the medium.

Appendix 5



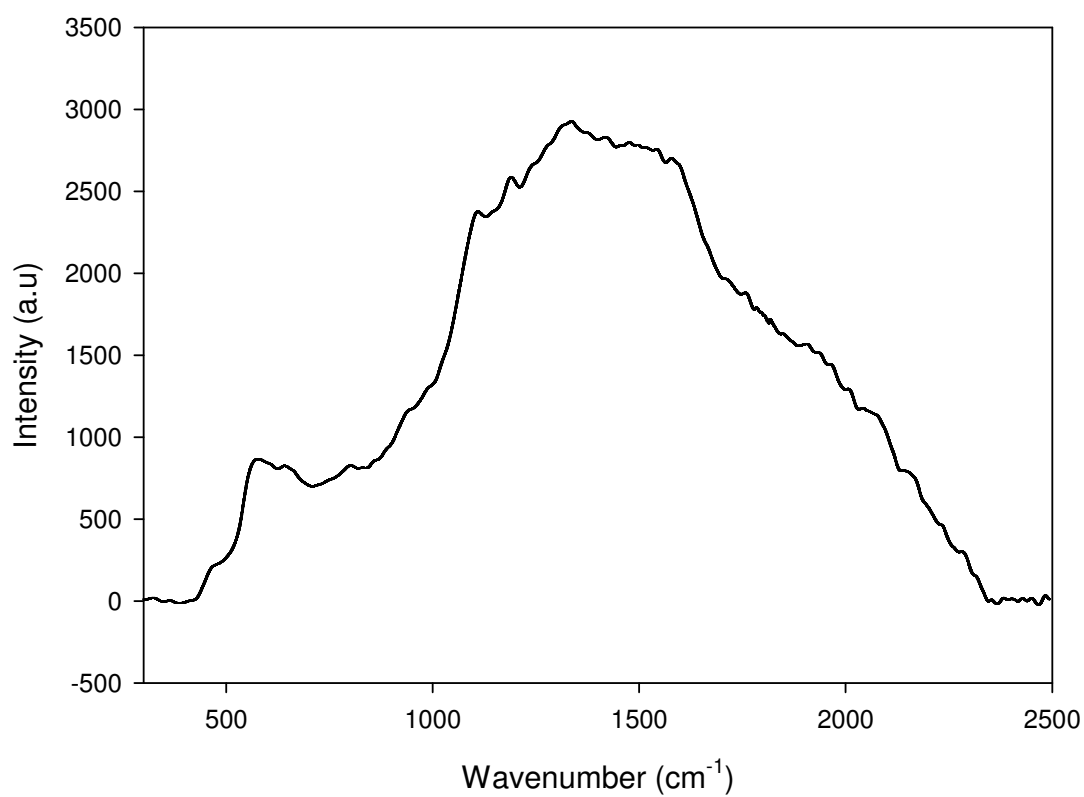
Appendix 5 displays the emission spectra obtained for (a) the tested cell culture medium, containing 5% FBS (protein supplement) by 268nm excitation (b) the quenched emission of this feature upon the addition of SWCNT. As was discussed in chapter 5 excitation of the medium by 268nm yielded an emission spectrum centred at 360nm. The origin of this feature was attributed to that the added protein supplement (FBS).

Appendix 6



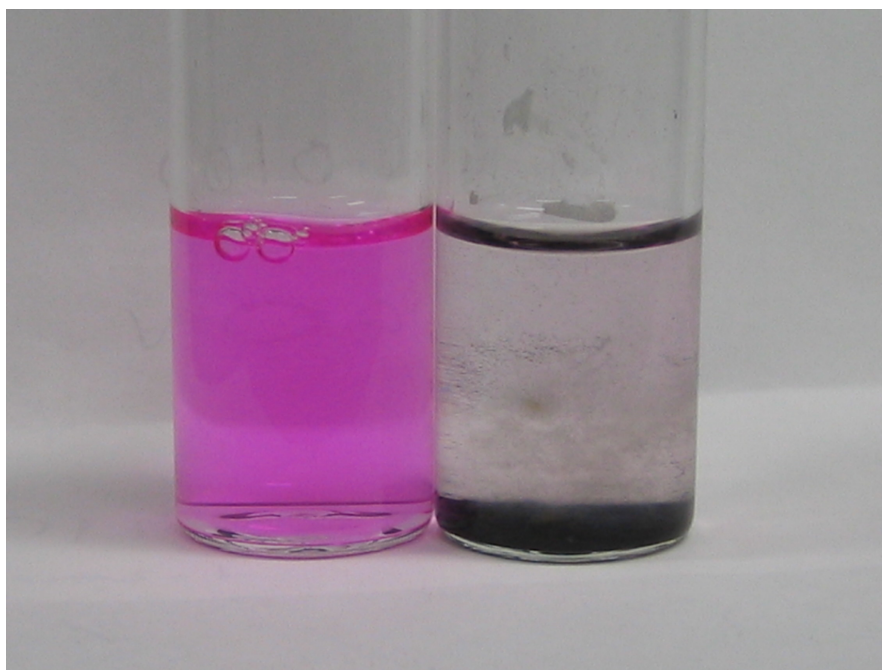
Appendix 6 displays the emission spectra obtained for (a) the tested cell culture medium, containing 5% FBS (protein supplement) by 410nm excitation (b) the quenched emission of this feature upon the addition of SWCNT. As was discussed in chapter 5 excitation of the medium by 410nm yielded an emission spectrum centred at 450nm. The origin of this feature was attributed to that the added protein supplement (FBS).

Appendix 7



Raman Signal of unprocessed Carbon Black (Printex 90) by 514nm laser excitation. As can be seen Carbon Black exhibits one dominant feature consisting of a broad band centred at approximately 1500 cm⁻¹ originating from graphene.

Appendix 8

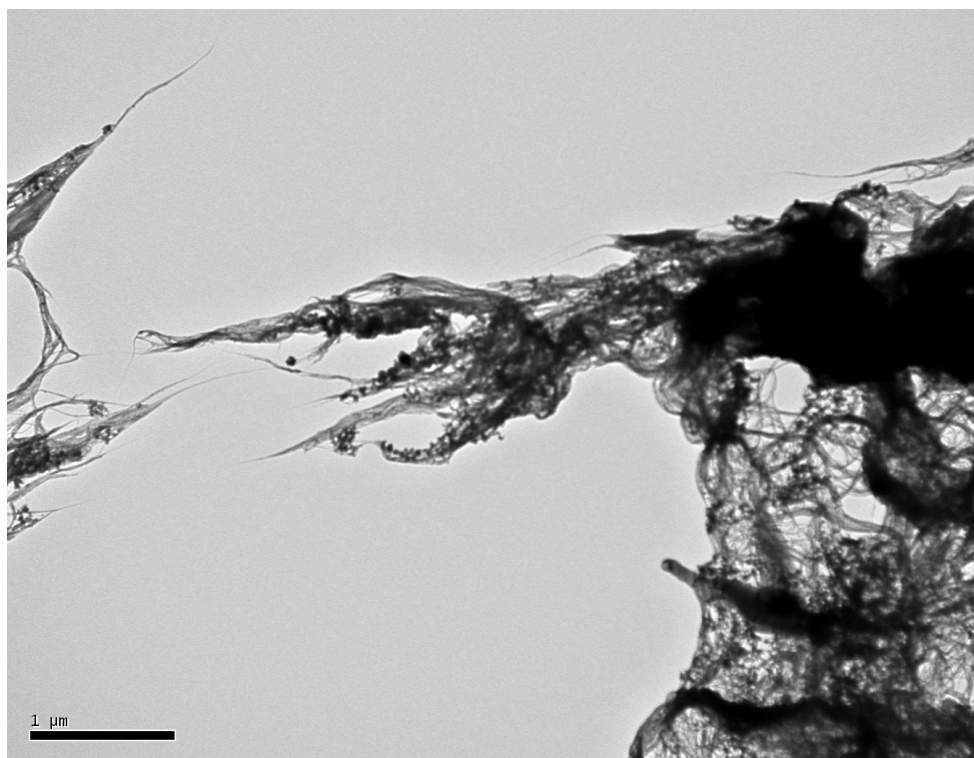


Photograph shows the observed colour change upon dispersing SWCNT within a solution of the converted form of the alamer blue assay.



Photograph shows the observed colour change upon dispersing SWCNT within a solution of the converted form of the WST-1 assay previously thought not to interact with SWCNT.

Appendix 9



Appendix 9 displays a Tem image of HiPco SWCNT dispersed in cell culture medium. As can be clearly seen the SWCNT remained as large aggregates. This verifies the conclusion draw from the emission and Raman spectroscopy of chapter 5 that due to the nature of the obtained ratio plots (figure 5.2 and 5.3) and radial breathing mode analysis (figure 5.6) no debundling of SWCNT sample occurred.

Peer Reviewed Publications

“Spectroscopic analysis confirms the interactions between single walled carbon nanotubes and various dyes commonly used to assess cytotoxicity.” A. Casey, E. Herzog, M. Davoren, F.M. Lyng, H.J. Byrne and G. Chambers.
Carbon, 2007, 45, 1425 – 1432.

“*In vitro* Toxicity Evaluation of Single Walled Carbon Nanotubes on human A549 lung cells.” M. Davoren, E. Herzog, A. Casey, B. Cottineau, G. Chambers, H.J. Byrne, F.M. Lyng.
Toxicology in Vitro. 2007, 21, 438-448.

“Probing the interaction of single walled carbon nanotubes within cell culture medium as a precursor to toxicity testing.” A. Casey, M. Davoren, E. Herzog, F.M. Lyng, H.J. Byrne and G. Chambers.
Carbon. 2007, 45, 34-40.

“Interaction of Carbon Nanotubes with Sugar Complexes” A. Casey, G.F. Farrell, M. Mc Namara, H.J. Byrne and G. Chambers.
Synthetic Metals. 2005, 153, 357–360.

Other Publications

“Single walled carbon nanotubes induce indirect cytotoxicity by medium depletion in A549 lung cells” A. Casey, E. Herzog, M. Davoren, F.M. Lyng, H.J. Byrne and G. Chambers. *Manuscript in preparation*.

Conferences

Irish Society of Toxicology (IST), Spring Meeting
Galway, Ireland.
March 30th-31st 2007.

Oral Presentation.

European Conference on Diamond, Diamond like materials, Carbon Nanotubes and Nitrides.

Estoril, Portugal. Sept 3rd –Sept 8th 2006.

Poster Presentation

The International Conference of Synthetic Metals (ICSM).
Trinity Collage, Dublin. July 2nd – July 7th 2006

Oral Presentation

The International Conference of Materials Energy and Design.
Bolten Street, DIT. Mar 14th –Mar 16th 2006.

Oral Presentation.

The International Conference on Nanotoxicology: Biomedical Aspects.
Miami, USA. Jan 29th – Feb 1st 2006.

Poster Presentation.

Opto Ireland Spie Conference
Dublin, Ireland. 4th -6th April 2005

Poster Presentation.

The Institute of Physics, Spring Meeting 2005
Naas, Ireland.

Poster Presentation.

The International Conference of Synthetic Metals (ICSM)
University of Wollongong, Australia. 28th June – 2nd July 2004

Oral Presentation

The 12th International Cyclodextrin Symposium.
Montpellier, France. 16th -19th May 2004.

Poster Presentation